The Optimal Layout of Electrical Interconnection and Transmission Systems of Offshore Wind Farms

Mohsen Sedighi

Submitted to the
Institute of Graduate Studies and Research
in partial fulfillment of the requirements for the degree of

Doctor of Philosophy
in
Electrical and Electronic Engineering

Eastern Mediterranean University
November 2017
Gazimağusa, North Cyprus

Approval of the Institute of Graduate Studies and Research

Assoc. Prof. Dr. Ali Hakan Ulusoy
Acting Director

I certify that this thesis satisfies the requirements as a thesis for the degree of Doctor of Philosophy in Electrical and Electronic Engineering.

Prof. Dr. Hasan Demirel
Chair, Department of Electrical and Electronic Engineering

We certify that we have read this thesis and that in our opinion it is fully adequate in scope and quality as a thesis for the degree of Doctor of Philosophy in Electrical and Electronic Engineering.

Assoc. Prof. Dr. Murat Fahrioğlu
Co-Supervisor

Prof. Dr. Osman Kükrer
Supervisor

Examining Committee

1. Prof. Dr. İsmail H. Altaş
2. Prof. Dr. İres İskender
3. Prof. Dr. Oman Kükrer
4. Prof. Dr. Şener Uysal
5. Assoc. Prof. Dr. Murat Fahrioğlu
6. Asst. Prof. Dr. Sahand Daneshvar
7. Asst. Prof. Dr. Reza Sirjani

ABSTRACT

Off-shore Wind Farm (OWF) is the largest renewable energy resource. The cost of electrical interconnection and transmission systems of OWFs is a considerable fraction of the overall design cost of the farm. In order to minimize the investment and operational costs, this thesis proposes an optimization formulation to find the optimal electrical interconnection configuration of Wind Turbines (WTs) and the optimal size of cables cross section (cable sizing) simultaneously, while the transmission system and other relevant components are optimized as well (e.g. the offshore platforms, offshore substation transformers, switchgears). This simultaneous minimization of total trenching length and cable cross sections creates a complex optimization problem that is solved by the Harmony Search (HS) algorithm. The optimization performance of HS has been compared with the genetic algorithm. The proposed simulations can be applied to a symmetric or asymmetric topology of OWF, which are applied in two case studies.

In the first case study, two distinct methods of full and partial optimal cable sizing have been considered to comprehensively assess the optimal interconnection layout of OWFs. Furthermore, various shipping and burying costs as well as various WTs power rating have been considered to investigate their impact on the layout of optimal electrical interconnection system.

In the second case study, the optimal layout of electrical interconnection, transmission system and other relevant components of a real OWF have been found simultaneously. In order to demonstrate higher performance of the proposed

optimization method and formulation, the results have been compared with another study, where a real OWF has identically been assumed to have a fair comparison, under identical conditions and constraints. The comparison results reveal that, our proposed optimal interconnection system reduces the interconnection cost, cable length and power loss of OWF.

Keywords: Off-shore Wind Farm (OWF), optimal interconnection configuration, cables cross section, transmission system, Harmony Search (HS) algorithm, and simultaneous optimization.

ÖZ

Kıyı ötesi rüzgar çiftliği en büyük yenilenebilir enerji kaynağıdır. Bir rüzgar çiftliğinin elektriksel bağlantı ve iletim maliyeti, çiftliğin toplam tasarım maliyetinin önemli bir oranıdır. Bu çalışma, yatırım ve işletme maliyetlerini en aza indirgeme amacıyla, eniyi elektriksel bağlantı yapılandırması ve eniyi kablo boyutlarını, iletim sistemini ve diğer ilgili elektriksel bileşenleri de eniyileştirme hedefli bir eniyileştirme formülasyonu önermektedir. Toplam hendek uzunluğu ve kablo boyutlarının eşzamanlı enaza indirgenmesi, "Uyumluluk Arayışı" algoritması kullanılarak çözülen karmaşık bir eniyileştirme problem yaratmaktadır. Uyumluluk Arayışı algoritmasının eniyileştirme başarımı genetik algoritması ile karşılaştırılmıştır. Benzetimler simetrik ve simetrik olmayan rüzgar çiftliği topolojilerine uygulanabilir. Bu topolojilerin iki farklı durumu üzerine çalışma yapılmıştır. Birinci durum çalışmasında, kıyı ötesi rüzgar çiftliğinin eniyi bağlantı düzeninin kapsamlı bir değerlendirmesini yapmak amacıyla, tam ve kısmi kablo boyutlandırmasından oluşan iki farklı yöntem üzerinde durulmuştur. Buna ek olarak, farklı taşıma ve gömme maliyetleri ile rüzgar türbinlerinin güç kapasiteleri de, eniyi elektriksel bağlantı sistemi üzerindeki etkilerini araştırmak amacıyla ele alınmıştır. İkinci durum çalışmasında, gerçek bir kıyı ötesi rüzgar çiftliğine ait elektriksel bağlantının eniyi düzeni, iletim sistemi ve diğer ilgili elektriksel bileşenleri de eşzamanlı bulunmuştur. Önerilen eniyileştirme yöntemi ve formülasyonunun daha üstün başarımını gösterme amacıyla, gerçek bir kıyı ötesi rüzgar çiftliğini esas alan başka bir çalışma ile karşılaştırmalar yapılmıştır. Karşılaştırma sonuçları önerilen eniyi bağlantı sisteminin, bağlantı maliyetini, kablo uzunluğunu ve rüzgar çiftliğinin güç kayıplarını azalttığını ortaya çıkarmıştır.

Anahtar Kelimeler: Kıyı ötesi rüzgar çiftliği, eniyi bağlantı yapılandırması, kablo boyutlandırma, iletim sistemi, Uyumluluk Arayışı algoritması, Eşzamanlı eniyileştirme.

DEDICATION

To my beloved wife, ***Shiva***

and

my great supporting ***parents***.

ACKNOWLEDGMENT

I am especially grateful to my supervisor and co-supervisor Prof. Dr. Osman Kukrer and Assoc. Prof. Dr. Murat Fahrioglu respectively, for providing the opportunity to do my research in the field I preferred most. They have been great advisor and mentor, while their vision and feedback have been significantly instrumental in the success of this research. I would like to extend my gratitude to Prof. Dr. Hasan Demirel for being a great respectful Chairman in our department, where I was a research assistant. Indeed, I am always indebted to their sincere supports and countless impact on my personal and professional growth.

In addition, I would like to acknowledge Assoc. Prof. Dr. Mohammad Moradzaheh from systems engineering research group in department of engineering and technology, University of Huddersfield, UK, for the collaboration and providing technical support in this research and the publications.

I am also honored to acknowledge Prof. Dr. István Erlich, chair of Electrical Power Systems department in Duisburg-Essen University, Duisburg, Germany, because of his technical support and admitting me into his fantastic institute as a visiting scholar for three months. It was really a great experience for me to work with them.

My deepest appreciation goes toward my parents, my father Ramezan Ali Sedighi, and my Mother Maryam S. Ghaheri, for their uninterrupted supports and encouragement throughout my study and life in general.

Finally, I would like to express my actual gratitude to my wife, S. Shiva Mousavi, for her aid, patience, exhortation, spiritual supports and endless love during these hard working years.

TABLE OF CONTENTS

LIST OF TABLES

LIST OF FIGURES

LIST OFABBREVIATIONS

AC	Alternating Current
AEP	Annual Energy Production
CAPEX	Capital Expenditure
CCP	Central Collection Point
HVAC	High-Voltage Alternating Current
HVDC	High-Voltage Direct Current
IGBT	Insulated Gate Bipolar Transistors
LCC	Line Commutating Converters
LCoE	Levelized Cost of Energy
MERRA	Modern-Era Retrospective Analysis for Research and Applications
MV	Medium Voltage
NREL	the National Renewable Energy Laboratory
OCP	Onshore Connection Point
OECD	Organization for Economic Cooperation and Development
OPEX	Operational Expenditure
OS	Offshore Substation
OWF	Offshore Wind Farm

O&M	Operation and Maintenance
PWM	Pulse Width Modulation
SCOE	Society‘s Costs of Electricity
VSC	Voltage Source Converters
WT	Wind Turbine

Chapter 1

INTRODUCTION

1.1 Background

Wind energy is the most promising source among the presently developed renewable energy supplies and it is the world's fastest growing renewable energy supply. Parallel with on-shore wind farms, Off-shore developing in large-scale Wind Farms (OWFs) can play a significant role in reducing the environmental implications of meeting the high electrical power demand of modern societies (Gonzalez-Longatt et al., 2012). The policy framework for securing 27% renewable energy and 40% reduction in greenhouse gas emissions could be met with OWFs solution with expected growth to 65 GW by 2030 (EY, 2015). In fact, the main advantage of OWFs compare to its onshore counterpart are harvesting wind with higher speed and more persistent in off-shore areas, thus Wind Turbines (WTs) can be designed for higher speed ratio and smaller weight for same power rating; moreover, land availability and acoustic emission, which are significant issues in on-shore wind farm design, are insignificant in the OWF design (Soukissian, 2013; Erlich et al., 2013). However, the foundations, installation and maintenance costs, as well as cost of the electrical interconnection system and transmission line to the shore are significantly higher in OWFs. These higher costs have demanded extensive technical developments and optimization challenges in order to reduce the Levelized Cost of Energy (LCoE). It is estimated that LCoE could be reduced to $100/MWh by 2030 (EY, 2015).

Figure 1.1: A large-scale offshore wind farm (London array)

Figure 1.1 shows a large-scale OWF. Year 2015 was a record in terms of total installed capacity of OWFs, where more than 20 billion Dollars was invested in 3.4 GW. Figure 1.2 shows that, by the end of 2015, worldwide OWFs installed capacity was about 12.1 GW, where portion of UK and Germany were nearly 8.4 GW and over 11 GW were located in waters off eleven European countries coast. However, offshore wind technology is still in its nascent stage, in contrast to the 429.5 GW worldwide capacity of on-shore wind energy (GWEC, 2015; Ederer, 2015).

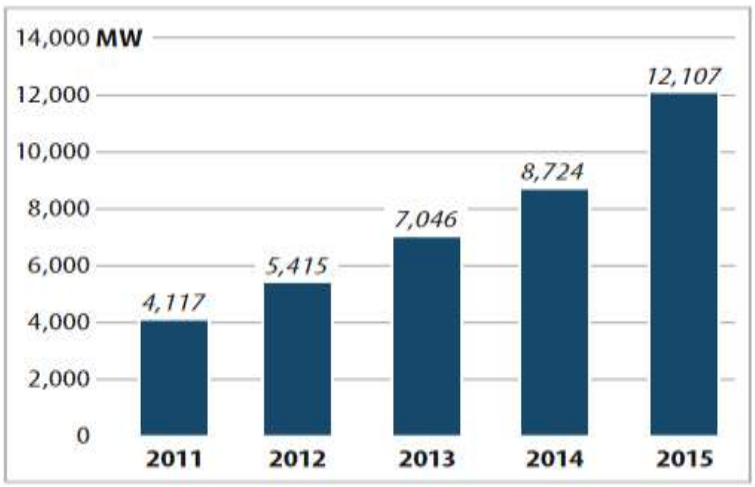

Figure 1.2: Worldwide annual cumulative capacity of OWFs (GWEC, 2015)

1.2 Problem Statement

Conventionally, the electrical interconnection system of OWFs could be structured in different configurations such as radial, star or loop design depending on the desired reliability level. Nevertheless, probability of a fault in buried subsea (submarine) cable is very low, about 0.001/km/yr (Kamalakannan et al., 2014), thus loop design justification may fail according to its higher cost. Actually, in the last few decades, most of the installed OWFs have been relatively small or employing WTs with low power rating. Hence, finding optimal interconnection layout was not necessary and a simple electrical design could be structured, e.g. mostly with typical radial configurations. The simplicity of the optimal interconnection configuration of an OWF with low power rating is also shown in chapter 4, where WTs with power rating of 3.6 MW were assumed in an OWF (Figure 4.4). On the contrary, recent large-scale OWFs with higher rated power WTs have created a new challenge of optimizing the electrical interconnection system, which are comprehensively investigated in this thesis.

In large-scale development of OWFs, since the WTs are scattered over vast areas, optimization of the electrical interconnection layout is significant and one of the most complex stages of the optimal design process. In addition, optimizing the transmission system infrastructure and other relevant components (e.g. the offshore substation transformers, switchgears, etc.) are necessary in order to ensure an efficient electrical connection to the main grid, as the penetration of large-scale OWF in electrical system is increasing.

1.3 Thesis Objectives

The objectives of this thesis are given as follows:

- To propose an optimization formulation in order to minimize the investment and operational costs of electrical connection in OWFs. The optimization problem is aimed to consider electrical interconnection configuration and subsea cables cross section (cable sizing) simultaneously, in the first case study.
- To perform a comprehensive investigation about the impact of the several parameters involved (*Csb* and power rating) on the optimal layout of electrical interconnection of OWFs.
- To investigate two different optimal cable sizing methods (full and partial) according to the change of *Csb* in different OWFs.
- To optimize the high voltage transmission system layout and ratings of other relevant components, together with the optimal layout of its interconnection system.

1.4 Literature Review

Since, large-scale OWFs have been recently developed in the last decade, more research works have recently conducted on the optimization of various aspect of OWF. As High Voltage DC (HVDC) transmission system is becoming a justified alternative solution for OWFs faraway from shore, recently some researchers suggest extending the DC nature to the interconnection system (Holtsmark et al., 2013; Chuangpishit et al., 2014). Moreover, a new AC interconnection system is assessed where the entire OWF is connected just to a single large power convertor, which operates at variable frequency (Gomis-Bellmunt et al., 2010; De Parda et al., 2014).

No optimal interconnection investigation is considered in any of these references. De Parda et al. (2015) also proposed an optimal design of hybrid AC-DC with variable frequency operation for individual clusters, while a simple radial configuration is considered. Dutta and Overbye (2011) proposed a clustering-based cable design, different from the typical configurations. In a later study, Dutta and Overbye (2012) proposed various clustering methods to decrease the problem size and find the optimal configuration of each cluster by Minimum Spanning Tree (MST) algorithm. Furthermore, they proposed an algorithm to introduce intermediate splice point to minimize the total trenching length. A similar clustering methodology based on MST algorithm was proposed for OWF by ignoring intermediate splice point (Shin et al., 2015), due to very high splicing cost on subsea cable. Banzo and Ramos (2011) proposed a stochastic programing model to find the optimal layout of electric power system of a real OWF in the UK. A Mixed Integer Programing (MIP) algorithm was used and a minor cost reduction was obtained. Lumbreras and Ramos (2013), proposed a similar tool with reasonable computational time to find the optimal electrical layout of OWFs by MIP algorithm and decomposition strategies. A Mixed Integer Linear Programming (MILP) approach was utilized by Pillaiet al. (2015) to minimize the total trenching length of OWFs to find optimal location of Offshore Substation (OS) and optimal interconnection configuration individually. Nevertheless, none of them could include cable cross sections in objective function to represent a realistic optimization, due to utilizing MST or analytical optimization methods that require weights for constant edges. Gonzalez et al. (2013) proposed an improved Genetic Algorithm (GA) to find optimal location of WTs to minimize the wake effect and then the total trenching length without cable sizing to find optimal electrical interconnection configuration of an OWF in two individual steps. In

addition, crossing cables was not avoided, which is impractical to bury the subsea cable in offshore area.

On the contrary, recent large-scale OWFs utilizing WTs with higher power rating ($P_G \geq 5MW$) have created a new challenge to optimize the electrical interconnection layout (interconnection configuration and cable sizing) of the OWFs. Recently, variable cable cross section has been also considered to find the optimal electrical interconnection configuration of OWFs; where heuristic optimization algorithms have been utilized.

Gonzalez-Longatt et al. (2012) proposed a modified approach to the Traveling Salesman Problem (TSP) for designing a radial configuration. This study used an improved GA to find the optimal electrical network design of a large-scale OWF, while cable cross sections were considered as a radial configuration without any tapering for cables away from the OS. A binary GA was used in (Dahmani et al., 2015) to find the optimal electrical network of an OWF where full cable sizing was considered. However, the optimal layout was found just for the pre-clustered nodes in order to decrease the problem size and power loss is not considered as operational cost. Hou et al. (2016) proposed an Adaptive Particle Swarm Optimization (APSO), which adjusts every individual solution to new integer solutions to solve discrete problems. In order to minimize the total cost of cables, an APSO-MST algorithm was utilized to find the optimal interconnection layout and OS location of an OWF simultaneously. However, the total power losses as well as shipping and burying costs (*Csb*) of subsea cables were not considered. Hou et al. (2017a) also found the optimal interconnection and transmission systems of an OWF, where APSO-MST

algorithm and C-means clustering method were utilized. In their recent studies (Hou et al. 2017b), the optimal location of OS and optimal topology of WTs location were simultaneously found together with the optimal interconnection layout of real OWFs. The same APSO-MST algorithm was adopted to minimize wake effect and cable cost of the OWF, due to high performance of PSO to solve such continuous problems (finding the optimal locations). However, the project area of the OWFs in case study was considered increasable during the optimization process, which would not yield to fair results. On the contrary, in these studies, finding the optimal electrical interconnection configuration and cable sizing of an OWF are inherently discrete problems. Thereby, the APSO, by adjusting real values to integers, may not be the best choice, as its performance was decreased to solve such a complex problem. Furthermore, in order to avoid crossing subsea cables, similar to (Dahmani et al., 2015), the edges with crossing potential are eliminated, which may miss some feasible solutions.

1.5 Contributions and Organization

The existing optimization methods or formulations mentioned in the literature do not seem to be completely satisfactory. This is because, finding the optimal electrical interconnection layout without cable sizing leads to over-sizing in the cross section of subsea cables in the interconnection system. Moreover, decreasing the problem size by any clustering method without considering integration of all WTs or utilizing an insufficient optimization algorithm may result in a local optimal solution. Furthermore, avoiding crossing of subsea cables by eliminating both feasible edges with crossing potential may lead to missing some feasible solutions.

In this thesis, the optimal configuration and cable sizing of interconnection system, as well as the optimal layout of HV transmission system and rating of other relevant components to connect an OWF to the onshore grid are found simultaneously, in order to minimize the Capital Expenditure (CAPEX) of the entire electrical connection system of an OWF.

The main contributions of this study are as follows:

- Formulation of the OWF interconnection system with two different cable sizing methods (full and partial), offering two distinct solutions according to the seabed conditions or cable installation constraints.
- Investigation of the impact of the WTs' power ratings and *Csb* on the optimal layout of electrical interconnection system.
- Proposing a new formulation for the detection and avoidance of cable crossing.
- Use of the Harmony Search (HS) as a high performance algorithm to solve the formulated discrete optimization problem, without the need for any clustering method.
- Provision of a useful tool to find the optimal interconnection layout of a large-scale OWF with any given topology, with possible adoption to on-shore wind farms.

The remainder of the thesis is organized as follows. Chapter 2 introduces the overview of on- and off-shore wind power. In chapter 3, the formulation of the optimization problem is described. Chapter 4 discusses the results, where the optimal

electrical connection layouts of two distinct case studies are investigated. Finally, the conclusion of the thesis is presented and future work is proposed in chapter 5.

Chapter 2

OVERVIEW OF ON- AND OFF-SHORE WIND POWER

2.1 Statistical Review of Wind Energy

Clearly, wind energy is now a mainstream renewable source and will play a leading role in de-carbonization. However, wind industry need to use technical innovation and optimization for cost reduction, improve the reliability and predictability of project and integrate large-scale wind sources into electricity systems. Worldwide annual cumulative installed wind capacity between 2000 and 2015 has been illustrated in Figure 2.1. "2015 was a stellar year for the wind industry and for the energy revolution, culminating with the landmark Paris Agreement in December" (GWEC, 2015). After first passing the 50 GW mark in 2014, wind technology had another record-breaking year in 2015 as annual installations increased by 21.9% and topped 63 GW, while China as usual led the way with as a new record (30.8 GW).

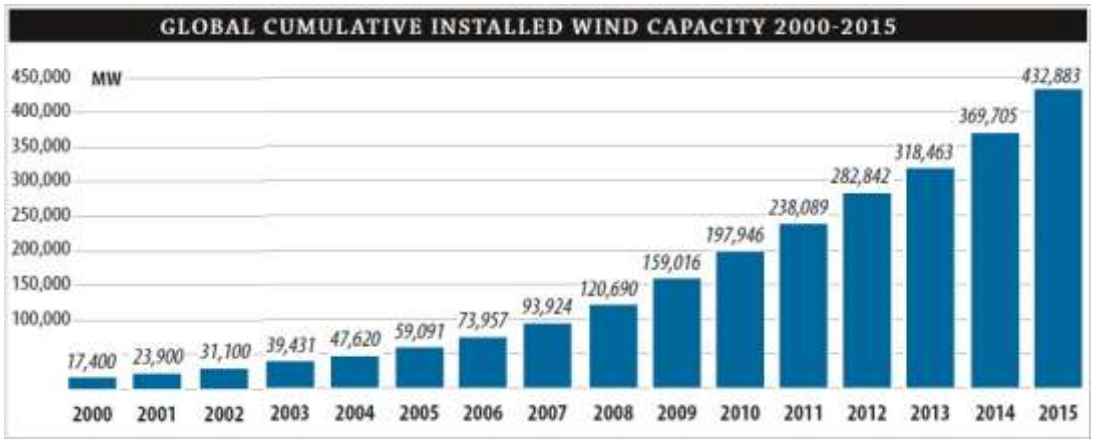

Figure 2.1: Worldwide annual cumulative installed wind capacity 2000-2015 (GWEC, 2015)

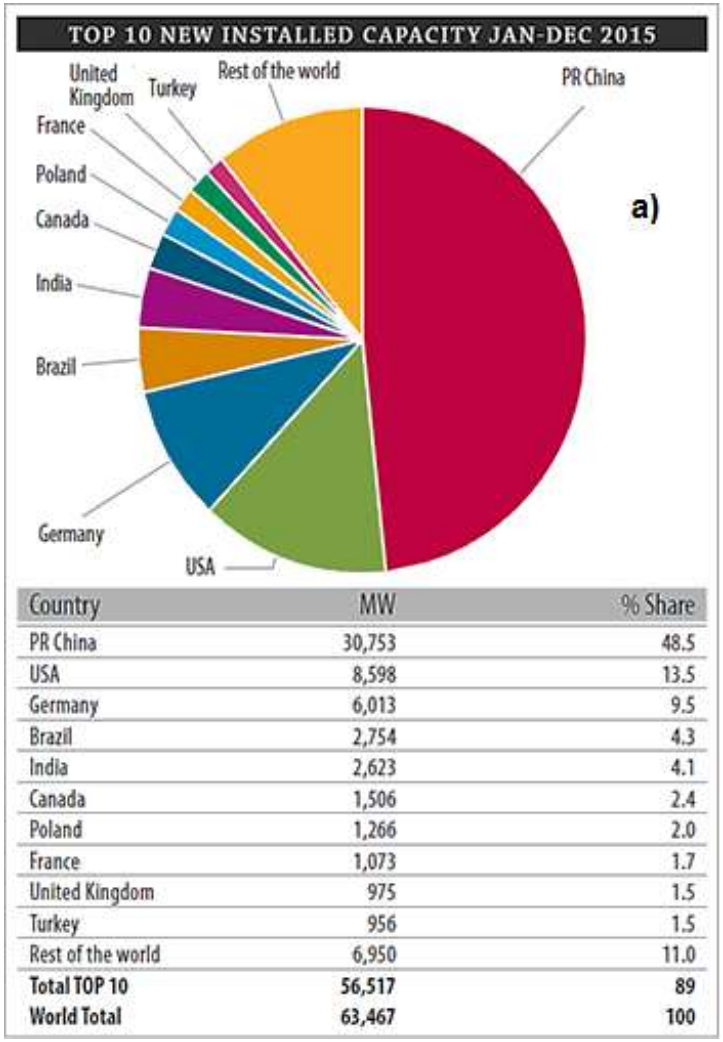

Country	MW	% Share
PR China	30,753	48.5
USA	8,598	13.5
Germany	6,013	9.5
Brazil	2,754	4.3
India	2,623	4.1
Canada	1,506	2.4
Poland	1,266	2.0
France	1,073	1.7
United Kingdom	975	1.5
Turkey	956	1.5
Rest of the world	6,950	11.0
Total TOP 10	**56,517**	**89**
World Total	**63,467**	**100**

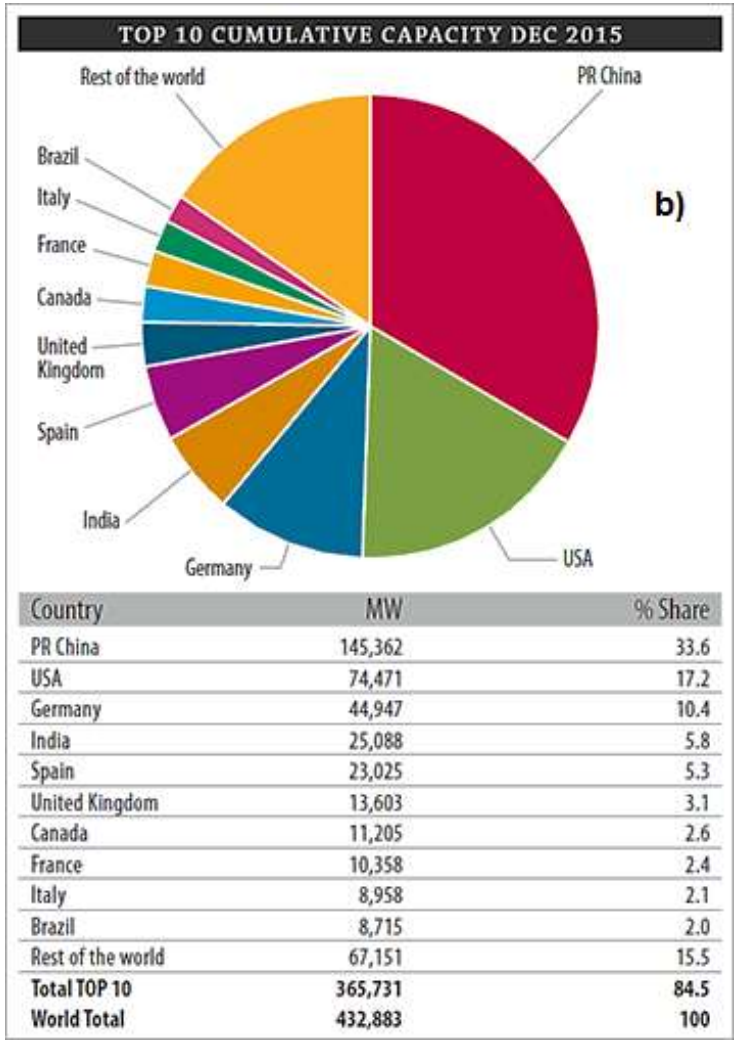

Country	MW	% Share
PR China	145,362	33.6
USA	74,471	17.2
Germany	44,947	10.4
India	25,088	5.8
Spain	23,025	5.3
United Kingdom	13,603	3.1
Canada	11,205	2.6
France	10,358	2.4
Italy	8,958	2.1
Brazil	8,715	2.0
Rest of the world	67,151	15.5
Total TOP 10	**365,731**	**84.5**
World Total	**432,883**	**100**

Figure 2.2: The portion of top 10 countries for new (a) and cumulative (b) installed wind capacity (including offshore) by 2015 (GWEC, 2015)

The portion of top 10 countries for new and cumulative installed wind capacity (including offshore) by 2015 are depicted in section a) and b) of Figure 2.2, respectively. Overall, China has the highest cumulative installed wind capacity (145.4 GW); even more than in all of the European Union, then USA with 74.5 GW while their offshore portion were negligible. Germany has the third rank of total installed wind capacity (44.9 GW) and the largest installed capacity in Europe; other European countries are followed by Spain (23 GW), the UK (13.6 GW), France (10 GW) and Italy (9 GW). “Beyond the EU, Turkey is the largest European market, with annual installations of 956 MW in 2015. Turkish market reached a cumulative installed capacity of 4,694 MW last year. Looking ahead, the future of Turkey’s wind sector looks promising" (GWEC, 2015).

Offshore wind technology had also an unprecedented year in 2015, especially in Europe. The worldwide portion of installed and fully connected to the grid OWFs in 2015 was about 3.4 GW, while Germany installed about 2.3 GW in an exceptional year. OWFs accounted for a quarter of total installations (over 3 GW) of European wind power in 2015. European annual offshore installations increased by 108% (€13.3 billion investment), compared to 2014, but the annual onshore installation in the Europe decreased by 7.8% in 2015. Figure 2.3 illustrates the countries portion and worldwide annual capacity of cumulative installed OWFs by the end of 2015. Over 91% of all 12.1 GW (global capacity of OWFs) have been located in Europe (11 GW). UK OWF market has the highest installed capacity (more than 5 GW) in the world by 2015; Germany has developed both on- and off-shore wind capacities in parallel with 41.7 and 3.3 GW, respectively. This year, Germany could pass Denmark and achieved the second rank in worldwide off-shore market; China with 1

GW installed OWF, has risen to the fourth rank as the largest non-European offshore market by 2015.

The OWFs are shaping tomorrow's de-carbonized economic development of Europe and elsewhere as secured and sustainable energy resources. Actually, in 2013 offshore wind industry in Europe committed to reach to cost reduction in their joint declaration and now it is delivering thanks to new development of larger wind turbines with higher yields. Hence, onshore wind technology has already become the most cost-competitive renewable energy supply in the Europe.

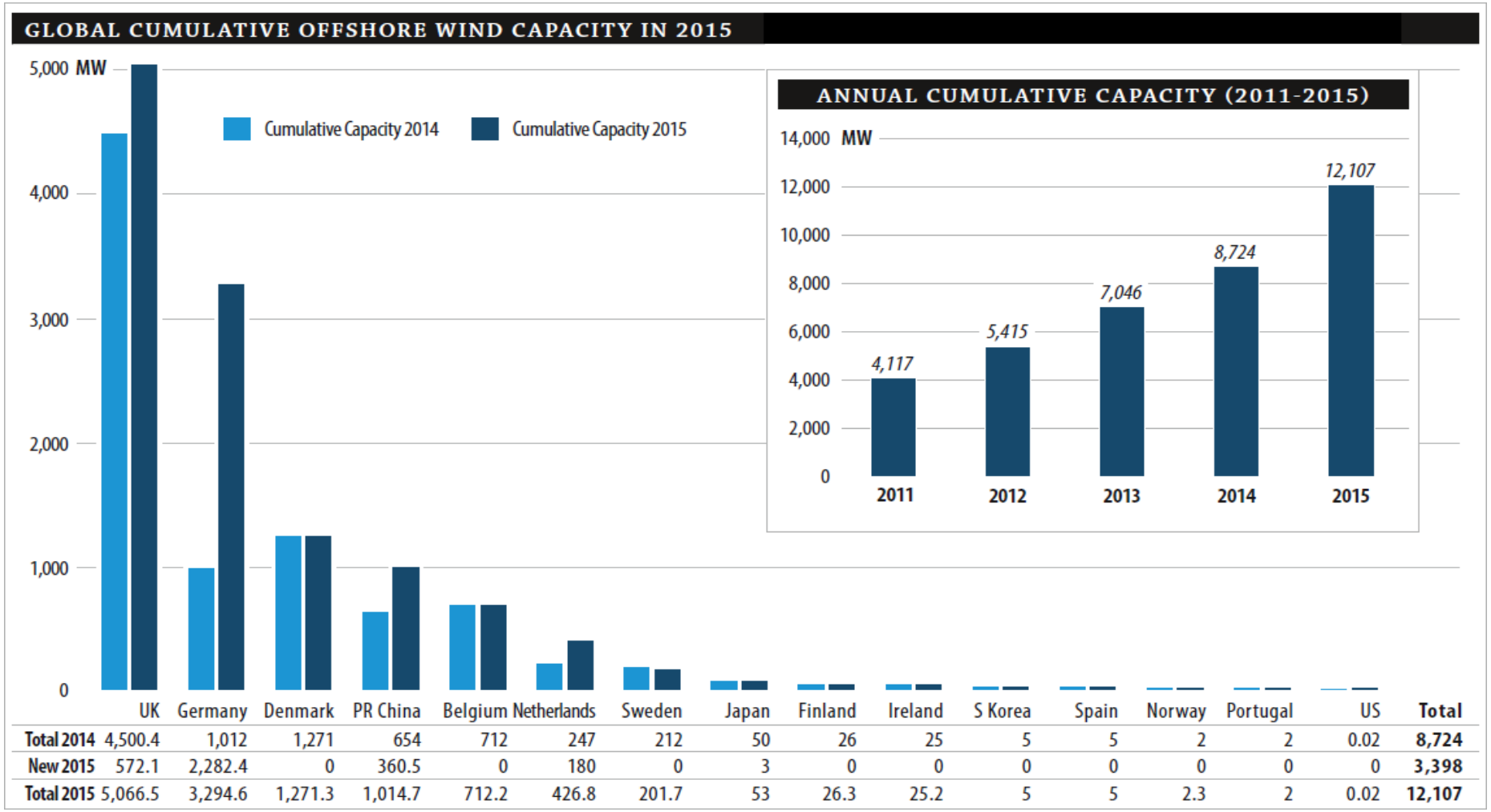

	UK	Germany	Denmark	PR China	Belgium	Netherlands	Sweden	Japan	Finland	Ireland	S Korea	Spain	Norway	Portugal	US	Total
Total 2014	4,500.4	1,012	1,271	654	712	247	212	50	26	25	5	5	2	2	0.02	**8,724**
New 2015	572.1	2,282.4	0	360.5	0	180	0	3	0	0	0	0	0	0	0	**3,398**
Total 2015	5,066.5	3,294.6	1,271.3	1,014.7	712.2	426.8	201.7	53	26.3	25.2	5	5	2.3	2	0.02	**12,107**

Figure 2.3: The countries portion and worldwide annual capacity of cumulative installed OWFs by the end of 2015 (GWEC, 2015)

2.2 Wind Market Forecast

Nevertheless, no one predicted about China with 23 GW new installing in 2014, as nobody predicted 30 GW in 2015. While their economy was slowing and demand was almost flat, actually just a flat market was forecasted in China for 2015. Therefore, it is hard to turn the wind market forecasts for several years, a sustained growth are anticipated, although spectacular growths that achieved in the last two years are not expected. In case, Europe wind market in 2015 reached to a record for wind energy installations, 40% more investment compare to 2014. It will be challenging for wind industry to beat this record in the coming years but 2020 outlook is encouraging (GWEC, 2015).

Figure 2.4 shows the global wind market forecast of cumulative capacity, cumulative growth rate, annual installed capacity and annual installed growth rate by 2020. It indicates that the cumulative and annual growth rate of onshore wind energy will even decrease as governmental funding and subsidies for onshore wind supply is reducing. In contrary, OWF will have more growth rate in future.

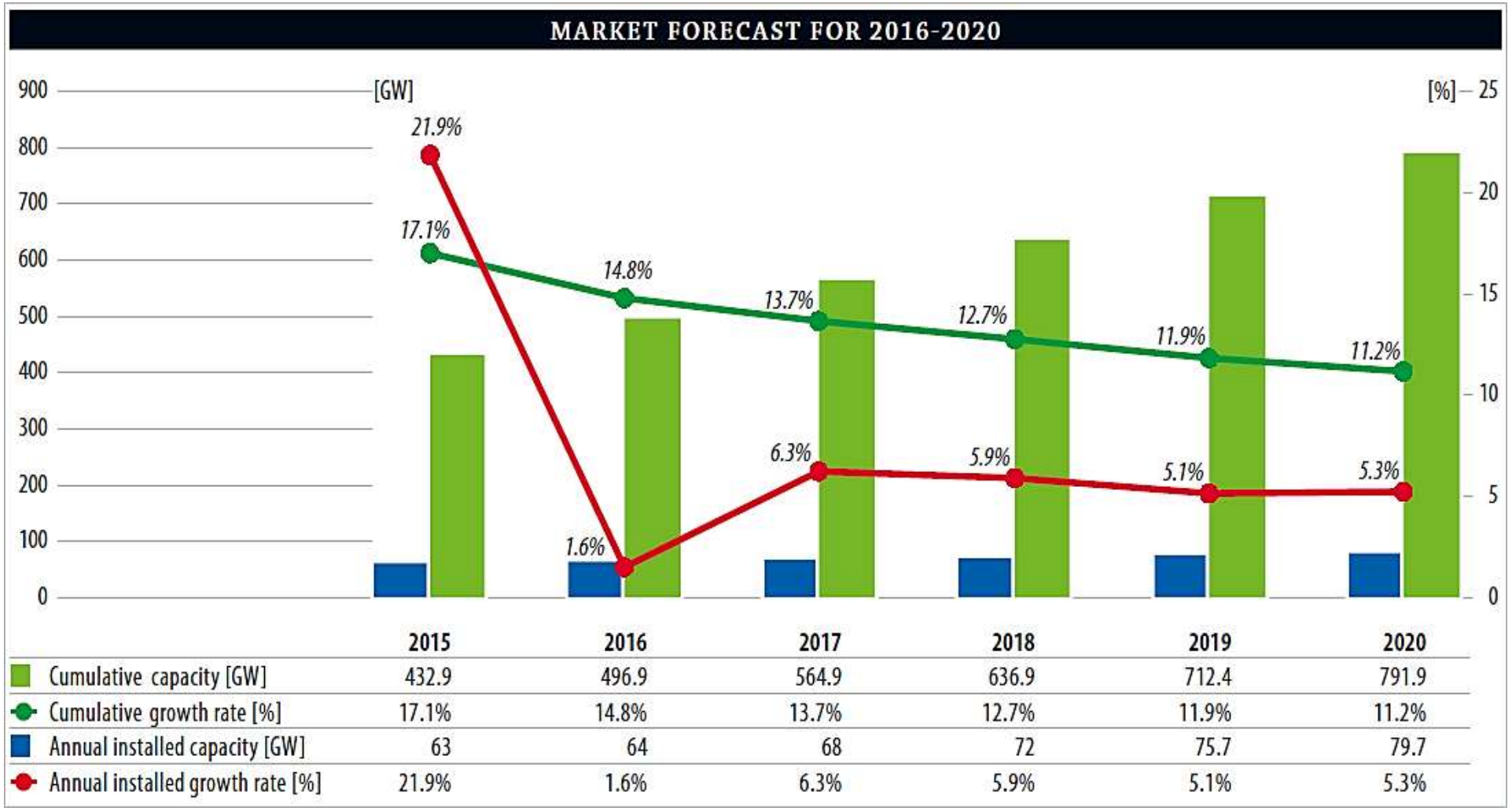

	2015	2016	2017	2018	2019	2020
Cumulative capacity [GW]	432.9	496.9	564.9	636.9	712.4	791.9
Cumulative growth rate [%]	17.1%	14.8%	13.7%	12.7%	11.9%	11.2%
Annual installed capacity [GW]	63	64	68	72	75.7	79.7
Annual installed growth rate [%]	21.9%	1.6%	6.3%	5.9%	5.1%	5.3%

Figure 2.4: Comprehensive evaluation of global wind market forecast by 2020 (GWEC, 2015)

It is also estimated that total investment in wind energy between 2015 and 2040 will be about USD 3.6 trillion, or more than one third of overall investment in renewable energy supplies. In some cases, onshore wind energy is already the cheapest source of energy supply and costs are decreasing: contracted prices for onshore wind in the next few years are about 30 USD/MWh. This is all good news as renewable energies must play the main role to achieve climate goals for 2^{o}C scenario. In recent years, both solar and wind technology cost have decreased dramatically. In some areas (Morocco), as the excellent wind resource are good example to explain this achievement, however the pressure to decrease the on will continue both technologies' price. The USA by having some of the best wind resources in the world is as a pioneer in the global wind industry. According to the location choices, companies' strategies and supply chain development, now the USA wind industry start a long period of policy to be a very different and much stronger in five years. Nevertheless, for some time, they have recently had much lower prices compare to most of their OECD[1] competitors (GWEC, 2015). Moreover, 20% wind energy influence will be reached in USA by 2030, based on development of OWFs proposed projects; 54 and 250 GW prediction for off- and on-shore wind farms, respectively (DOE, 2008). The National Renewable Energy Laboratory (NREL) has estimated potential of 907 GW offshore wind resource off the USA coasts, with high speed wind. About 10% (98 GW) of the offshore wind potential has been found in shallow water (Blohm, 2010).

Recently, Europe has been the lead the offshore wind technology development. They also count on offshore wind power as an unlimited renewable resource, which can be

[1] Organization for Economic Cooperation and Development

an attractive asset for European investors. Therefore, industries effort is to reduce the costs as much as they can. The goal is to decrease LCoE of OWF to €100/MWh by 2020 and €90/MWh by 2030 as it shown in Figure 2.5 (EY, 2015).

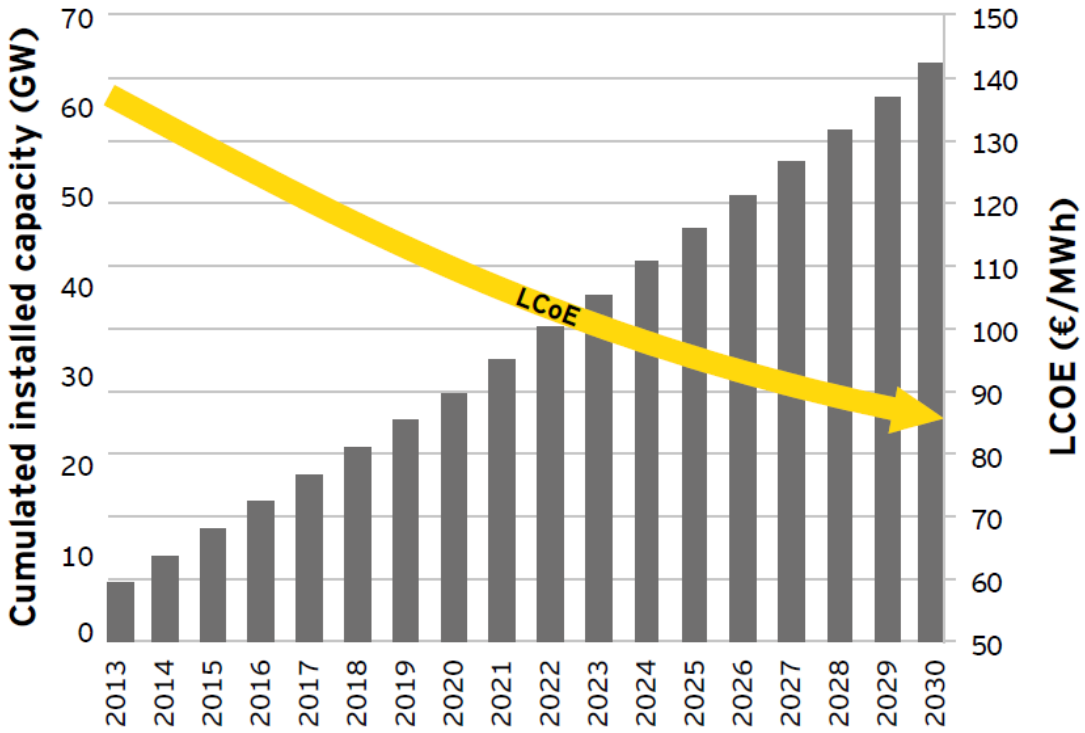

Figure 2.5: LCoE reduction with respect to cumulative OWF market forecast (EY, 2015)

Medium-term perspectives are forecasted that the installed capacity of European offshore wind market will reach to 23.5 and 66 GW by 2020 and 2030, respectively (EWEA, 2014a; EWEA, 2015). However, Europe is not the only market that is developing the offshore wind industry. By 2020, a potential of 35 GW has been found in Asia (more than the plans in Europe), where China followed by Japan and South Korea are developing the OWFs in their shallow waters (EY, 2015).

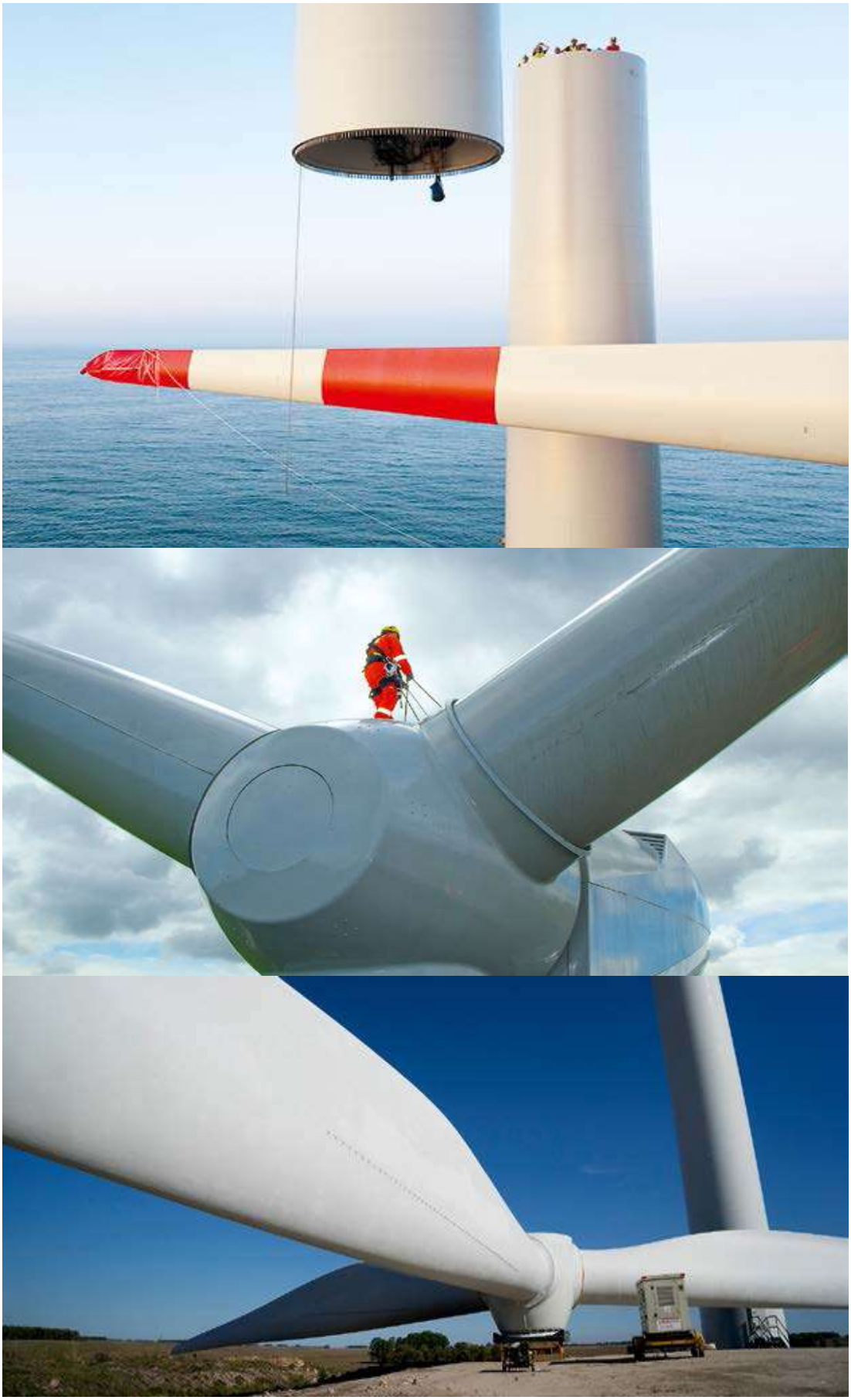

Figure 2.6: Some steps of installation process of off- and on-shore wind farms

2.3 Offshore vs. Onshore Wind Technology

On the one hand, the scarcity increase of feasible onshore sites, the abundant of offshore wind sites as well as the consistent and less intermittent characteristics of offshore wind are increasing the attraction of OWFs. Generally, OWFs can provide clean power over 340 days in a year. In addition, higher distance to shore leads to increase the wind speed sharply and mitigate the public acceptance about noise and visual impacts of WTs. As Figure 2.7 shows, many of civilizations and big cities in the countries with long coast line (e.g. USA, China, etc.) are located near or exactly beside the shores; thereby shorter and less investment transmission system may require where adequate OWFs allocated near urban load center compare to onshore wind farms.

Figure 2.7: At least 40% of the world population lives beside the shore, with less than 100 km distance, NASA 2000 (Siemens, 2014a)

On the another hand, according to the location of OWFs at the sea, they cost much more than onshore wind farms to design and construct the tower and under burying subsea cables as well as dealing with operating and maintenance system. The major difference for investment cost between on- and off-shore wind farms is the cost of foundation and electrical connections. Required investment for an OWF with capacity of 300-400 MW could be about one billion Euros, even far more in deep water projects. Nevertheless, compare to onshore wind, the offshore industry is much younger, thus in a few years, the researches, innovations, optimizations and new technologies (larger WTs with less operating cost) offer a lot of potential to decrease LCoE of offshore wind power significantly. Generally, the OWF is 10-15 years behind its onshore counterpart, but on the right way, and onshore wind success can be adapted to OWF.

The WT in off- and on-shore wind farms are almost the same, but higher power and speed ratio are utilized in OWFs. The control concepts and basic technology of WTs in both off- and on-shore installations are rather the same. Figure 2.8 Shows part of installation procedure for off- and on-shore wind farms in Europe.

Figure 2.8: Part of assembling procedure for off- and on-shore wind farms in Europe

2.4 Development in Offshore Wind Technology

Twenty five years ago in 1991, the world's very first OWF at Vindeby had been constructed by Dong Energy with total capacity of just 5MW, which is still operational off the shore of the island of Lolland in Denmark. They also constructed the first two large-scale OWFs, Horns Rev 1 (2002) and Nysted (2004) OWFs with total capacity of 160MW and 165.6MW, respectively.

In the last decade, majority of OWFs have been installed in shallow waters (5-8 m), while most of them were installed off the shores of Northern countries in Europe. There were two exceptions: the Beatrice project in 2007 that located off the Scotland coast and the Hywind project in 2009 that located off the Norway coast with water depths of 45 and 220 m, respectively (Blohm, 2010). The Beatrice project was the first offshore wind project that deployed more advanced foundation types with transitional technology water depths and the first OWF with 5 MW WTs. The Hywind project was the first installed full-scale project on a floating platform by utilizing 2.3 MW WTs. Currently, Europe is forerunner in offshore wind industry in both manufacturing and design. They have even installed OWFs faraway from shore and in deeper waters. By 2015, the average power rating of offshore WTs in European waters was 4.2 MW, while the average water depth and distance of OWFs to shore became 27.1 m and 43.3 km, respectively. The information about some of the installed European OWFs in the last decade is indicated in Table 2.1.

Table 2.1: Detailed information about OWFs in North Europe by June 2007 (Breton and Moe, 2009)

Name/location	Developer	Manufacturer	Turbines × rating (MW)	Depth (m)	Dist. to shore (km)
Built					
Beatrice/UK	Talisman energy Inc., Scottish and southern energy	REpower	2 × 5	45	25
Blyth/UK	AMEC/Shell/Nuon/powergen	Vestas	2 × 2	6–11	0.8
Barrow-in-Furness/UK	Barrow offshore wind Ltd	Vestas	30 × 3	21–23	7
Burbo/UK	DONG energy A/S	Siemens windpower	25 × 3.6	1–8	6.4
North Hoyle/UK	National windpower	Vestas	30 × 2	10–20	6
Scroby sands/UK	E.ON UK	Vestas	30 × 2	4–8	2.3
Kentish flats/UK	Elsam	Vestas	30 × 3	5	8.5
Arklow bank/Ireland	Airtricity	GE Wind	7 × 3.6	2–5	10
Q7-WP/Netherlands	Econcern, energy investments holding, ENECO energy	Vestas	60 × 2	20–24	23
Egmond ann Zee/Netherlands	Noordzee wind (Shell, NUON)	Vestas	36 × 3	19–22	10
Lely/Netherlands	ENW	Nedwind	4 × 0.5	5–10	0.75
Irene Vorrink/Netherlands	NUON*	NordTank	28 × 0.6	5	0.02
Ems-Enden/Germany	Enova	Enercon	1 × 4.5	3	0.04
Breitling/Germany	WIND-projekt GmbH	Nordex	1 × 2.5	2	0.5
Nysted/Denmark	Elsam/Elkraft/Energy E2	Bonus	72 × 2.3	5–9.5	10
Samso/Denmark	Samso Havvind A/S*	Bonus	10 × 2.3	20	3.5
Frederikshavan/Denmark	Elsam	Vestas, Bonus, Nordex	1 × 3 + 2 × 2.3	4	0.2
Ronland/Denmark	Two local cooperatives	Bonus/Vestas	4 × 2.3 + 4 × 2	1*	0.2*
Horns Rev/Denmark	Dong energy*	Vestas	80 × 2	6–12	14–20
Middelgrunden/Denmark	Kobenhavns Energi*	Bonus	20 × 2	3–6	3
Vindeby/Denmark	Dong energy*	Bonus	11 × 0.45	3–5	1.5
Tuno/Knob/Denmark	Dong energy*	Vestas	10 × 0.5	3–5	6
Yttre Stengrund/Sweden	Vindkompaniet	NEG-Micon	5 × 2	6–10	5
Utgrunden/Sweden	GE wind energy	GE wind energy	7 × 1.425	7–10	8
Bockstigen-Valor/Sweden		Windworld	5 × 0.5	6	3
Under construction					
Robin Rigg/UK	E.ON UK	Vestas*	60 × 3	3–21	9
Inner Dowsing/UK	Centrica	Siemens	27 × 3.6	10*	5
Lynn/UK	Centrica	Siemens	27 × 3.6	6–13	5
Alpha Ventus/Germany	E.ON Energy, EWE, Vattenval	Multibird-RePower	12 × 5	30	43–50
Lillgrund Bank/Sweden	Vattenvall AB, Nordic Generation	Siemens	48 × 2.3	4–8	7
Kemi, Ajos/Finland	PVO innopower Oy	WinWind	8 × 3		0.05–1
Planned					
Kish Bank/Ireland	Powergen Renewables/Saorgus/ESB		50 MW total*		
Rhy1Flats/UK	RWE npower	Siemens	25 × 3.6		8
Scarweather Sands/UK	E.ON UK/eEnergy E2		30 × 3		5–10
Gunfleet Sands/UK	GE Gunfleet Ltd.	GE	30 × 3.6	8*	7
Cromer/UK	Norfolk Offshore Wind		30 × 4	23*	7
Breedit-Mardyck Bench/Erance	Nord-Pas-de-Calais/Shell/TFE/Jeumont	Jeumont	8 MW total		
Vlakte van Raan/Belgium	Seanergy		20 MW total		
Thornton/Bank/Belgium	C-power	GE wind energy	60 × 5*	12–27.5	27–30
Jade/Germany	Winkra-Energie GmbH	Enercon	1 × 4.5	5	0.55
Butendiek/Germany	OSB/Bürger-windpark	Vestas	80 × 3	20	34
Sky 2000/Germany	GEO		100 MW total	−20*	17*
Mecklenburg-Vorpommern/ Germany	Neptun		40 MW total		
Skabbrevet/Sweden	Renewable energy/Cynergy global power		54 MW total		
Klasarder/Sweden	NEG-micon	NEG-micon	16 × 2.75*	7–11*	1.5*

Today, OWFs mostly install in water depths of up to 20-30 m and they largely utilize monopile technology (e.g., Horns Rev 1-2 in Denmark, Robin Rigg and Thanet in UK etc.) as well as several gravity-based structures (e.g., Nysted and Rodsand 1-2 in

Denmark etc.). However, by increasing WT size, the offshore wind industry moved to deeper waters, thus jackets/tripods uses in water depths of up to 50-60 m and over 60 m floating structures will be required. Figure 2.9 indicates the various structure types and their installed sharing in Europe by the end of 2013.

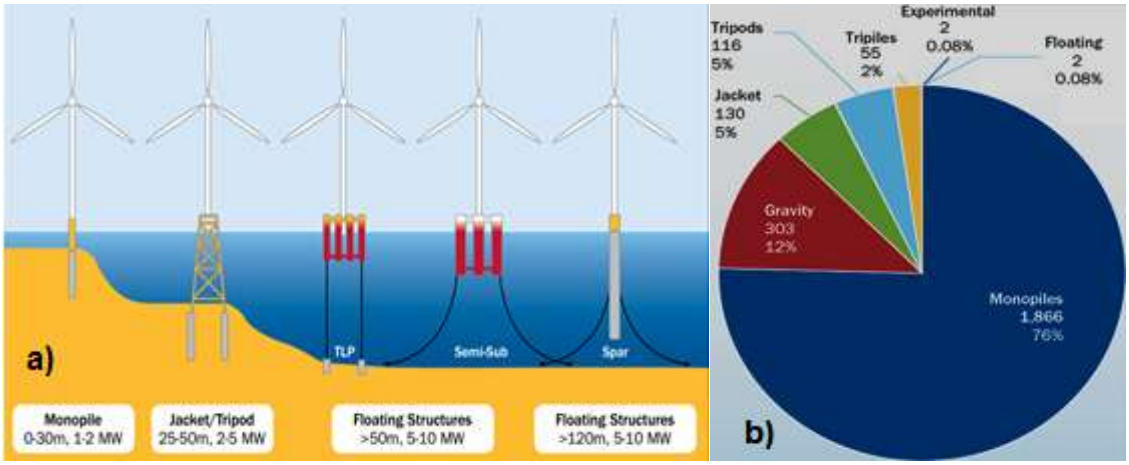

Figure 2.9: a) development of OWF foundation according to water depths (EWEA, 2013), b) share of installed structure type, by the end of 2013 (EWEA, 2014b).

An overview of the average water depth and shore distance is illustrated in Figure 2.10 for European OWFs. Figure 2.11 depicts the wind speeds average at 10 m above the sea in Northern Europe area, according to MERRA[2] dataset.

[2] Modern-Era Retrospective Analysis for Research and Applications in NASA

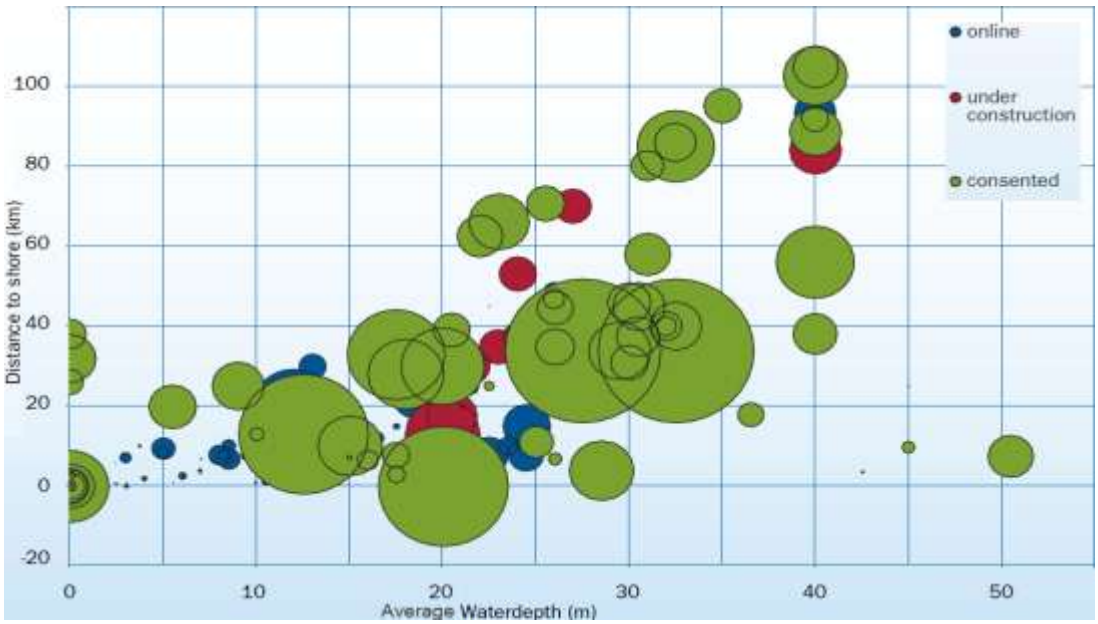

Figure 2.10: Average water depth and shore distance for under construction, constructed and online OWFs, where the capacities are represented by bubbles size (EWEA, 2014b)

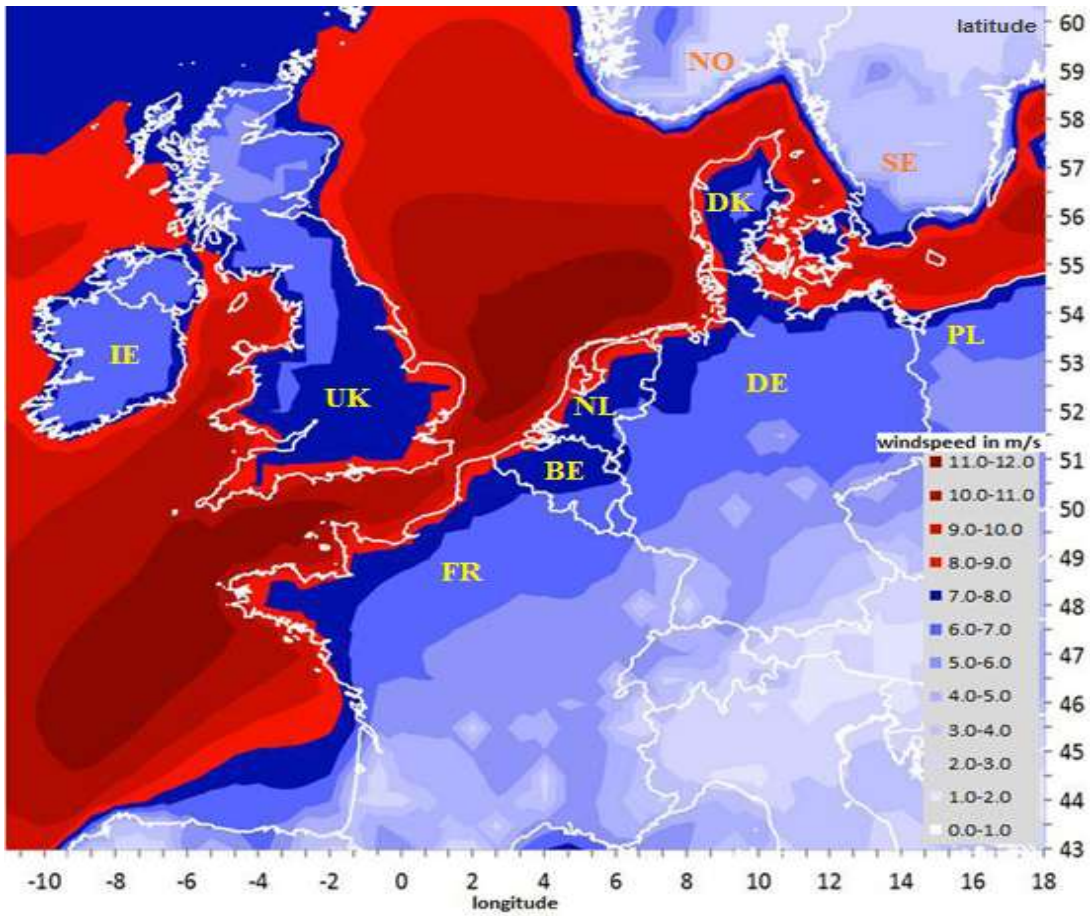

Figure 2.11: Wind speeds average at 10 m above the sea in Northern Europe area (Cole, 2014)

By increasing water depth, the higher foundation complexity and required resources below the waterline will come up; therefore the costs of OWF foundations will increase as well. Actually, water depths of over 25 m lead to a dramatic foundation costs increasing, in monopole and gravity-based. Consequently, floating WTs have been introduced to reduce the cost of foundation in deeper water, in order to take advantage of higher and more persistent wind flow, where WTs can be installed far away from the shore. The cost comparison between these three foundation methods with respect to water depth is indicated in Figure 2.12.

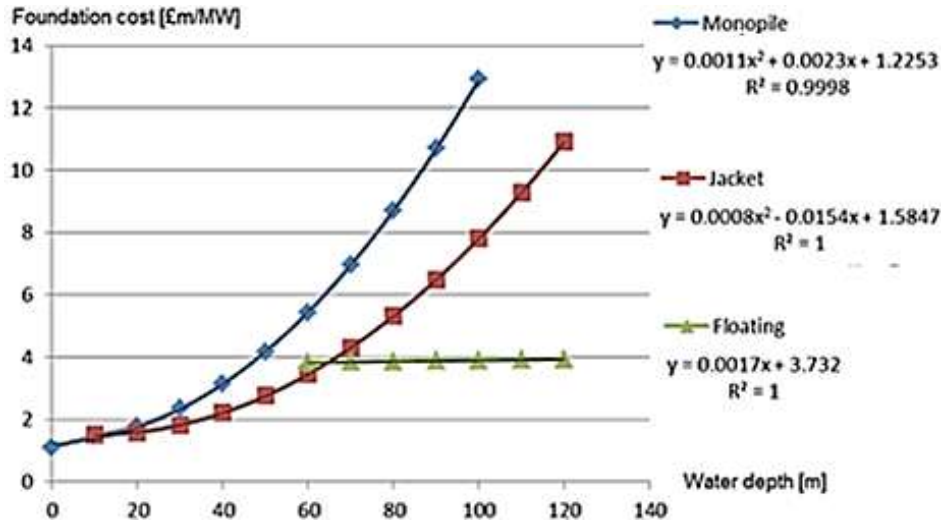

Figure 2.12: The foundation cost of OWFs with respect to water depths, steel price of $3200/Ton and exchange rate of £1 = $1.6

According to higher hub height in greater power rating (particularly for offshore WTs), the evaluation of average wind speed above the sea level should be converted from 50 m to 100 m, by logarithmic wind characteristic above the water.

The time series of yearly wind speed in a typical OWF area as well as its respective generated output offshore wind power are presented in Figure 2.13, where they almost fluctuate together.

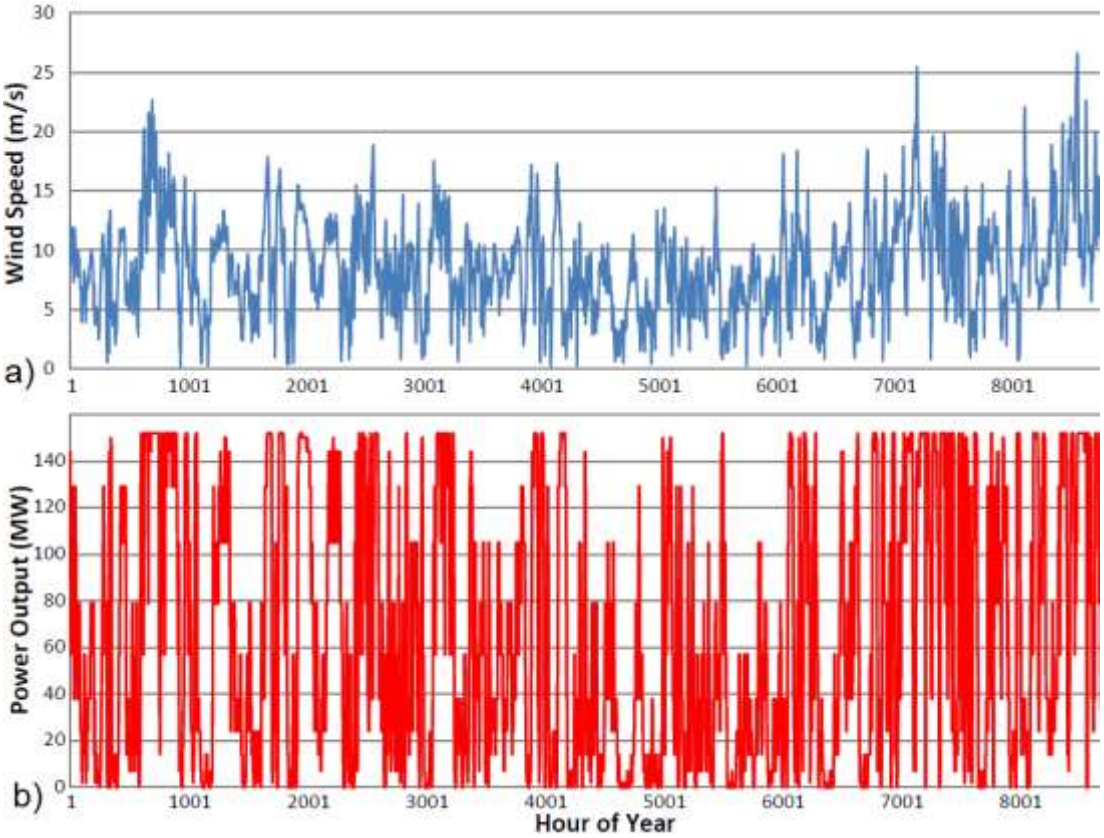

Figure 2.13: Time series of wind speed (a) and respective generated output wind power (b) in a typical OWF area in a typical OWF area, according to MERRA dataset (Cole, 2014).

Currently, Dong Energy has been the largest OWF owner/developer, while they cumulatively constructed 26% of European installation by the end of 2013; Siemens is the lead supplier for offshore WT, whereas they manufactured the majority of the total installed capacity of OWFs in Europe. By the end of 2014, their share has been increased to 65.2%, in term of MW installed capacity. The cumulative share of OWF owner/developer and WT manufactures in Europe are illustrated in Figure 2.14, by the end of 2013.

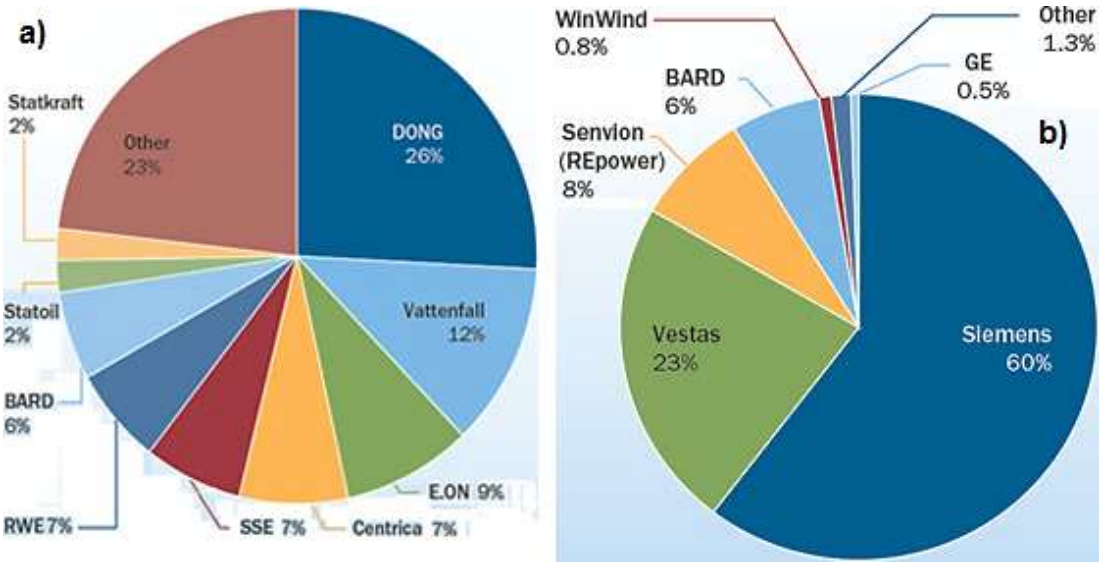

Figure 2.14: Cumulative share of OWF owner/developer (a) and offshore WT manufactures (b) in Europe, by the end of 2013 (EWEA, 2014b).

Figure 2.15 indicates new installation procedure to minimize the shipping and assembling cost by using only one vessel for several WTs in OWFs far away from the shore as well as shows typical 5 MW offshore WT.

a)

b)

Figure 2.15: a) Installation technique by using one vessel in long distance OWFs, and b) Close shot of nacelle of a 5MW offshore WT

2.5 Real Cost of Offshore Wind Energy

In order to analyze the total economy costs and benefits of energy production fairly, comparing OWF vs. the alternatives only with LCoE is not a complete and justly measure. LCoE [€/MWh] can be calculated as follows (Siemens, 2014a):

$$\text{LCoE} = \frac{CAPEX + \sum_{y=1}^{LT} \frac{OPEX}{(1+i)^y}}{\sum_{y=1}^{LT} \frac{AEP}{(1+i)^y}} \qquad (2\text{-}1)$$

where, i is interest rate, LT lifetime of the energy source, AEP the annual energy production, $CAPEX$ the capital expenditure and $OPEX$ the operational expenditure, which include the Operation and Maintenance (O&M) fuel and CO_2 cost.

The real costs of energy can be revealed by Society‘s Costs of Electricity (SCoE). For example, decreasing house prices near the onshore wind farms or power planets is one of social costs. In addition, it is expected that the LCoE of OWFs will decrease according to development of offshore wind technology and optimization tasks as well as increase in CO_2 price, due to recent global efforts to decrease greenhouse gas emissions. Hence, OWF competitively parallel with onshore wind technology will be a significant primary power supply as a renewable energy by 2025. Comparison of different level of LCoEs and SCoE is depicted in Figure 2.16 between Nuclear, Coal, Gas, Photovoltaic (PV), Onshore Wind and OWF power supplies in Germany. These costs might be different in other countries as Figure 2.17 indicates the UK projection (with details) for LCoE and SCoE of all these primary power supplies.

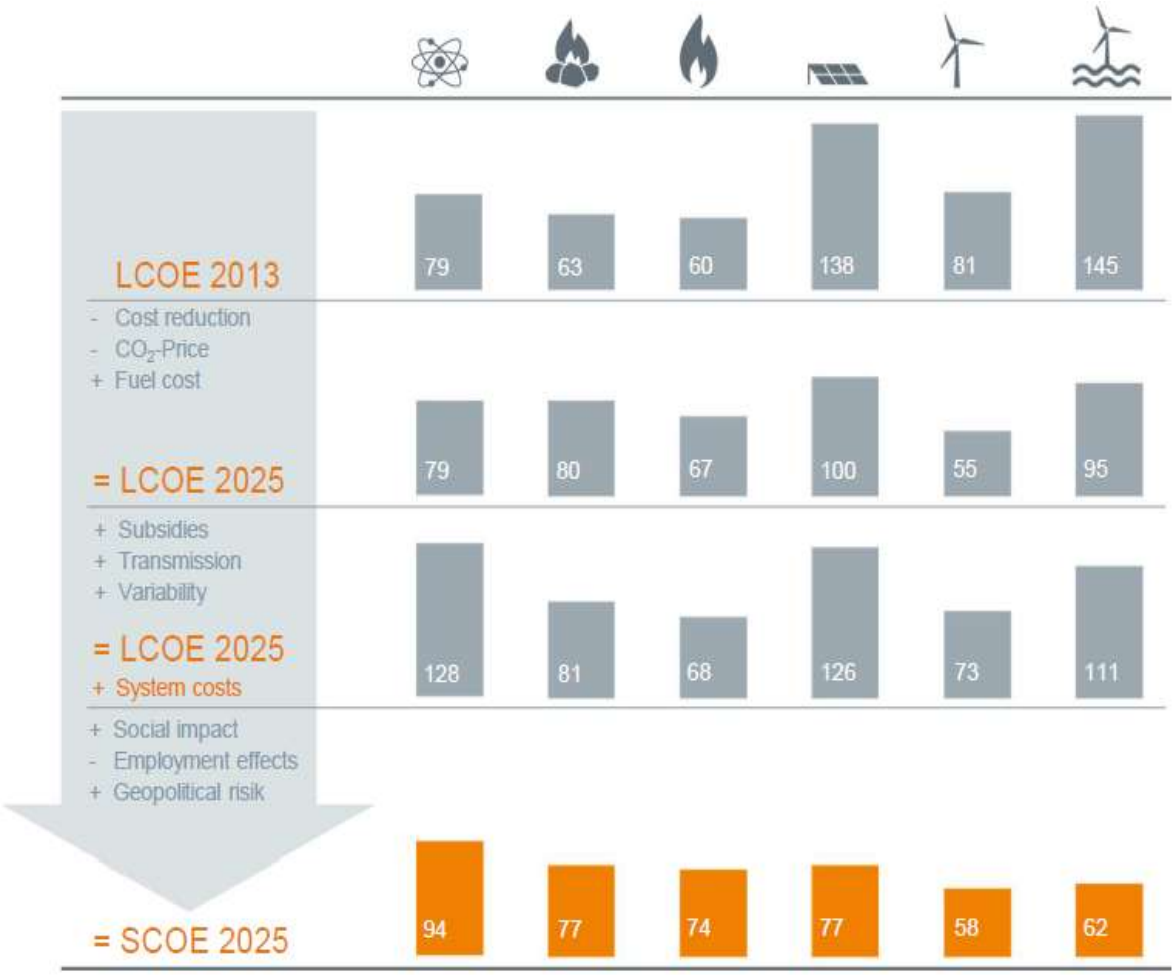

Figure 2.16: German Projection to compare the LCoE and SCoE by 2025, (Siemens, 2014b).

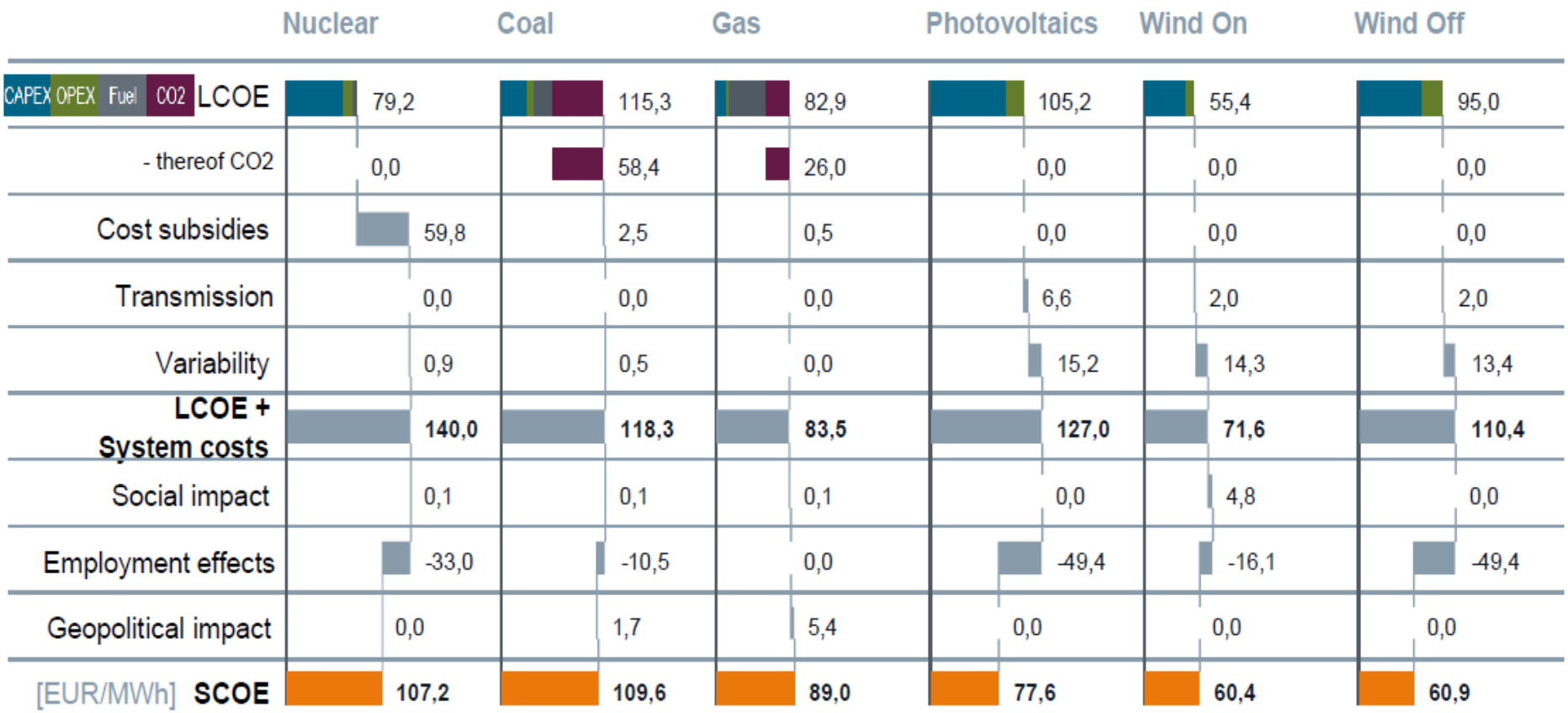

Figure 2.17: UK Projection for 2025 to compare the LCoE and SCoE, average scenario (Siemens, 2014a).

The cost of OWF also needs to become more competitive. Cost reduction can be likely achieved by WT development and investment in research as well as optimization in supply chain, operations and maintenance.

In 2013, two outstanding projects have reached financial close: the “Butendiek” project in Germany, as well as refinancing of Masdar’s stake in the largest worldwide OWF project installed in the UK, the “London Array” project (EWEA, 2014b).

2.6 Wind Turbine Technologies

The control concepts and basic technology of WTs in both off- and on-shore installations are rather the same. Majority of the generators typically have relatively LV levels of 400-690 V due to voltage limitations of power electronics devices and safety regulations. Therefore, high current flowing through long cables induces significant power loss and high cost of complex cooling systems in the high-power WTs. In order to cope with increasing power loss and cabling costs, a step-up transformer is required to interface with a medium voltage (MV) network, which is typically 25-40 kV. The generator is placed in nacelle on the top of a tower and usually the converter systems as well, but the step-up transformer could be located in the base or nacelle of the tower. Table 2.2 lists some advantages and disadvantages of different location for additional electrical system (power converter and/or transformer) in a WT.

Table 2.2: Advantages and disadvantages for location of WT electrical components

electrical components location	Advantage	Disadvantage
Top of tower (in nacelle)	- Lower cable cost - Lower power loss	- Limited availability for maintenance - Higher mechanical stress and vibration due to wind load hitting
Base of Tower	- Fast availability for maintenance - lower weight nacelle	- Higher cable cost - Higher power loss

The weight of installed components in the nacelle directly influences mechanical and structure design as well as their costs to decide about their location.

In order to use the great potential of wind in offshore area, higher power rating of WTs is developing to achieve the main cost reductions of OWFs in term of LCoE. Figure 2.18 shows a comparison and WT development between on- and off-shore wind farms, while the blades size are compared visually with Airbus 380 and football field. Additionally, increasing the portion of higher power rating WTs is shown in Figure 2.19.

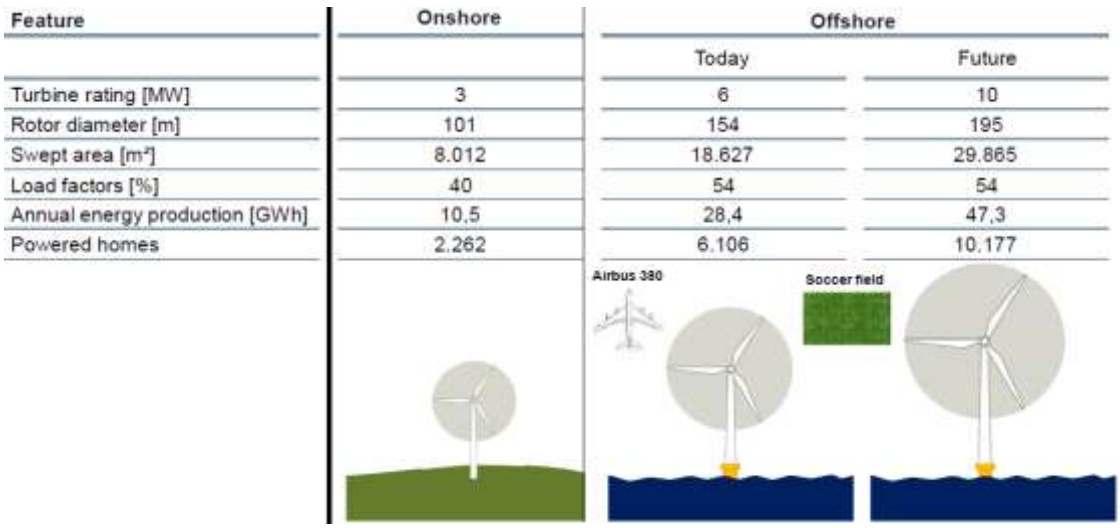

Figure 2.18: WT development in on- and off-shore technology (Siemens, 2014a)

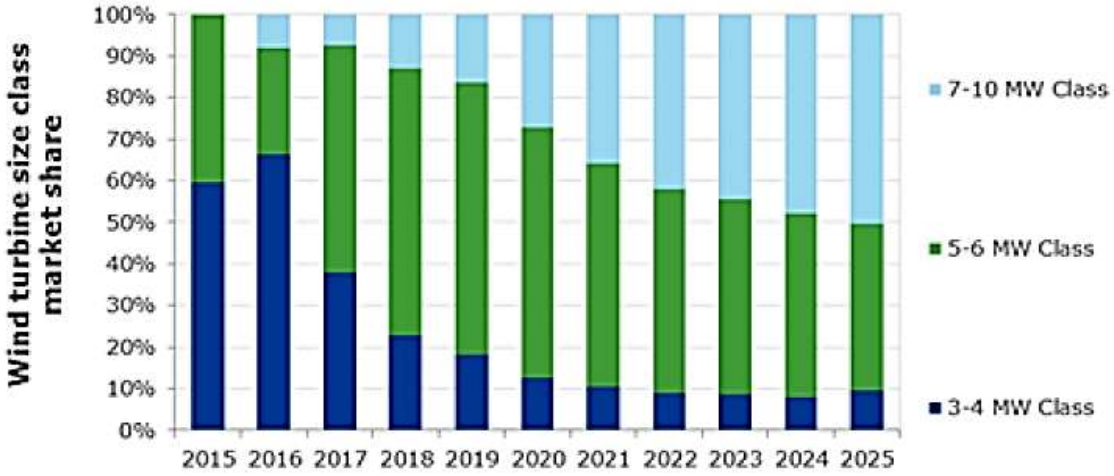

Figure 2.19: Increasing the power rating of WTs for OWFs and their portion in market

The power curve of WTs from various companies that have been manufactured for OWFs are shown in Figure 2.20, where their rated wind speed is started in range of 12-15 m/s. Recently, MHI-Vestas has manufactured WTs with power rating of 8MW (V164-8MW) to be installed in OWF project in UK, 19 km off England's northwest coast.

Wind turbines typically generate power at a voltage of 690 V, up to 1 kV AC. A transformer located either in the nacelle or at the bottom of the tower steps the voltage up to either 11 kV or 33 kV. The power from the wind turbines is transmitted at to an offshore substation, which increases the voltage for transmission to shore. In an HVAC transmission system, a typical transmission voltage to shore is 132 or 220 kV, which can be connected directly to the electricity grid or stepped-up at an onshore substation if it is to be connected at 400 kV. Alternatively, where the distance or transmitted power is high, the AC voltage can be converted to DC by an HVDC converter on the offshore platform and then converted back to AC by a HVDC converter located onshore.

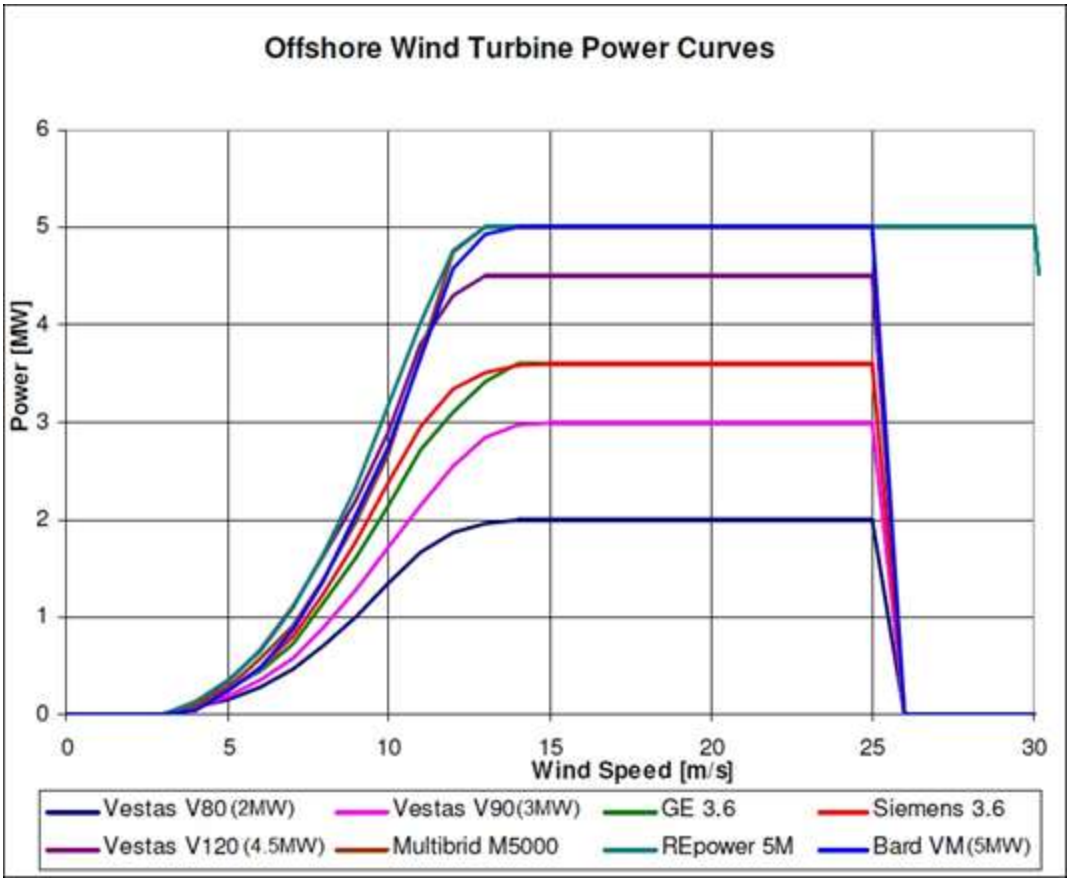

Figure 2.20: Overview of power curves of offshore WTs (Schoenmakers, 2008)

The typical energy conversion systems of exist WTs that using in OWFs are Doubly-Fed Induction Generator (DFIG), Squirrel-Cage Inductive Generator (SCIG) and Permanent Magnet Synchronous Generator (SCIG). SCIG and PMSG conversion systems are used for variable speed operation and DFIG system is partially used for variable speed operation. Where, DFIG system is assumed in this thesis. Figure 2.21 illustrate the configuration of these energy conversion systems (a and b) as well as two different arrangement of step up transformer and other electrical components inside the WT tower.

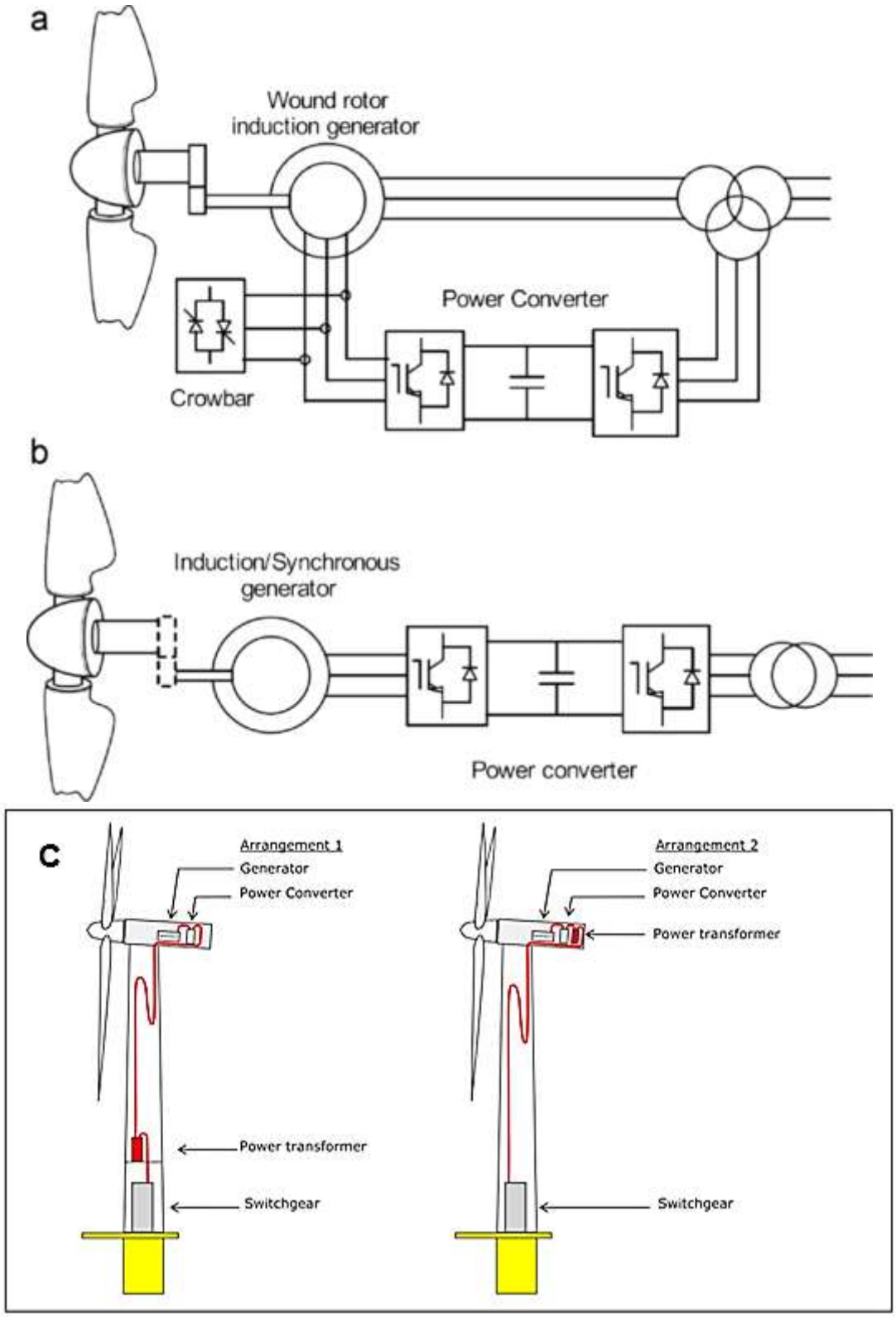

Figure 2.21: Energy conversion systems of exist WTs. a) DFIG in partially variable speed operation, b) SCIG and PMSG in variable speed operation (Madariaga et al., 2012) and c) various arrangement of step up transformer and other components inside WT tower.

2.7 Electrical Connection System of OWFs

There are two tasks about electrical connection of OWFs: the transmission system from OWF to the onshore grid and the electrical interconnection system between WTs inside the OWF. The offshore power transmission system and laying offshore submarine cables have had several experiences in oil and gas industries as well as telecom system. High Voltage AC (HVAC) and DC (HVDC) compete in OWFs to transmit the generated power to the main onshore grid, however the HVDC transmission system is not considered in this thesis. Nevertheless, electrical interconnection system has never been applied in any offshore industry, before offshore wind industry.

The generated power of WTs is collected into the Offshore Substation (OS) or Central Collection Point (CCP) by utilizing Medium Voltage (MV) AC cables, which can be extended to onshore grid directly in very close OWF projects.

2.8 Power Transmission System

Majority of installed OWFs are using HVAC cables to connect the collected power at offshore substation to an onshore substation. HVAC system has yet been the dominant transmission technology as it is cost effective solution, since most of current OWFs are relatively close to the shore (in the range of 20-60 km). However, development of OWFs is moving further offshore and longer cables required. Thereby, HVDC system becomes viable alternative due to distance limitation and higher reactive losses in HVAC cables. Since cable-based HVAC transmission systems (currently, the only available technology in AC system) has higher capacitive nature than overhead lines.

2.8.1 HVAC Transmission System

HVAC has been the standard technology for onshore power transmission system; step up/down voltage transforming is easy for the required level of voltage; it is a cheap technology and it has proved its reliability. HVAC has also been used to link different large-scale OWFs to the main onshore grid. Additionally, its reliability under offshore conditions has been proven (i.e. moist and salty conditions). All these advantages make HVAC a suited technology for the grid connection of OWFs. The main drawback of HVAC transmission line is the generated reactive power by HVAC cables (capacitive line), which limits the maximum transmission distance due to the limitation in maximum transmission of active power. The active and reactive power flow over a transmission line is given by well-known Eq. (2-2). In addition, by increasing the overall reactance of transmission line (X_{line}) the reactive power losses will be increased as well.

$$P=\frac{|V_1|.|V_2|}{X_{\text{line}}}\sin\delta \qquad \rightarrow \qquad \downarrow P_{\max}=\frac{|V_1|.|V_2|}{\uparrow X_{\text{line}}} \tag{2-2}$$

$$Q=\frac{|V_1|^2-|V_1|.|V_2|.\cos\delta}{X_{\text{line}}} \tag{2-3}$$

The critical distance is defined while the flowing injected reactive current reached to half of the nominal current of the HVAC cable. Therefore, for long HVAC transmission cable complex or simple compensation equipment is indispensable, which should also be controlled to avoid system instability. Figure 2.22 depicts the relation between maximum transmitted power and admissible distance at various voltage levels (132, 220 and 400 kV) with respect to two compensation methods: compensation only onshore side (100%) and at both ends (50%-50%).

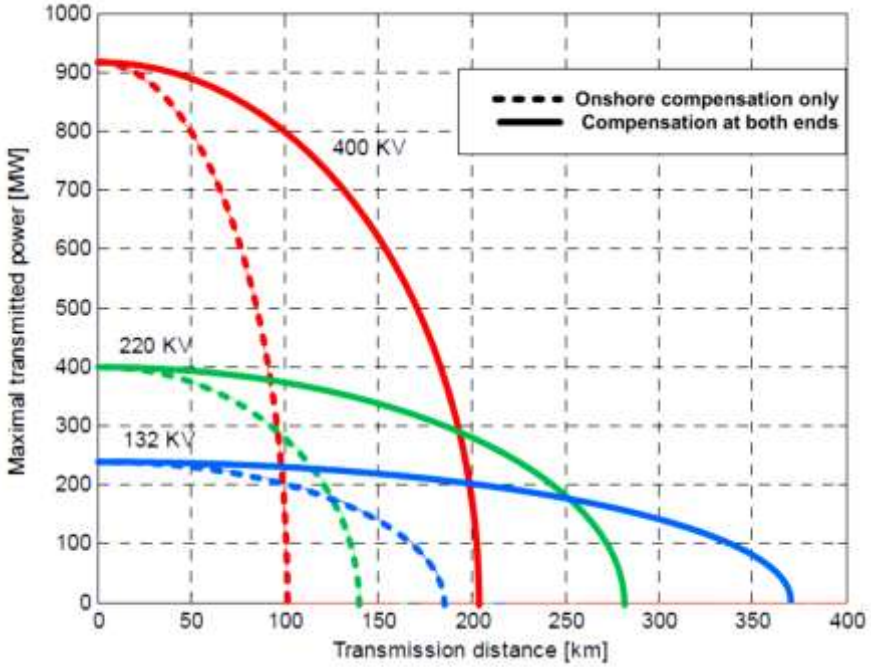

Figure 2.22: Critical distances offshore HVAC cable with respect to various compensation and voltage levels (Baring-Gould, 2014)

Nevertheless, the maximum distance of these curves (touching distance axis) are not feasible, due to relevant zero transmitted power. According to following equation, higher voltage level clearly increases the maximum transmitted power of the cable (by identical cable cross section), while the reactive charging current is relatively increased. Hence, the critical/admissible distance is decreased (Schoenmakers, 2008).

$$I_{\text{charge}} = \frac{U}{\sqrt{3}} \times 2\pi f \times C \times L \qquad (2\text{-}4)$$

Where, C is the cable capacitance per phase in each km that is given by submarine cable manufactures in the datasheet [F/km], f the system frequency [Hz], U the nominal voltage [V] and L transmission line distance [km].

2.8.2 HVDC Transmission System

HVDC transmission system can offer zero reactive charging current as well as reactive losses, since the alternative frequency could be zero or negligible in an appropriate DC system. In addition, HVDC system is useful to increase system reliability during the fault with higher voltage stability and it allows providing a connection between two grids with different frequency or asynchronous operation. In HVDC system with identical transmission capacity, the cost of transmission cables itself less than the HVAC, because of absence of skin effect. However, the cost and loss of HVDC substations (both off- and on-shore) are much higher, because additional high voltage convertor systems are required in both sides (AC to DC, then back again). Hence, the HVDC can only dominate the HVAC in transmission systems with long distance, where higher transmitted power and lower losses in cables is a big advantage for HVDC transmission system, however the HVDC transmission system is not considered to compete with HVAC transmission system in this thesis.

A “brake-even” distance can be defined between cable-based HVAC and HVDC system; Figure 2.23 illustrates their cost comparison with respect to distance as well as the brake-even distance.

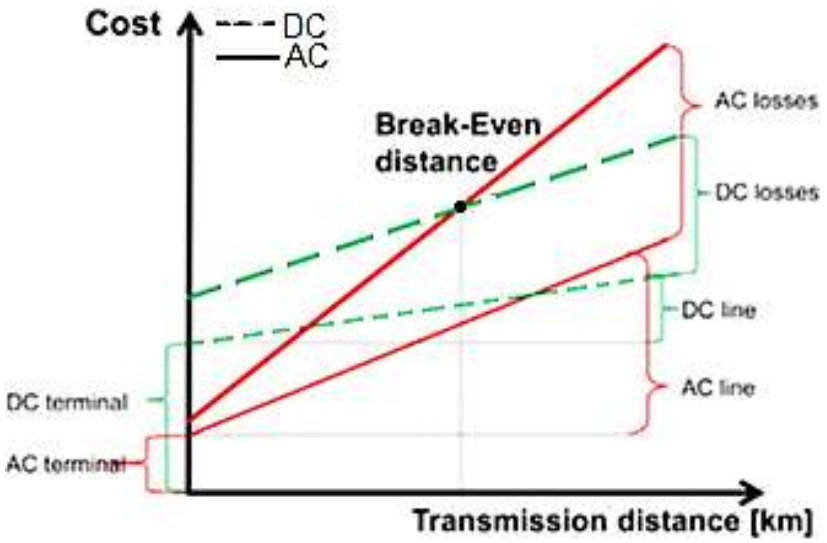

Figure 2.23: Comparison between HVAC and HVDC cable to find Break-Even distance

Therefore, according to the distance to the shore, the generated power of OWF can be transmitted with any conventional AC or DC high voltage technology. Actually, no certain break-even distance or identical range has been defined, whereas the nominal transmitted power is an influencing factor as well. Nevertheless, most literature approximately defined between 45 and 95 km in average, moreover a decision formula is empirically defined (Ergun et al., 2012) to find the break-even distance:

$$L_{\mathrm{DC}} = \max\{\, 40 \,,\, \min\{200 \,,\, 832.5 \times P_n^{-0.4}\} \,\} \qquad (2\text{-}5)$$

where, P_N is the transmitted power and L_{DC} the break-even distance, thus every OWF with 200 km and no OWF with less than 40 km distance to the shore are recommended to use HVDC transmission system.

In this regard, the HVDC transmission system promises a very flexible and efficient technology for offshore wind farms because no reactive power is generated/consumed by DC transmission cables.

LCC-HVDC is known as traditional (classical) HVDC, is a mature technology that just uses thyristors and requires an existing AC line to commutate. About 100 small and large worldwide projects have been already installed, while the largest one is a ±800 kV of LCC-HVDC transmission line with distance of 2000 km and power rating of 7.2 GW. Many important and large projects have been implemented with LCC-HVDC as the efficiency is very high, usually 97-98% including the conversion at both end of the link. Thyristors can stand large currents and voltages with lower cost and loss compare to other power semiconductors. Generally, it operates around ±400 kV, but according to large breakdown voltage in the thyristors the nominal voltage can even be to ±800 kV (Ultra HVDC). Since thyristors can only be turned OFF when their current flowing becomes zero, LCC system has less controllability and phase difference between voltage and current. Hence, the whole LCC-HVDC transmission system demands large reactive power that should be compensated by capacitors. Moreover, some other supplementary equipment is required e.g. DC smoothing reactors and AC (as well as DC) filters at both ends convertor substations as well as control and telecommunications system etc. A simple diagram of LCC-HVDC transmission system has been indicated in Figure 2.24.

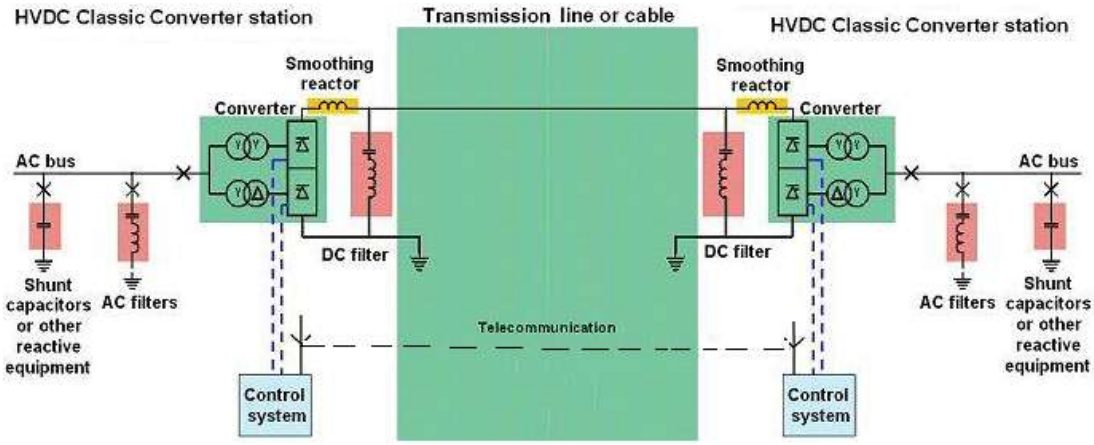

Figure 2.24: The diagram and components of a LCC-HVDC transmission system (ENTSOE, 2011)

As LCC-HVDC system depends on a strong external AC grid on the normal operation, in case of failure in AC grid the LCC system will fail as well (Schoenmakers, 2008). In spite of high efficiency and low loss of LCC system, there are some important drawbacks to be used at offshore substation: voluminous and the expensive required supplementary equipment; e.g. the transformers should be specially designed with higher level of winding insulation due to DC offsets and higher leakage impedance as well as capable of withstanding abrupt DC voltage change and harmonics. In addition, a back-start diesel generator is necessary in case of failure in order to transmit the initial voltage signal for normal operation of LCC system. Therefore, LCC-HVDC technology has not been yet implemented as offshore transmission system (Lancheros, 2013).

VSC-HVDC technology utilizes Insulated Gate Bipolar Transistors (IGBTs) as self-commutating semiconductors, which can be switched OFF and ON several times by using Pulse-Width Modulation (PWM) technique as signal control. IGBT rating in current and voltage level have been increased up to 2 kA and 4.5kV per device, respectively; Parallel and/or series connection are required for each switching valve to increase its rating current and voltage, respectively. Moreover the power loss for both switching and conduction has reduced to even 1% and switching frequencies is nominally about 2 kHz, which can lead to lower current harmonic insertion and decrease AC filter size (Lancheros, 2013). VSC technology initially constructed for low and medium voltage (e.g. motor drives), by using lower level of power switches. Adopting IGBTs could enter this technology to the high range of voltage (up to ±500 kV). Currently, only ABB and Siemens companies are delivering VSC-HVDC technology to the market (ENTSOE, 2011). The diagram and components of a simple two-level VSC-HVDC transmission system is depicted in Figure 2.25.

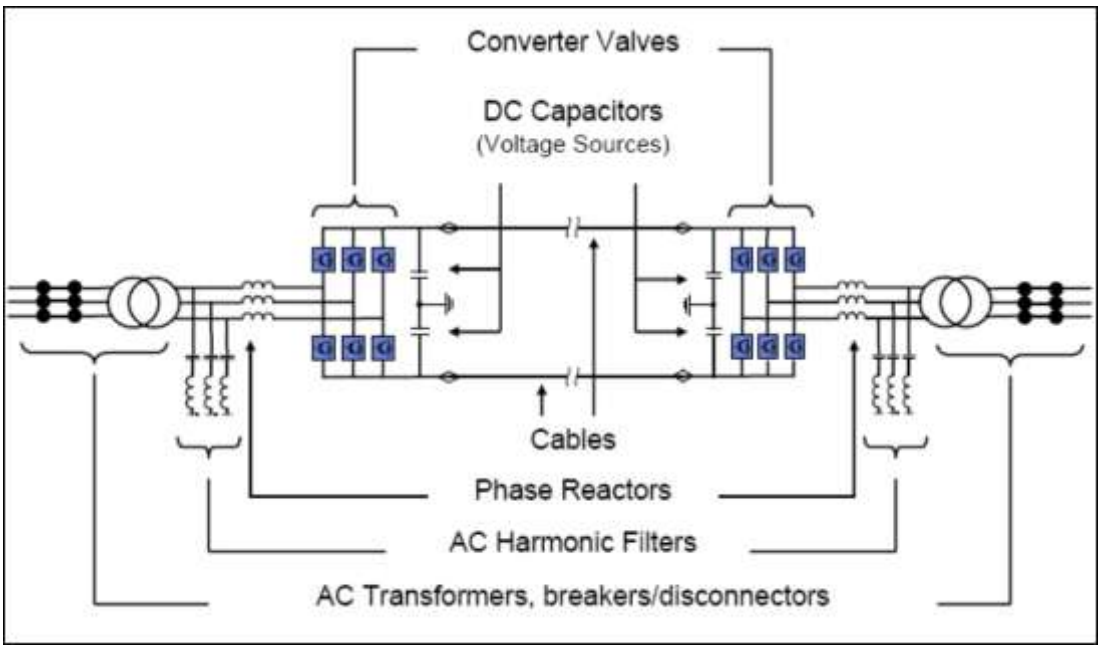

Figure 2.25: Simple diagram and components of a two-level VSC-HVDC transmission system (Schoenmakers, 2008)

The DC capacitors by acting as an energy store, helps to reduce the voltage harmonics ripple on the DC side and minimize any voltage variations under dynamic condition by disturbances on the AC side. The harmonic filters (50% smaller than LCC-HVDC filter size) eliminate the AC harmonics that created because of the high-frequency switching of IGBTs. The three-phase series reactor is a voluminous air-cored coil to help controlling the active and reactive power flow. It also acts as a low pass filter of AC wave form and limits any possible short circuit current.

Furthermore, VSC technology can rapidly control reactive and active power flow independently without any additional compensation equipment. Continuous and fast control of reactive power in VSC-HVDC transmission system improves voltage stability and transferring capacity of the AC grids at the both ends, while it is not depends on AC grid. VSC-HVDC system can also support weak AC networks or even start non-energized networks. Since, it can separately control frequency and

voltage variation in the AC side by controlling active and reactive power flow independently (Schoenmakers, 2008). Hence, VSC-HVDC technology could be a suitable alternative for long distance offshore transmission system. In order to control the frequency and amplitude of the AC output voltage independently, various VSC topology (e.g. two-level, three-level, etc.) have been so far implemented. The higher converter level leads to less switching frequency and filtering necessity in order to achieve lower power loss and perfect sinusoidal AC, respectively. General control system for VSC-HVDC is shown in Figure 2.26.

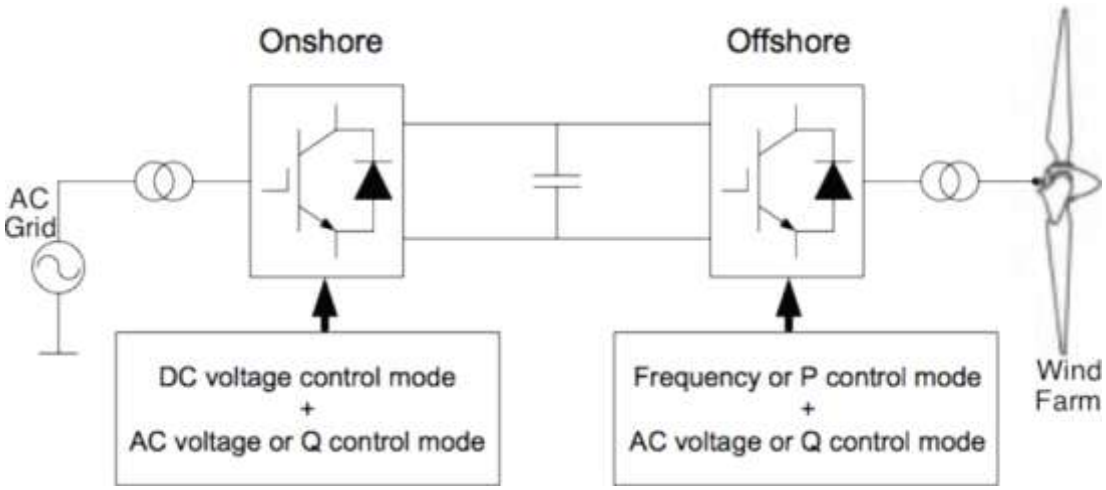

Figure 2.26: General control system for VSC-HVDC

Table 2.3 compares various issues of these two commercially available technologies for OWF usage to illustrate the advantages and disadvantages HVAC and VSC-HVDC transmission technologies.

Table 2.3: Comparison between HVAC and VSC-HVDC technologies for OWF usage (Schoenmakers, 2008)

	HVAC	HVDC VSC
Voltage levels	132 kV, 150 kV, 220 kV	±150 kV, ±300 kV
Maximum transmission capacity per cable system	190 MW at 132 kV 215 MW at 150 kV 310 MW at 220 kV	740 MW at ±150 kV 1480 MW at ±300 kV
Type of cable used	XLPE Three phase offshore Single phase onshore	XLPE Single phase both offshore and onshore in bipolar systems
Transmission capacity distance depending	Yes, reactive power compensation required	No
Black start capability	Yes	Yes
Fault contribution	Yes	Low compared to HVAC
Technical capability for network support	Limited, additional systems required for voltage and frequency support	Large range of possibilities for voltage and frequency support
Space requirement offshore substation	Small Relative volume 1	Large Relative volume 2.5 - 3
Modularity possible	Yes	Yes
Redundancy	High in case of multiple cables	Low compared to HVAC due to high transmission power of single bipolar system

The first installed (in 2009) VSC-HVDC offshore transmission system was BorWin1 in order to link BARD 1 OWFs (inaugurated in 2013) that is located off the shore of North-West Germany. The distance of HVDC transmission line was 200 km (125 km submarine and 75 km land) with power rating of 400 MW at ±150 kV.

Nevertheless, the HVDC solution is not considered for transmission system in this thesis. Because, the main optimization of connection for OWFs has been applied for interconnection system and HVAC link with single or parallel line transmits the generated power to the main grid.

2.9 Electrical Interconnection System

In order to collect the generated power of WTs to an OS all electrical interconnection systems are currently based on Medium Voltage (MV) AC cables (typically 33 kV). However, new researches are also conducting on scenarios with DC series interconnection system, which is not considered in this study since it just used for OWFs with HVDC transmission system.

The proposed project for Cape Wind OWF contains 130 WT with 3.6 MW power rating. The maximum capacity is designed for 545 MW in 62 square kilometers, as it has been shown in Figure 2.27. The location of proposed OWF is 7.6 km away from Cape Cod shore, Massachusetts (Blohm, 2010). Figure 2.28 and Figure 2.29 show two real OWFs with typical radial and mixed configuration.

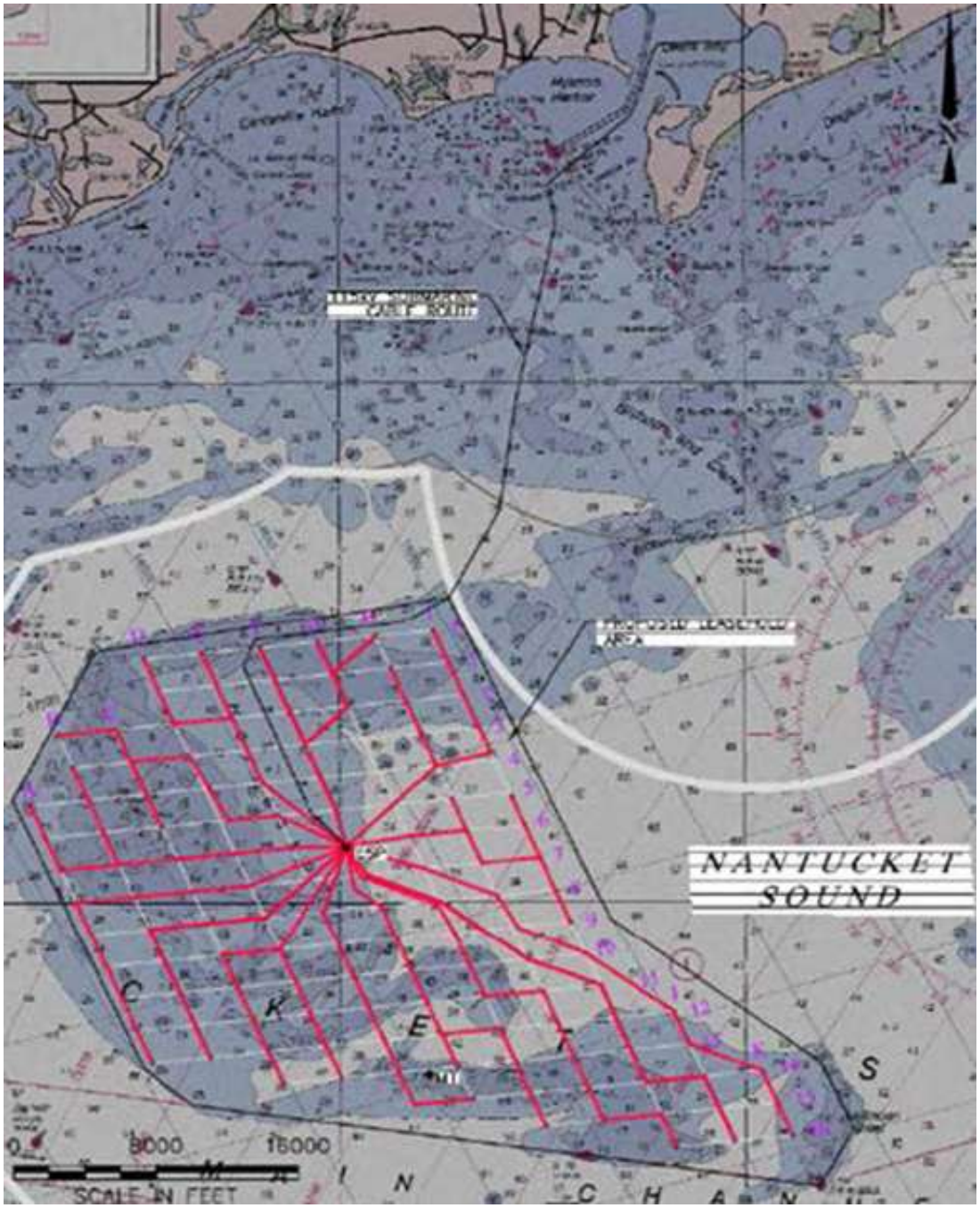

Figure 2.27: Proposed layout of Cape Wind OWF, Massachusetts State (Blohm, 2010)

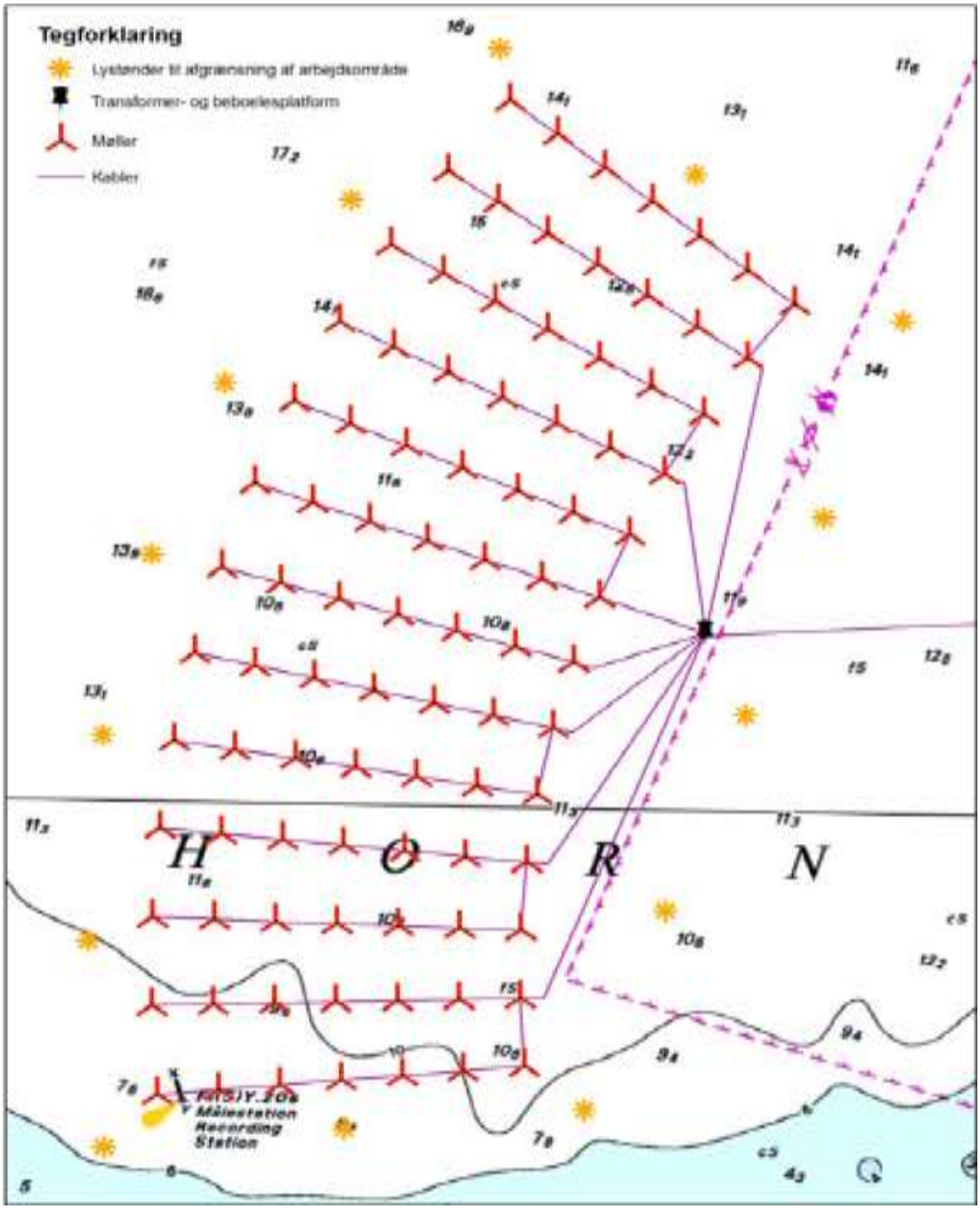

Figure 2.28: Layout of Horns Rev 2 Wind Farm (Baring-Gould, 2014)

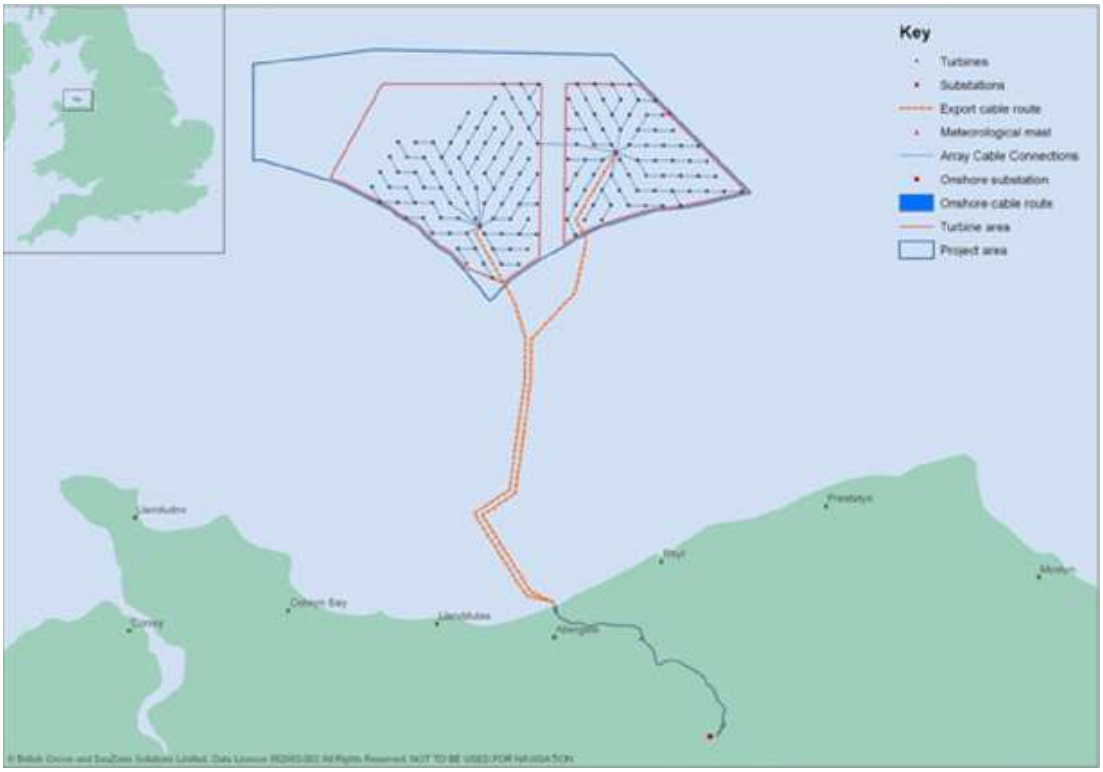

Figure 2.29: Electrical interconnection and transmission systems of an OWF (Madariaga et al., 2012)

2.9.1 Installation of Submarine Cables

Installation of any submarine/subsea cable (transmission or interconnection system) is a challenging operation, which requires specific expertise and equipment. Submarine cables should be installed by cable laying vessel. The vessels are mostly equipped with a turntable (carousel) to store the submarine cable to be installed. Moreover, the cable should be buried to avoid possible damage from fishing gear, or anchors, etc. Subsea cables are typically buried between 1.5 and 3 meter blow the seabed. Usually, laying and burying subsea cables are simultaneously accomplished either by utilizing a cable laying vessel and a plough. If the time of burying process may take longer than laying or burying close to WT's foundation, they are accomplished in two-stage process: first subsea cables are laid on the seabed and then a water jetting machine can provide a trench to fall the subsea cable into the assigned depth. In order to install transmission cables utilizing a large capacity of

cable laying vessel and its turntable are required to lay subsea cables as long as possible in order to avoid an extra subsea connections. While just few expertise companies and limited vessels are currently available to install subsea cables. The largest available can carry about 70 km or 7000 tonnes high voltage subsea cable (BVG, 2010). Nevertheless, cutting the cables in interconnection system of a wind farm is inevitable, due to joining tree cables under each WT (after the first WT of each cluster), thus smaller with lower cost can be utilized.

Submarine cables are supported with more robust armoring and tested mechanically in order to withstand both compressive and tensile forces during installation according to vessel motion. Hence, sophisticated tools are utilized to predict and minimize the risks after surveying the seabed geology and other relevant parameters.

Cut section of a three-phase HVAC submarine power cable (132 kV) together with fiber optic is shown in Figure 2.30.

Figure 2.30: Three-phase copper core HVAC submarine power cable (132 kV) together with fiber optic, Prysmian manufacture

The cost of shipping and burying per meter are varies greatly with respect to several environmental and practical parameters in each individual OWF (e.g. seabed geology, distance to shore, burial depth, the OWF size, etc.). Since no detailed costs information has been found in the published resources. They have been usually considered all as constant value, summation of shipping and burying. In different references, rang of 150-1000 $/m is assumed for *Csb* of Medium Voltage (MV) cables (Dahmani et al., 2015; ENTSOE, 2011). The required equipment to lay and bury the subsea cable is shown in Figure 2.31.

a)

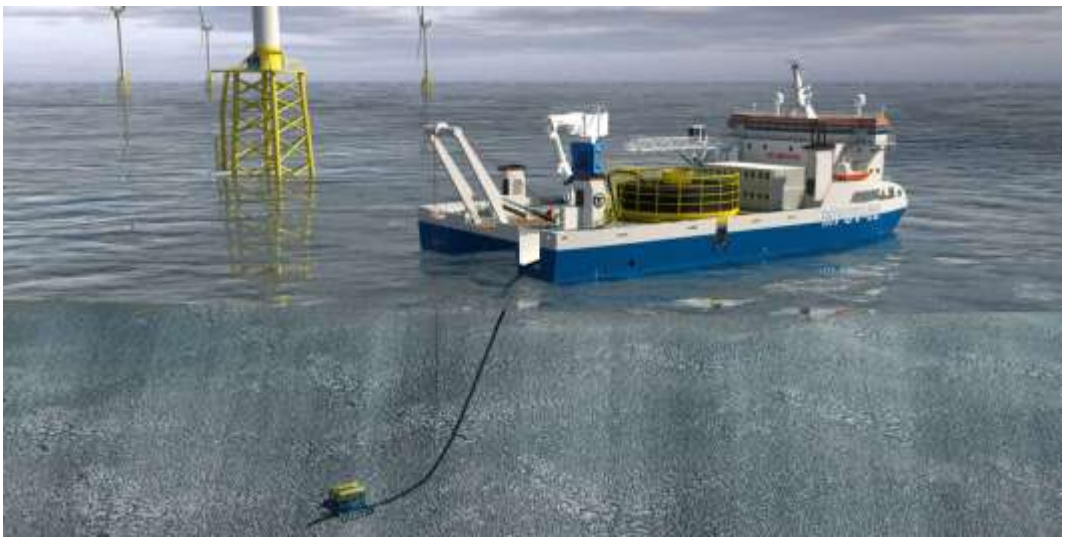

b)

c)

Figure 2.31: a) the cable laying vessel, b) turntable (carousel), and c) burying plough

Chapter 3

THE OPTIMIZATION PROBLEM AND FORMULATION

3.1 Introduction

In order to minimize the investment and operational costs, this thesis proposes an optimization formulation to find the optimal electrical interconnection configuration of Wind Turbines (WTs) and the optimal cable sizing simultaneously. In addition, the optimal layouts of interconnection and transmission systems as well as rating of other relevant components are found simultaneously in the second case study. The simultaneous consideration of all components is significant to find the optimal electric system layout of an OWF.

Including corresponding cost of cables cross sections into the objective function causes variable cost branches (edges) for each individual solution, thus creating an extremely complex and inherently intractable discrete optimization problem. Generally, these optimization problems can be regarded as a class of complex combinatorial problems that cannot be mathematically modeled, and be solved with analytical optimization algorithms or they may result in a local optimal solution. Therefore, metaheuristic optimization techniques (e.g. GA) would be required to solve such complex problems.

This simultaneous minimization of total trenching length and cable cross sections creates a complex discrete optimization problem that is solved by the Harmony

Search (HS) algorithm, as a metaheuristic optimization technique. Because of the inherent discrete characteristic of HS algorithm, it has been chosen to solve this completely discrete optimization problem. Finding the optimal layout of transmission system and other relevant components are also discrete problems. However they are not as complex as finding the optimal layout of interconnection system.

3.2 Computational Complexity of the Optimization Problem

The simultaneous optimal electrical interconnection configuration and cable sizing of an OWF as a discrete optimization problem is rather similar, but harder than both the Traveling Salesman Problem (TSP) and optimizing pipe diameters in the Water Distribution System (WDS) problem. It is harder, because the traveling cost of each individual road (branch) in the TSP is constant, and the network configuration in the WDS problem is given according to urban design restrictions. In fact, simultaneous optimal pipe diameters design and configuration of system network in a WDS problem have never been optimized. This simultaneous optimization problem was defined as an extremely complex optimization problem (Dan et al., 2007). Note that, these two well-known discrete optimization problems are also non-smooth and non-convex problems. Thereby, they are defined as NP[3]-complete problems (Chu et al., 2008; Yun et al., 2013). However, finding the simultaneous optimal configuration and cable sizing of an OWF without any clustering method can be embedded in the category of NP-hard or at least NP-complete problem (Gonzalez-Longatt et al., 2012).

[3] NP stands for Nondeterministic Polynomial time, which means that the problem can be solved in Polynomial time only by using a Non-deterministic Turning machine. In addition, NP-Hard and NP-Complete is a way of showing that certain classes of problems are not solvable in realistic time. In order to compare the difficulty of problems: NP-hard ≥ NP-complete ≥ NP ≥ P

On the one hand, the complexity and the number of possible solutions for the optimal electrical interconnection configuration problem generally increases dramatically with factorial factor of the number of optimization variables. However, by an intuitive engineering insight, it can easily be understood that most of the possible power flow directions cannot comprise an optimal power flow path. Hence, a generalized sub-algorithm has been developed to reduce the search space of a given topology OWF, according to the location coordinates of WTs and OS with respect to each other (either symmetric or asymmetric topology of OWF). The proposed reduction sub-algorithm identifies only the feasible connecting nodes (either WTs or OS) to each individual WT with acceptable paths to the OS location. Nevertheless, any unlikely but feasible connecting nodes have been considered in the decision set. Only the paths between WTs in opposite of OS direction are not included into the decision set. Thereby, the number of feasible solutions for interconnection configuration problem can be reduced from $N!/2$ to $\prod_{i=1}^{N} k_i \cong \overline{K}^N$ (exponential-time problem), where N is the number of WTs (optimization variables), k_i is the number of feasible choices in the decision set of i^{th} WT (usually it is found that: $1 \leq k_i \leq 7$) and $\overline{K}$ represents an approximate average value of k_is among all WTs. On the other hand, adding cable sizing to the problem increases the problem complexity by an exponential-time factor. Number of possible solutions for the cable sizing problem is m^N, where m is limited to the number of available cable cross sections (for example only three choices in partial cable sizing). The ampacity and required cable cross section of each individual branch can easily be determined after finding the interconnection configuration of each individual solution.

3.3 Harmony Search (HS) Algorithm

Heuristic optimization algorithms mimic natural phenomena such as biological evolution in Genetic Algorithms (GA), physical annealing in Simulated Annealing (SA), human/animal memory in Tabu Search (TS) and Particle Swarm Optimization (PSO). Geem at el., (2001) conceptualized the Harmony Search (HS) algorithm as another artificial phenomenon from the musical process of searching for a perfect state of harmony such as jazz improvisation.

HS algorithm is a new heuristic optimization method and has been used to tackle various optimization problems in discrete and continuous space successfully (Wang et al., 2010). The capability of solving complex and discrete optimization problems was demonstrated by finding the most proper solution in TSP and WDS in comparison with GA and other analytical optimization methods (Geem at el., 2001; Geem, 2006; Yun et al., 2013).

The steps in the HS algorithm procedure are as follows:

step 1. Initialize a Harmony Memory (HM).

step 2. Improvise a new harmony from HM or random.

step 3. If the new harmony is better than the worst harmony in HM, include the new harmony in HM, and exclude the worst harmony from HM.

step 4. If stopping criteria are not satisfied, go to Step 2.

An HM with Harmony Memory Size (HMS) of four, shown in Figure 3.1, is a memory location where all the solution vectors and their corresponding fitness values are stored. This HM is similar to the genetic pool in the GA. Consider a jazz trio

composed of fiddle, saxophone and keyboard (three optimization variables). Initially, the memory is stuffed with four random harmonies vector: (C,E,G), (B,D,A), (C,F,A), and (B,D,G) that are sorted with their corresponding aesthetic estimation. Every note in HM has the same opportunity to be selected. In the improvising procedure, three instruments produce a new harmony; for example, (C,D,A).

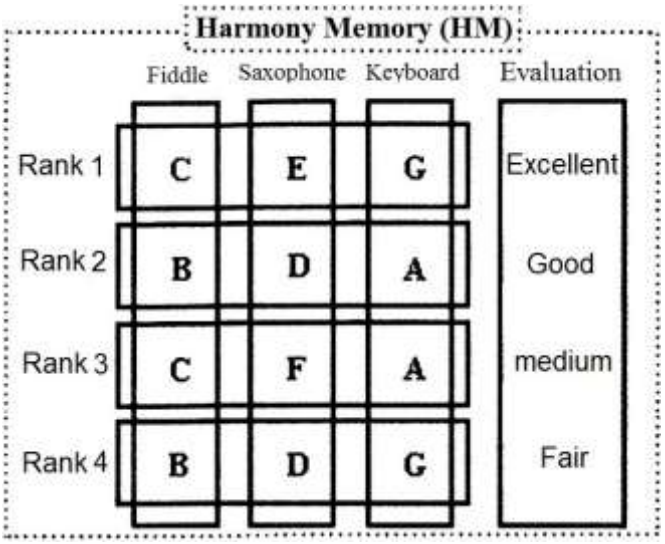

Figure 3.1: Structure of Harmony Memory (Geem at el. 2001)

If evaluation of the new harmony vector is better than the worst harmony (4^{th} rank) in HM, then the new harmony is included into the HM and the worst harmony is excluded. After ranking the HM again, this process is repeated until satisfying results according to the stopping criteria are obtained. (Geem at el., 2001; Geem, 2006).

There are two other parameters that should be considered in improvisation steps: Harmony Memory Considering Rate (*HMCR*) and Pitch Adjusting Rate (*PAR*). The *HMCR* and *PAR* parameters help HS algorithm to find improved solutions globally and locally, respectively. Improvising procedure of a new harmony for each variable (musical note) in HS is based on the following three rules (Geem, 2006):

1) random selection with probability of (1- *HMCR*),

2) HM consideration with probability of *HMCR*,

3) if #2 has happened, extra pitch adjustment can be applied with probability of *PAR*.

The pitch adjustment value should be assigned with a limited bandwidth (*bw*). Hence, according to the defined *bw*, a local search around the optimum point can be provided. The improvisation process is defined as follows:

for $i = 1 : N$

if $rand1 < (1 - HMCR)$

$X_{new}(i) = LB(i) + [UB(i) - LB(i)] \times rand$

elseif $rand1 \leq HMCR$

$r = \text{randi(HMS)}$

$X_{new}(i) = HM(r , i)$

if $rand2 \leq PAR$

$X_{pitch1}(i) = X_{new}(i) + rand \times bw$

$X_{pitch2}(i) = X_{new}(i) - rand \times bw$

end

end

end

where, N number of variables, $randi(\text{HMS})$ a function to create an integer random value between 1 to HMS; *rand*, *rand*1 and *rand2* are various random values with uniform probability between 0 to 1; $UB(i)$ and $LB(i)$ are the upper band and lower band for i^{th} variable.

By applying pitch adjustment, three new harmonies might be generated for i^{th} variable $\{X_{new}(i),\ X_{pitch1}(i),\ X_{pitch2}(i)\}$, thus the one with minimum fitness value will be chosen. Note that, in order to assign the pitch adjustment value a random value between 0 to *bw* is applied in continuous optimization problems (continuous variable), while in discrete optimization problems the *bw* and the selected random value should be integer.

Since the optimization variables in this optimization problem are the node index, the numbers of choices as integer variables are limited and changed nonlinearly. Hence, the pitch adjustment value for improvisation process is applied from the values in HM, while an integer random value with limitation of *bw* is applied to the node index. In addition, the random new harmony is generated by selecting a random value from the decision set (B_i). The improvisation process for this discrete problem is defined as follows:

for $i = 1 : N$

if $rand1 < (1 - HMCR)$

$r1 = \text{randi}(length(B_i))$

$X_{\text{new}}(i) = B_i(r1)$

elseif $rand1 \leq HMCR$

$r = \text{randi}(\text{HMS})$

$X_{\text{new}}(i) = \text{HM}(r, i)$

if $rand2 \leq PAR$

$X_{\text{pitch1}}(i) = \text{HM}(r + \text{randi}(bw), i)$

$X_{\text{pitch2}}(i) = \text{HM}(r - \text{randi}(bw), i)$

end

end

end.

Recommended ranges for parameter value are 0.7-0.95 for *HMCR* and 0.05-0.7 for *PAR*, according to the frequently used values in other HS applications. Besides, according to the number of optimization variables, HMS value of 10-100 is recommended (Geem, 2006).

Under investigation in this study, the HS parameters are assumed as follows:

- Harmony Memory Size (HMS) = N (number of discrete variables),
- Harmony Memory Considering Rate (*HMCR*) = 0.7 - 0.95,
- Pitch Adjusting Rate (*PAR*) = 0.1,
- Discrete bandwidth (*bw*) = 1,
- Maximum number of iterations = $2N \times 10^3$;

where, a variable *HMCR* has been used that it increases with the rate of 0.0001 from 0.7 to 0.95 per iteration.

3.4 Mathematical Formulation of the Optimization Problem

In this study, the simultaneous optimal electrical interconnection configuration and cable sizing of OWFs minimizes the trenching length and cable cross sections of a given topology. In order to minimize the investment and operational costs, the proposed optimization formulation considers both cable cost as well as the sum of shipping and burying costs (*Csb*), as a significant influencing term in this optimization problem.

Csb varies greatly with respect to several environmental and practical parameters in each individual OWF (e.g. seabed geology, distance to shore, burial depth, the OWF size, etc.). In this study, if practical detailed costs are provided, even a variable *Csb* can be applied, i.e. different value of variable *Csb* can be considered for each individual choice (according to its corresponding seabed condition) of the discrete decision set (B_i). However, similar to all recent studies in the literature a constant value for *Csb* has conventionally been considered. In different references, an extensive range of 150-1000 $/m is assigned for *Csb* of Medium Voltage (MV) cables (Dahmani et al., 2015; ENTSOE, 2011). In case of adopting the proposed formulation in on-shore wind farms, laying cost itself with other additional limitation (e.g. land unavailability or other practical restrictions) can be considered as a variable cable installation cost instead of a constant cost for each individual choice of the discrete decision set (B_i).

Due to the significant influence of *Csb,* two methods of cable sizing are proposed as distinct scenarios. The methods are defined as follows:

a) **Full cable sizing:** the cable cross section of each branch is assigned individually according to its ampacity.

b) **Partial cable sizing:** limited number of cable cross section is considered to be available in the decision set (three available cross sections in this study). Moreover, cable cross sections of all branches on each route are identically assigned according to the ampacity of last branch before joining another route or connecting to the OS.

Note that, due to the existence of MV switchgears and junction terminals (at least three cables) below every WT, cutting the subsea cable is inevitable in electrical interconnection of wind farms, thus connecting different cable cross sections in full cable sizing method can be possible. However, changing in cable cross section or utilizing more choices in the decision set of cable cross sections may increase *Csb* practically. Thereby, a method of partial cable sizing is also proposed in this study.

For integration of all WTs, during the evolutionary optimization process the WTs could be clustered randomly according to the maximum ampacity of the largest cable cross section, with different shapes and sizes in any iteration. Note that, no specific clustering method is applied before solving the optimization problem. Thereby, in this complex optimization problem, only a small difference may occur between fitness values of the global optimal and local solutions, where it may change the shape and size of clusters as well as the corresponding cable cross section of several paths. Therefore, escaping from local optimum solutions and finding the global optimal solution would be very difficult in a large problem, even with metaheuristic optimization algorithms. In fact, including the cable costs into the objective function creates variable cost branches for each individual solution, thus a complex, non-convex and non-linear optimization problem is formed. Hence, before running the optimization algorithm, the reduction sub-algorithm identifies the discrete decision set (B_i) of the interconnection configuration problem for each individual WT (i^{th}). The sub-algorithm can identify B_i either for symmetric or asymmetric topology of the OWF, while the location coordinates of all WTs and OS are considered as given input data. After that, the OS location coordinates is considered to be set at the

origin. In addition, every WT in its decision set has a chance to be connected to the OS directly, while B_i consists of k_i feasible choices that are found as follows:

$$B_i = \sum_{\substack{n=1 \\ n \neq i}}^{N+1} \delta_n \,.\, n \qquad \forall \; i \in \{1, 2, \ldots, N\} \tag{3-1}$$

$$\text{S.t.} \quad \sum_{n=1}^{N+1} \delta_n = k_i \qquad \forall \; \delta_n \in \{0,1\}$$

where, i is WT (optimization variable) index, n the node (either WTs or OS) index, N the number of WTs, k_i the number of choices in the decision set for i^{th} WT, N+1 represents the OS index, δ_n is a binary variable [0, 1] that is assigned 1 if nth node is a feasible choice according to the reduction sub-algorithm to be selected in the decision set, otherwise zero.

$$\begin{cases} \delta_n = 1 & |\mathrm{Re}(loc_i)| > |\mathrm{Re}(loc_n)| \text{ or } loc_n = loc_{N+1} \\ \delta_n = 0 & \text{otherwise} \end{cases} \tag{3-2}$$

where, loc_i and $loc_{\boldsymbol{n}}$ are Cartesian location coordinates of i^{th} WT and its n^{th} feasible choice, respectively ($loc_i \in \mathbb{C}$).

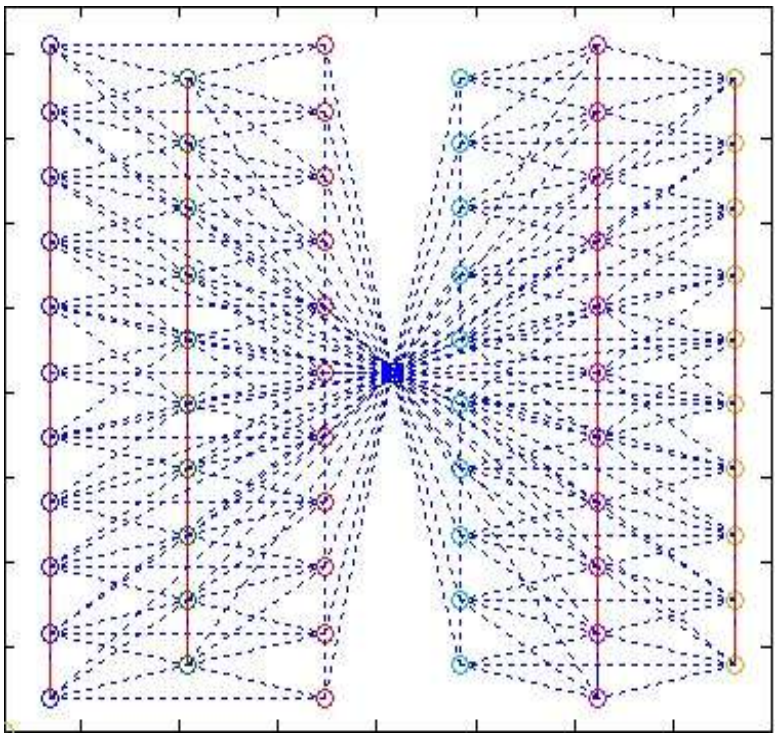

Figure 3.2: All feasible choices (B_i s) of an 11*6 OWF with semi-symmetric rectangular topology that found from reduction sub-algorithm

Figure 3.2 shows all identified feasible choices that directed to the OS, after applying the reduction sub-algorithm for an OWF (11*6) with semi-symmetric rectangular topology. Dotted lines are one-direction feasible choices and the red vertical lines represent two individual choices in both directions between two nodes.

The optimization variable of the electrical interconnection problem (y_i) is the index of the next connected node to i^{th} WT. The value of this optimization variable can be chosen among the discrete decision set of i^{th} WT (B_i) with k_i choices.

$$y_i = \sum_{x=1}^{k_i} \beta_x \,.\, B_i(x) \quad \forall\, B_i \subseteq \{1, 2, \ldots, N, N+1\}, \quad i \notin B_i \tag{3-3}$$

$$\text{S.t.} \sum_{x=1}^{k_i} \beta_x = 1 \qquad \forall\, \beta_x \in \{0,1\}$$

where, x is the choice index of the decision set and β_x is a binary variable [0, 1] that is assigned 1, if x^{th} choice of the decision set is chosen randomly, otherwise 0.

In order to represent an iterative output solution for the interconnection configuration problem an *N*-length vector (*Y*) has been defined as Eq. (3-4) for all WTs.

$$Y = \{y_1, y_2, \dots, y_N\}, \quad y_i \neq i \tag{3-4}$$

Since a fixed voltage is assumed for all nodes, no power flow analysis is required for the interconnection system. Thereby, after finding the interconnection configuration and assigning y_is, the ampacity of each branch (I_{i,y_i}) between i^{th} WT and y_i^{th} node is just determined analytically by the Network Flow method, according to the injected current of each WT (I_G):

$$I_{i,y_i} - \sum_{j=1}^{N} \sigma_{j,i} \cdot I_{j,i} = I_G \qquad \forall\, i, j \in \{1, 2, \dots, N\} \tag{3-5}$$

$$\text{S.t.} \quad I_{i,y_i} > 0 \qquad \forall\, y_i \in \{1, 2, \dots, N, N+1\}, \quad y_i \neq i$$

where I_G is the injected current by each WT, $I_{j,i}$ is the ampacity of connected branch from former WT (j^{th}) to i^{th}, $\sigma_{j,i}$ is a binary variable [0, 1] that represents the branch connection between i^{th} and j^{th} WTs; is assigned 1 if such a connection exist, otherwise 0.

$$\begin{cases} \sigma_{j,i} = 1 & y_j = i \\ \sigma_{j,i} = 0 & y_j \neq i \end{cases} \tag{3-6}$$

In the full cable sizing method, the assigned cable cross section (cs_i) of each branch is found individually with respect to its ampacity (I_{i,y_i}) for each particular

configuration. In the partial cable sizing method, the number of cable cross sections in the decision set is limited (three available cross sections in this case) and the cable cross sections of all branches of each route are assigned according to the ampacity of last branch before joining another route or connecting to the OS for each particular configuration.

$$cs_i = \sum_{d=1}^{m} \lambda_i(a_d) \,.\, a_d \qquad \forall\, cs_i \,,\, a_d \in \mathrm{A} \tag{3-7}$$

$$\text{S.t.} \sum_{d=1}^{m} \lambda_i(a_d) = 1 \qquad \forall\, \lambda_i \in \{0,1\}$$

where, d is the element index of the set of available cable cross sections (A), m number of available cross sections in the set of subsea cables, a_d cross section of d^{th} element, cs_i the assigned cable cross section for i^{th} WT, $\lambda_i(a_d)$ a binary variable [0,1] of i^{th} WT that represents d^{th} cable cross section index, assigned 1 as defined in Eq. (3-8), otherwise 0.

$$\begin{cases} \lambda_i(a_d) = 1 & I_{d-1}^{\max} < I_{i\,,\,y_i} \leq I_d^{\max} \\ \lambda_i(a_d) = 0 & \text{otherwise} \end{cases} \tag{3-8}$$

where, $I_d^{\max}$ is the admissible ampacity of d^{th} index of cable decision set. In order to represent another iterative output solution for cable sizing problem, second N-length vector (CS) has been defined as follow:

$$CS = \{cs_1,\, cs_2, \ldots, cs_N\} \tag{3-9}$$

Table 3.1 shows the output vectors (Y and CS) of an individual solution corresponding to the optimal solution of the first case study of this study

(Figure 4.2). Due to space limitations, instead of all 63 WTs, only the output vectors of the first eleven WTs are depicted.

Table 3.1: Part of output vector of an individual solution

Index (i)	1	2	3	4	5	6	7	8	9	10	11
Y(y_i)	2	3	14	5	16	5	17	7	8	9	10
CS [mm^2]	50	50	95	50	95	50	300	185	95	50	50

Figure 3.3 provides a flowchart of the optimization algorithm in HS algorithm (or GA). Three penalty terms are applied in this optimization process (cable crossing, looping and overloading), so that if any of following penalty terms are flagged that solution is eliminated.

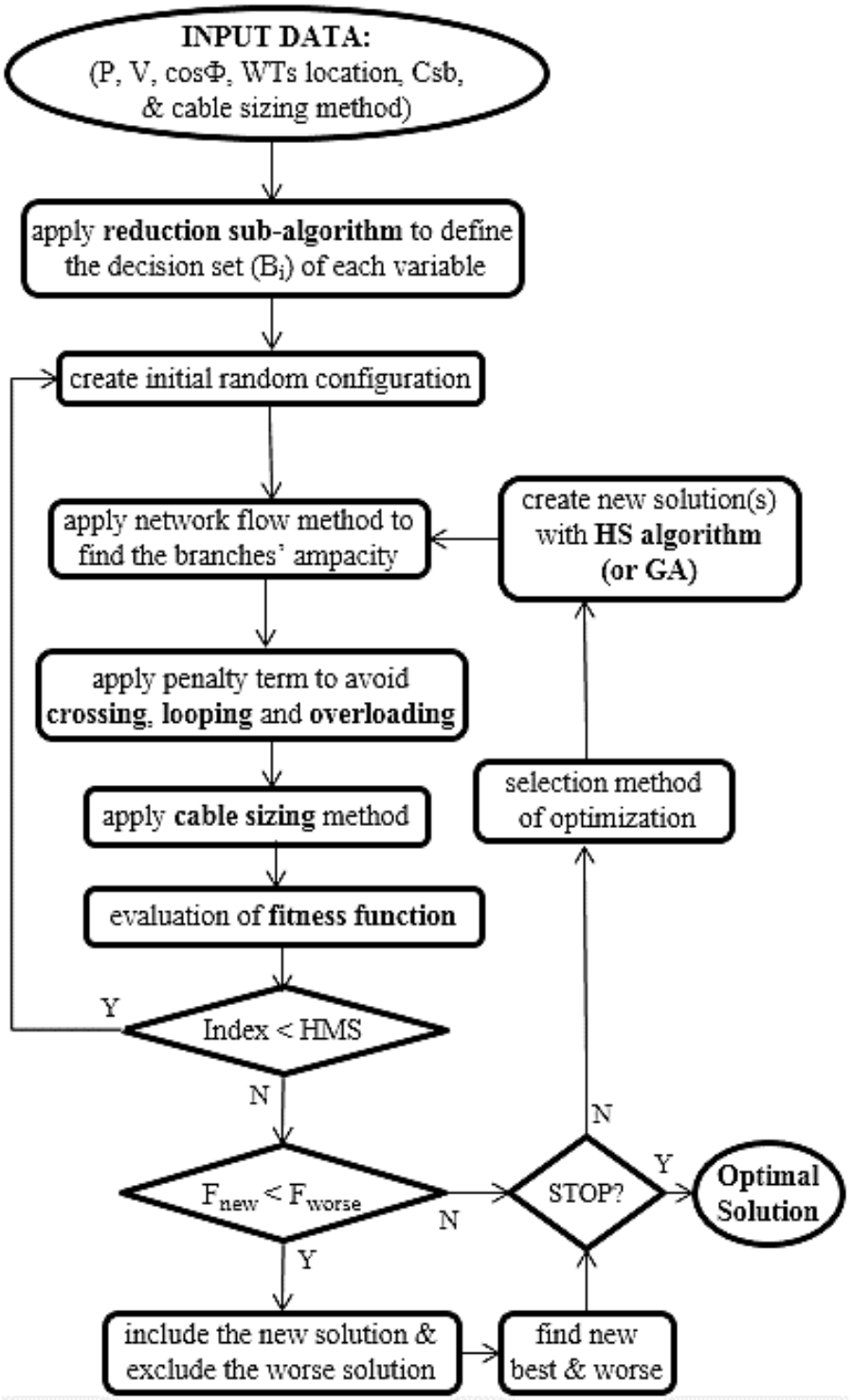

Figure 3.3: Flowchart of the optimization algorithm

1) Cable crossing: In this study, both crossed edges (branches) have the chance to be selected individually. Before running the optimization process, the joint of every two-edges that may cross are detected and stored in a set. After that,

during the optimization process, cable crossing can be detected in a solution, if any of those two-edges appears together.

2) Looping: A loop can be detected by comparing the total generated power of WTs and the summation of gathered power of all clusters into the OS.

3) Overloading: When the ampacity of a branch is higher than the admissible ampacity of the largest available cross section of subsea cables, overloading can easily be detected.

For the GA, a roulette wheel selection and k_i-based encoding method have been used, where k_i is the number of choices for each individual optimization variable, which may not be a constant value. Therefore, both GA and HS algorithms are dealing with integer values and various numbers of choices for each individual optimization variable, according to the discrete decision set (B_i). In order to improve the performance of GA multipoint crossover with random splice points has been considered, while mutation probability and population size are assumed as 0.1 and *N*, respectively.

3.5 The Objective Function

Our proposed simultaneous optimization consists of two terms in order to minimize the trenching length and cable cross sections simultaneously. A constant *Csb* is considered in this thesis, however even variable *Csb* ($Csb_i = \sum_{x=1}^{k_i} \beta_x \,.\, Csb_{i,x}$) could be easily applied to each optimization variable in the objective function, where *i* is optimization variable index, x choice index of the decision set and β_x a binary variable [0, 1] that is defined in Eq. (3-3).

The following objective function is formulated to minimize the CAPEX of electrical interconnection system of a given topology OWF.

$$\min \quad \sum_{i=1}^{N} D_{\boldsymbol{i},\, y_i} \times \left(Csb + \sum_{\mathrm{d}=1}^{m} \lambda_{\boldsymbol{i}}(a_{\boldsymbol{d}}) \,.\, Cc_{\boldsymbol{i}}(a_{\boldsymbol{d}}) \right) \tag{3-10}$$

$$\text{S.t.} \quad \sum_{d=1}^{m} \lambda_{\boldsymbol{i}}(a_{\boldsymbol{d}}) = 1 \qquad \forall\, \lambda_{\boldsymbol{i}} \in \{0,1\}\,, \quad a_d \in \mathrm{A}$$

where:

a_d is d^{th} cross section of the cable decision set [mm^2],

m number of available cross sections in the cable decision set,

N number of WTs (optimization variables),

y_i the assigned value to i^{th} WT as optimization variable (index of the next connected node),

$Cc_i(a_d)$ the corresponding cost of assigned cable ($a_{\boldsymbol{d}}$) to i^{th} turbine for each individual configuration [$/m],

Csb the sum of shipping and burying costs [$/m],

$D_{\boldsymbol{i},\, \boldsymbol{y_i}}$ the distance between i^{th} WT and $y_i^{\,th}$ [m], which can be calculated as follow:

$$D_{\boldsymbol{i},\, \boldsymbol{y_i}} = \sqrt{(x_i - x_{\boldsymbol{y_i}})^2 + (y_i - y_{\boldsymbol{y_i}})^2} \tag{3-11}$$

where $(x_{\boldsymbol{i}}, y_{\boldsymbol{i}})$ and $(x_{\boldsymbol{y_i}}, y_{\boldsymbol{y_i}})$ are location coordinates of i^{th} WT and the next connected node index (y_i^{th}) respectively.

In order to have an admissible total power loss, an inequality constraint has been added to the objective function as a penalty function:

$$\Delta P_{\text{tot}} = \sum_{i=1}^{N} \Delta P_i \leq \Delta P_{\max} \tag{3-12}$$

where, ΔP_{tot} is the total power loss [MW], ΔP_{max} the total maximum permitted active power loss [MW] and ΔP_i the active power loss of the connected branch to i^{th} WT in the worst case [MW]:

$$\Delta P_i = 3 \,.\, R_{\boldsymbol{i}}(a_d).\, I_{i,y_i}{}^2 \times D_{i\,,\,y_i} \qquad (3\text{-}13)$$

where, $R_i(a_d)$ is AC resistance [Ω/m] of assigned cable cross section (a_d) connected to i^{th} WT at 90°C.

According to Eq. (3-13) the power loss is proportional to the square of flowing current, thus in Eq. (3-14) the total cost of average power loss during a year is affected by square rate of the capacity factor (CF) in practice. In addition, due to smaller farm area of OWFs in comparison with its on-shore counterpart (identical power rating), the power loss of its electrical interconnection system is relatively lower (mostly, it is just about 1%). Note that, according to the offshore wind characteristic, the annual capacity factors of installed OWFs are generally in the range of 0.33-0.54 (Cavazzi and Dutton, 2016; Levitt et al., 2011).

In order to minimize the CAPEX for investors, the power loss is defined as a penalty function with its admissible value (lower than 2%) (Gonzalez-Longatt et al., 2012). Moreover, in case of obtaining identical fitness function among different optimal solutions the one with lower total power loss is selected, which coded as follow:

$$\text{if} \quad F^{new} = HF^{best} \quad \& \quad \Delta P_{tot}^{new} < \Delta P_{tot}^{best} \xrightarrow{yields} F^{new} \text{ replace as the best}$$

where, F^{new} and HF^{best} are the fitness value of the new harmony and fitness value of the best harmony in harmony memory respectively.

The annual cost of energy loss can represent the economic performance during the operational phase of the OWF over its lifetime, while maintenance cost is considered a constant value in all cases of this thesis:

$$C_{\Delta W} = 8760h \times \text{LCoE} \times CF^2 \times \Delta P_{tot} \quad \textbf{(}3\text{-}14)$$

where $C_{\Delta W}$ is the annual cost of approximate energy loss; CF is the capacity factor; LCoE is the levelized cost of energy of OWF. In order to find the total cost of energy loss as an operational cost at the investment date, its net present value (NPV) during the OWF lifetime has been calculated (Voormolen et al., 2016; Levitt et al., 2011). However, the annual profit of OWF is not considered, since it is the same in all cases. The aim is only to minimize some of the influencing terms of LCoE.

$$NPV_{\Delta W} = \sum_{y=1}^{LT} \frac{C_{\Delta W}}{(1+r)^y} \quad (3\text{-}15)$$

$$= \sum_{y=1}^{LT} \frac{8760\text{h} \times \text{LCoE} \times CF^2 \times \sum_{i=1}^{N} \Delta P_i}{(1+r)^y}$$

Where $NPV_{\Delta W}$ is the NPV term of the total cost of energy loss (without considering any LCoE reduction for OWF in the future); r is the interest rate [per unit]; LT is the lifetime of the OWF [year]. Therefore, the NPV term of power loss could easily be added to the objective function as a realistic term to find the overall cost of the electrical interconnection system. However, including this term into the objective function is not necessary. Because, the total power loss of OWFs is relatively low (about 1%), and minimizing the CAPEX is a more significant issue for investors.

3.6 The Performance of Optimization Algorithms

This simultaneous optimization is solved offline, relying on the HS algorithm as well as integer-based GA. Each algorithm is run 100 to 1000 times to frustrate the uncertainty of the metaheuristic algorithms and calculate their performances. In order to compare the performances of these two algorithms fairly, the stopping criteria of both algorithms set to individual maximum number of iteration so that only running times of the algorithms are relatively similar. This is because the number of generated offspring in any iteration of GA is much higher than in the HS algorithm (only one offspring). In order to evaluate the average performances of the GA and HS algorithms in different ranges of WTs, the optimal solutions of both cable sizing methods are calculated for various topologies of OWFs; e.g. 4*5 (with 18 WTs) and 4*6 (with 22 WTs). Table 3.2 indicates average estimations for the performance of various topologies and various cable sizing methods.

Table 3.2: Comparison between performance of GA and HS

	Genetic Algorithm (GA)		Harmony Search (HS) algorithm	
Cable sizing method	full	partial	full	partial
Range of 18-22 WTs	84.9%	91.5%	97.6%	94.8%
Range of 37-43 WTs	73.3%	84.3%	91.3%	88.6%
Range of 58-65 WTs	57.1%	72.4%	83.7%	76.8%

The results confirm the better performance of the HS algorithm to find the global optimal solution of this complex optimization problem, compared to the GA. This is because the new harmony (new solution) in the HS algorithm is improvised with a random selection for each optimization variable individually, by considering all existing harmonies (solutions) in HM. This feature increases the flexibility of the HS algorithm to produce better solutions in iterations compared to the GA as it was also

demonstrated in the literature (Geem at el., 2001; Geem, 2006; Yun et al., 2013). On the contrary, the GA only considers the two parent chromosomes (solutions) with single- or multi-point crossover. However, the GA simulation would be more compatible and perform well for partial cable sizing method, where multipoint crossover is considered; even its performance was relatively close to the HS algorithm or even better in some particular topologies. Because, in the partial cable sizing method, the cable cross sections of all branches in each route are the same and assigned only according to the ampacity of the last branch before joining to another route. On contrary, according to individual improvising of each optimization variable in the HS algorithm, it shows more compatibility with full cable sizing rather than partial cable sizing method. Higher performance and faster convergence of the HS algorithm compared to the GA is demonstrated together in Table 3.2 and Figure 3.4 (fitness value vs. iteration). Note that, the illustrated fitness value is about optimization for first scenario of case study one in chapter 4. Conventionally, in HS, only one new harmony is generating per iteration, while in GA the number of generated offspring per iteration is same as number of parents. In order to have fair comparison according to the number of iteration, the HS formulation is changed similar GA so that each iteration generating N new harmonies and the best one is found easily, instead of generating only one new harmony.

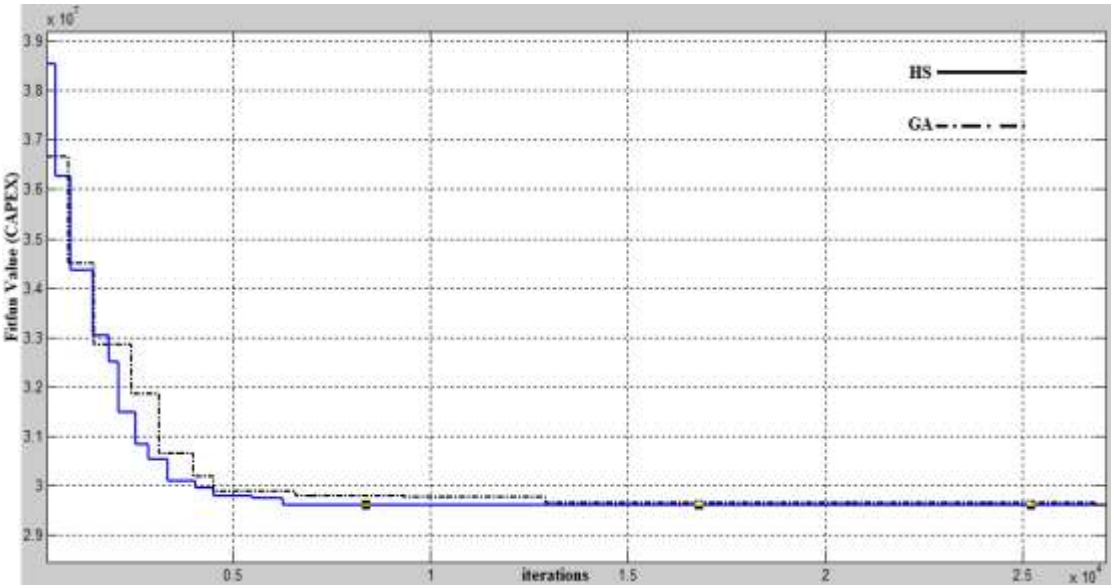

Figure 3.4: Performance of HS (line) and GA (dash line)

Additionally, the HS algorithm has found the optimal solution by considering all possible node connections (even non-feasible ones) in the decision set. Nevertheless, due to increased number of iterations to find global optimal solution of a larger problem, each optimization process takes much longer and obviously with lower performance. The fact that, full optimization yields identical results as the reduced optimization problem, verifies the functionality of the proposed reduction sub-algorithm.

Chapter 4

RESULTS AND DISCUSSIONS

4.1 Introduction

In this chapter two OWFs are investigated as distinct case studies to comprehensively assess the optimal electrical interconnection layout of OWFs and the transmission system to the main grid, so that the investment and operational costs are minimized.

The first case study is an OWF with rectangular topology while any given size (n*m) can be considered. The WTs and OS(s) are allocated according to number of arrays (n) and number of WTs in each array (m). The optimal electrical interconnection configuration and cable sizing of a large-scale OWF with any given topology is found simultaneously. Optimizing of transmission system and other relevant components are not considered in this case.

The second case study is a real OWF in France that called “Banc de Guerande” (Projet, 2013). It has 80 WTs with power rating of 6 MW. Simultaneous optimization is formulated to find the optimal electrical interconnection configuration and cable sizing, transmission line and other relevant components. The results are compared with another study (Dahmani et al., 2015) on the same OWF to illustrate the improvement of the optimization formulation.

4.2 The First Case Study: OWF with Rectangular Topology

In this case, the WTs and OS are allocated according to number of arrays (n), and number of WTs in each array (m) to create a symmetric or semi-symmetric rectangular topology (n*m). However, in very large OWFs multi-OS substations could be also investigated. A semi-symmetrical rectangular topology (11*6) consisting of 63 WTs is considered, where eleven turbines can harvest direct wind and WTs on the next arrays allocated with larger space particularly in order to minimize the overall wind wake effect. The WTs' spacing is assigned according to WT blades diameter (D). Different admissible spacing has been defined in the literature, e.g. 3D-7D and 7D-12D (Pookpunt and Ongsakul, 2016; Xiaoxia et al., 2016; Siemens, 2014a; Samorani, 2013; Gonzalez-Longatt et al., 2012). Thereby, the spacing of 5D and 9D are assumed between the WTs along an array (dy) and between the arrays (dx), respectively. Moreover, an intermediate single OS is assumed at the centroid of the OWF to decrease the interconnection CAPEX as well as the total power loss (Hou et al., 2016; Lumbreras and Ramos, 2013; Banzo and Ramos, 2011). The OWF is assumed to be far from the shore, thus a high voltage transmission system is required for the connection of the OWF to the main grid, which is not investigated in this study. According to the available literature, the assumption values for optimization are given in Table 4.2 (Voormolen et al., 2016; Li and DeCarolis, 2015; GWEC, 2015; Siemens, 2014a), while the lifetime, interest rate, LCoE and the average capacity factor of OWF are considered to be 20 years, 5%, $140/MWh and 0.45 respectively. Two different Siemens WTs with 3.6 and 6.0 MW power rating have been assumed in this study while the diameters are 120 and 154 m, respectively (SWT-3.6-120 and SWT-6.0-154). The above-mentioned WTs employ a variable-speed DFIG and an individual step-up transformer with output

voltage of 33 kV at nacelle or pad-mount, according to the structure stamina of WTs. The DFIG manufacturers offer different characteristics options for reactive power generation (Erlich et al., 2007). Figure 4.1 shows the characteristic of active power (*P*) versus reactive power (*Q*) of a typical DFIG (Gashi et al., 2012).

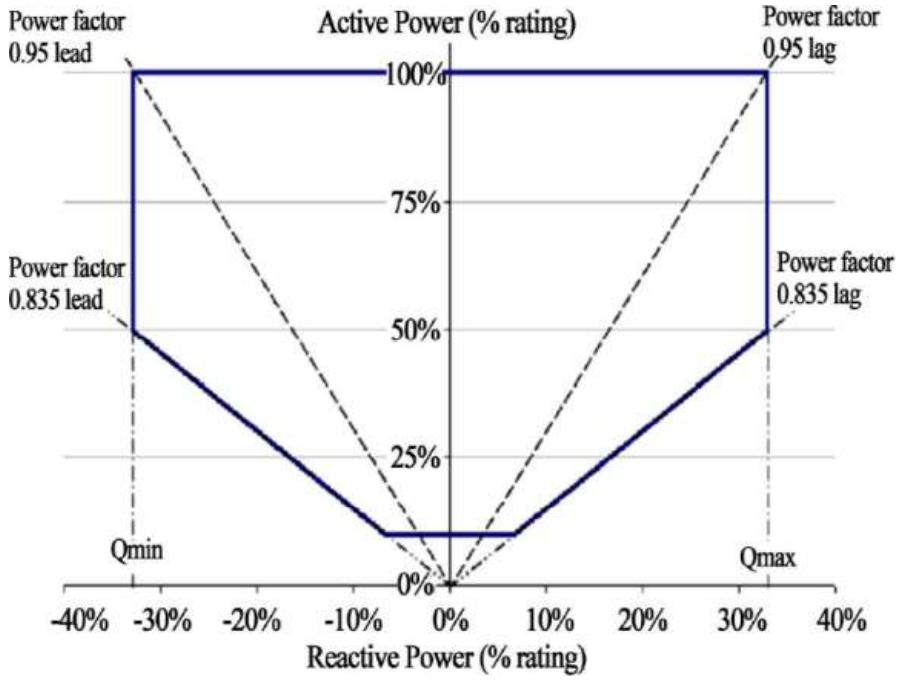

Figure 4.1: P-Q characteristics of DFIG base WTs (Gashi et al., 2012)

In order to consider the worst case in cable sizing (maximum ampacity), the power factor has been considered at 33% leading or lagging reactive power, at fully rated active power ($\cos\emptyset = 0.95$). The injected current of each WT is calculated as:

$$I_{\mathrm{G}} = \frac{P_{\mathrm{G}}}{\sqrt{3} \,.\, V_{\mathrm{L}} \,.\, \mathrm{Cos}\emptyset} \qquad (4\text{-}1)$$

where P_G is the rated power of each WT; V_L is the output line voltage of its internal transformer. A 690V/33kV step-up transformer is used to boost the voltage up to 33 kV, since the stator output voltage of the WTs generator is typically 690 V. The

maximum permitted active power loss ($\Delta P_{\max}$) of the electrical interconnection system is conventionally considered as 2% of the OWF capacity.

All available cross sections of subsea (submarine) MV cables have been considered in the decision set of cable sizing problem, where *A* = {50, 70, 95, 120, 150, 185, 240, 300, 400, 500, 630}. According to shipping limitation or unavailability, a new set with a few choices can easily be replaced, thus it may even decrease *Csb*. The parameters of three-core copper conductor with XLPE insulator and armored subsea cable for 18-30 kV (36 kV) are shown in Table 4.1 (Orient Cable, 2015; Nexans, 2013). Note that, it represents only the cross sections that have been used in this case study.

Table 4.1: Submarine and subsea cable parameters (Orient Cable, 2015; Nexans, 2013)

MV Cable [mm2]	50	70	95	185	240	300	400	500	630
Current [Amp] (on seabed)	241	281	335	473	540	601	671	742	812
AC resistance at 90oC [Ω/Km]	0.493	0.342	0.247	0.127	0.1	0.08	0.063	0.05	0.041
Cost [$/m]	89	118	152	250	283	320	381	430	490

The *Csb* has significant contribution in the electrical interconnection CAPEX and may vary in different OWFs. A constant value has been assumed in this thesis, conventionally; because, the outer diameter and weight of a subsea cable with maximum cross section of 630 mm^2 is just about twice as thick and heavy as 50 mm^2. However, variable *Csb* ($Csb_{i,x}$) can be easily applied to the objective function, if more practical detailed cost information about *Csb* is provided.

In this section, the optimal electrical interconnection layout is comprehensively assessed. Variation in different influencing parameters and cable sizing methods are considered via three distinct scenarios to investigate their impact on the CAPEX and the optimal interconnection layout of a given OWF. Scenario I uses the full cable sizing method to find the simultaneous optimal interconnection configuration and cable sizing. Moreover, the impact of different *Csb* and different WT power rating are investigated. Scenario II uses the partial cable sizing method to solve the similar simultaneous optimization. Scenario III employs a conventional radial configuration in order to compare and investigate different aspects. Nevertheless, power rating of 6 MW and constant *Csb* of 250 $/m are considered to have a fair comparison among all the scenarios. The data the OWF considered for optimization is described in Table 4.2.

Table 4.2: Assumption for optimization

No. of WTs	63		Capacity Factor	0.45
Topology	n*m: 6*11		OWF lifetime	20 years
Spacing	Lx = 9D & Ly = 5D		LoCE	$140/MWh
Csb (various in scenario I)	**$250/m** $500/m	$250/m	Interest rate (r)	5%
Rated power	6 MW	3.6 MW	Rated voltage	33 kV
OWF capacity	378 MW	226.8 MW	$cos\emptyset$	0.95

4.2.1 Results of Scenario I: Full Cable Sizing Method

In this scenario, full cable sizing method is used for the simultaneous optimization. Two different comparisons are made to investigate the impact of various *Csb* and power ratings of WTs on the CAPEX and the optimal interconnection layout of a given OWF. In addition, any change in the space between the WTs along an array or between the arrays obviously changes the optimal interconnection layout.

In the first comparison, the optimal electrical interconnection layouts of the identical OWF with the WT's power rating of 6MW are found in two cases with *Csb* of 250 and 500 $/m and shown in Figure 4.2 and Figure 4.3 respectively, where corresponding values are mentioned in the captions.

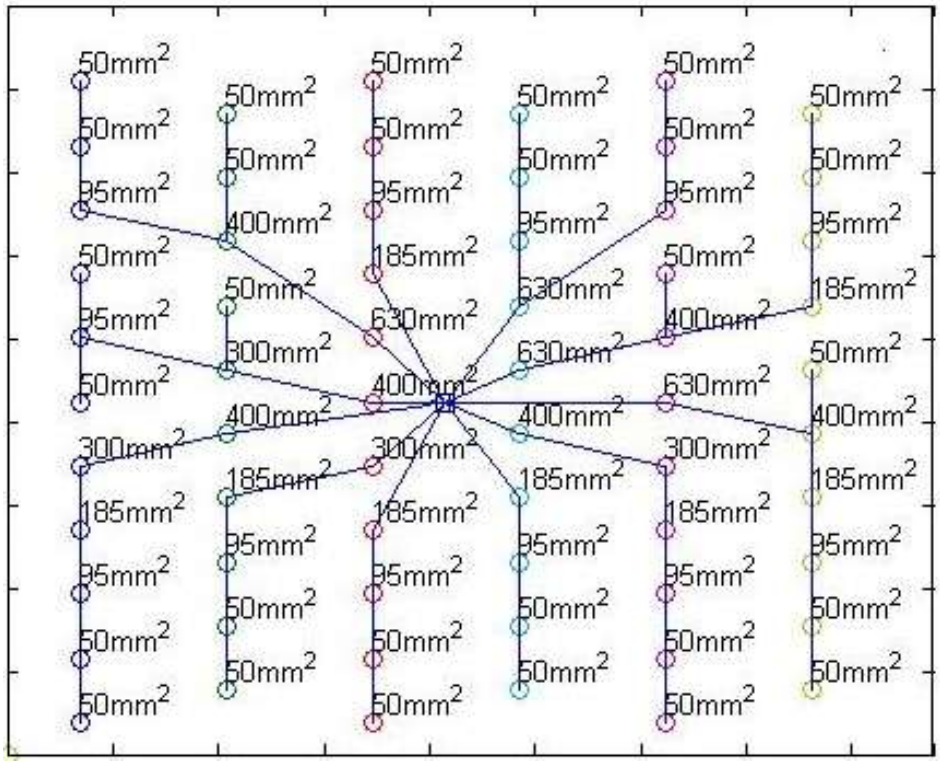

Figure 4.2: *Scenario I*, optimal layout (*Csb* of $250/m with 6MW), CAPEX= M$ 29.352 & Losses = 4.039MW & L_T = 62.740km

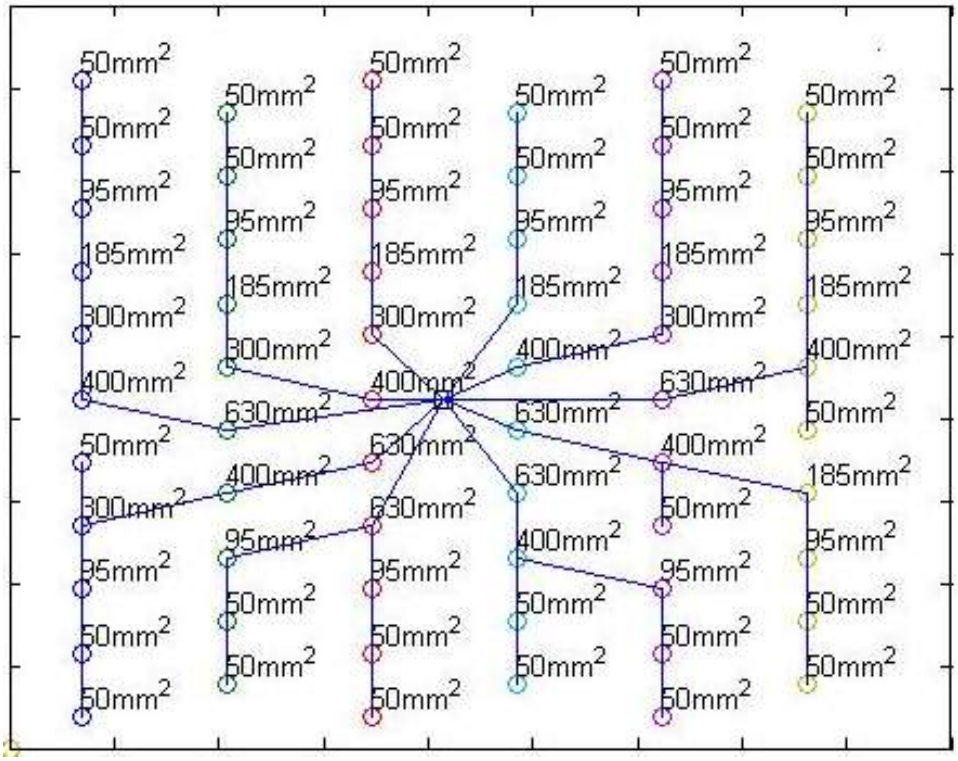

Figure 4.3: Optimal layout (*Csb of $500/m* with 6MW),
CAPEX= M$ 44.656 & Losses = 3.927MW & L_T = 60.421km

The results reveal that 100% increase in *Csb* (from 250 $/m to 500 $/m) leads to 52% increase in the electrical interconnection CAPEX (from M$ 29.352 to M$ 44.656). However, the total trenching length is decreased by 3.7% (2.318 km) as *Csb* affects about the length term of the simultaneous optimization formulation. The total active power loss in both optimal interconnection layouts (Figure 4.2 and Figure 4.3) are about 1% (387 MW), which is just half of the admissible loss in full capacity of the OWF.

In the second comparison in scenario I, the optimal electrical interconnection layouts of the identical OWF with *Csb* of 250 $/m are found, where WTs are considered with the power rating of 3.6 MW and the total capacity of 226.8 MW. Note that, the original diameter is 120 m instead of 154 m, thus only per unit values can be compared. The optimal interconnection layout is shown in Figure 4.4.

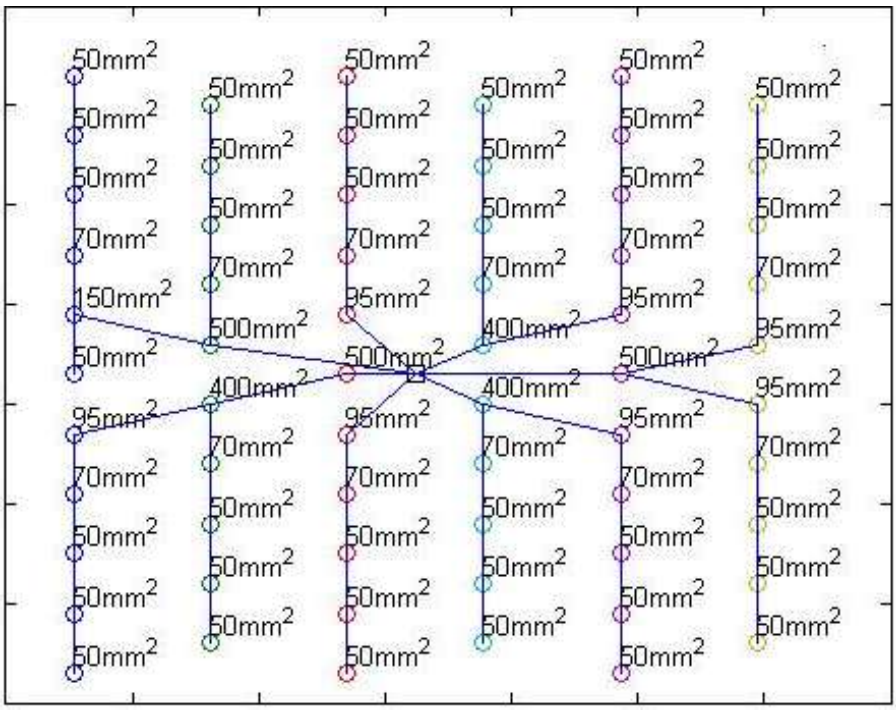

Figure 4.4: Optimal layout (*Csb* of \$250/m with *3.6MW*),
CAPEX= M\$ 17.686 and Losses = 2.3507MW & L_T = 43.904km

The results indicate that CAPEX of the interconnection system for both 6 MW and 3.6 MW are relatively similar (about 76 \$/kW). In addition, the percentage of their total power losses is almost the same (about 1%). However, the total trenching length is decreased, due to spacing reduction. It is also found that the optimal interconnection configuration of an OWF with lower power rating would be similar to the simple configuration of a traditional OWF, as the power rating of WTs in the last decade was in the range of 2-3.6 MW, and where a single low cross section cable could collect the generated power of several WTs.

4.2.2 Results of Scenario II: Partial Cable Sizing Method

In this scenario, the partial cable sizing method is applied in the objective function so that only limited number of cable cross sections is considered to be available in the decision set (50, 185 and 630 mm^2). In addition, cable cross sections of all branches on each route are identically assigned according to the ampacity of the last branch

before joining another route or connecting to the OS. In partial cable sizing, shipping or burying might be easier and *Csb* may decrease in practice, according to fewer changes in cable cross sections or using only a few cable cross sections. However, partial cable sizing may lead to over-sizing of cable cross section in some branches and increasing the CAPEX, which is investigated in this section. Figure 4.5 shows the optimal interconnection layout of the identical OWF in Scenario II.

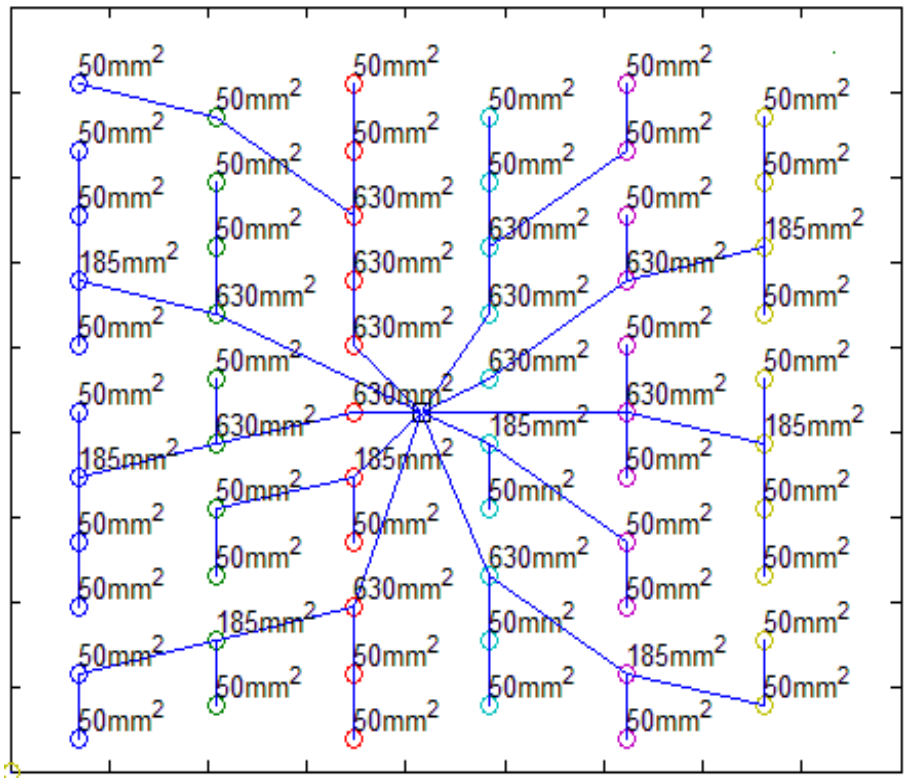

Figure 4.5: *Scenario II*, optimal layout (*Csb* of \$250/m with 6MW), CAPEX= M\$ 31.897 and Losses = 3.557MW & L_T = 67.278km

The optimal interconnection layout of this scenario can be compared with the main case in scenario I (Figure 4.2). The investment and operational costs of the electrical interconnection systems, and the overall cost of all scenarios are indicated in Table 4.3. The NPV terms of the total cost of energy losses during the OWF lifetime

are calculated as a variable operating cost, while maintenance cost is considered a constant value in all scenarios.

Table 4.3: Comparison between capital investment and operational cost of different scenarios, (according to *Csb* of $250/m and power rating of 6MW)

	Scenario I	Scenario II	Scenario III
CAPEX (investment cost)	M$ 29.352	M$ 31.897	M$ 38.755
% Total power losses (378MW capacity)	1.04%	0.92%	0.69%
Cost of Energy losses (operational cost as NPV)	M$ 12.501	M$ 11.008	M$ 8.257
Overall costs of interconnection system	M$ 41.853	M$ 42.905	M$ 47.012

The results reveal that the CAPEX of interconnection system in scenario II is increased by 8.67% compared to scenario I. However, the overall costs increase will be only by 2.5% (M$ 1.052), due to obtaining lower power loss, which is less than 0.92% (3.557 MW). Hence, scenario II also has good potential to be a justified solution, if partial cable sizing can provide just about 5.02% *Csb* reduction (if *Csb* ≈237 $/m instead of 250 $/m) in practice[4]. Note that, it is only an estimation according to the first comparison, since any change in *Csb* for the new optimization process may change not only CAPEX but also the optimal layout.

4.2.3 Results of Scenario III: Conventional Radial Layout

Most of OWF projects in the last decade have used a typical conventional radial configuration (Projet, 2013). In order to illustrate the significance of the proposed simultaneous optimization, the optimal interconnection layouts in scenarios I and II are additionally compared with a conventional radial layout, which is shown in

[3] No details have been published about effective parameters in *Csb*, e.g., vessel capacity for various number cables cross sections or the length of subsea cables to ship in each journey to the OWF area.

Figure 4.6 for the identical OWF while cable crossing is avoided.

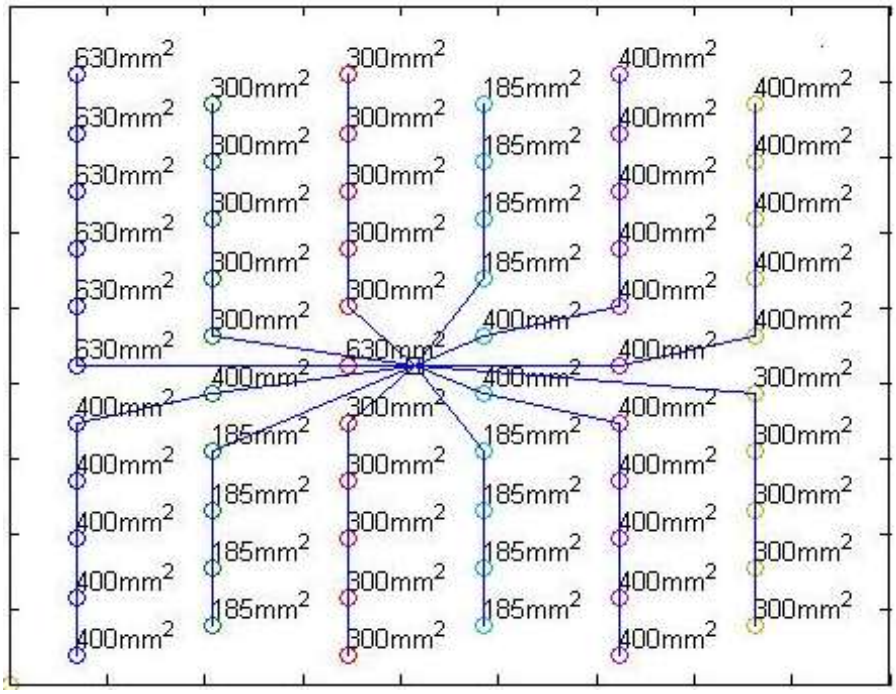

Figure 4.6: *Scenario III*, optimal layout (*Csb* of $250/m with 6MW), CAPEX= M$ 38.755 & Losses = 2.668MW & LT = 63.163km

The results of the typical radial electrical interconnection layout indicate that the CAPEX of interconnection system is increased to M$ 38.755. Table 4.3 reveals that, according to the CAPEX, the optimal electrical interconnection of the scenarios I and II would save about 24.3% and 17.7%, respectively. However, the total power loss of 0.69% (2.668MW) in this scenario is relatively low as expected, due to the over-sizing of the cables cross sections away from the OS. Hence, the overall cost saving during the OWF lifetime will be M$5.159 (about 10.97%) and M$4.107 (about 8.74%), respectively.

4.3 The Second Case Study: a Real OWF

"Banc de Guerande" is an OWF in France, which has 80 WTs with power rating of 6 MW and the main data of this OWF is available in (Projet, 2013). In this section the

optimal electrical interconnection configuration and cable sizing as well as the optimal layout of HV transmission line and other relevant components are found simultaneously. In order to demonstrate the improvements of the proposed optimization formulation, the results are compared to another study (Dahmani et al., 2015) with the same OWF.

In this case study, in order to have fair comparison all assumptions, constraints and OWF parameters are considered identically, however the optimization formulation is different. Dahmani et al. (2015) utilized a binary GA to find optimal interconnection configuration and full cable sizing, while only five cable cross sections were considered in decision set. Crossing cables was avoided so that no crossed edges were considered in MST to find the optimal interconnection configuration, which may miss some feasible solutions. Moreover, the optimal layout was found just for pre-clustered nodes in order to decrease the problem size and be solved with MST algorithm. Nevertheless, decreasing the problem size by any clustering method without considering integration of all WTs or utilizing an insufficient optimization algorithm may result in a local optimal solution.

Some of the important optimization assumptions, constraints and OWF parameters that were considered in Dahmani et al. (2015) are listed as follows:

- The location and power rating of WTs are fixed.
- Loop design configuration is not considered, as the reliability of buried subsea cable is not an issue.
- Only HVAC solution is considered in for transmission system.
- Fixed voltage is considered for both MV and HV sides.

- No parallel MV subsea cable is considered between WTs, however parallel HVAC line might be required, according to the total transmitted power.
- Only one Onshore Connection Point (OCP) is considered, while multi-OS can be considered in optimization.
- Three-core submarine MV cables (33kV) are utilized for interconnection system, where only five cable cross sections were considered in decision set (120, 240, 300, 500 and 800 mm^2).
- The investment that is minimized, supposed to be made today and paid off during of OWF lifetime, which is found as follows:

$$C_{inv}=\frac{r.LT.(1+r)^{LT}}{(1+r)^{LT}-1}\times\frac{1}{1-PR}\times[C_{MV}+C_{HV}+C_{pl}+C_{tr}+C_{sw}] \quad (4\text{-}2)$$

where, C_{inv} is the total investment cost, C_{sw} the initial invest for MV and HV switchgears, C_{tr} the initial invest for step up transformer(s) on OS, C_{pl} the initial invest for the platform of OS(s), C_{MV} and C_{HV} are the initial invest for MV and HV cables respectively (by considering *Csb*), and, r is the interest rate (4%), PR the annual profit (2%) and LT is OWF lifetime (20 years). The WTs topology in the studied OWF is shown in Figure 4.7, where the OCP is assumed to have the coordinates $\{-20, -20\}$.

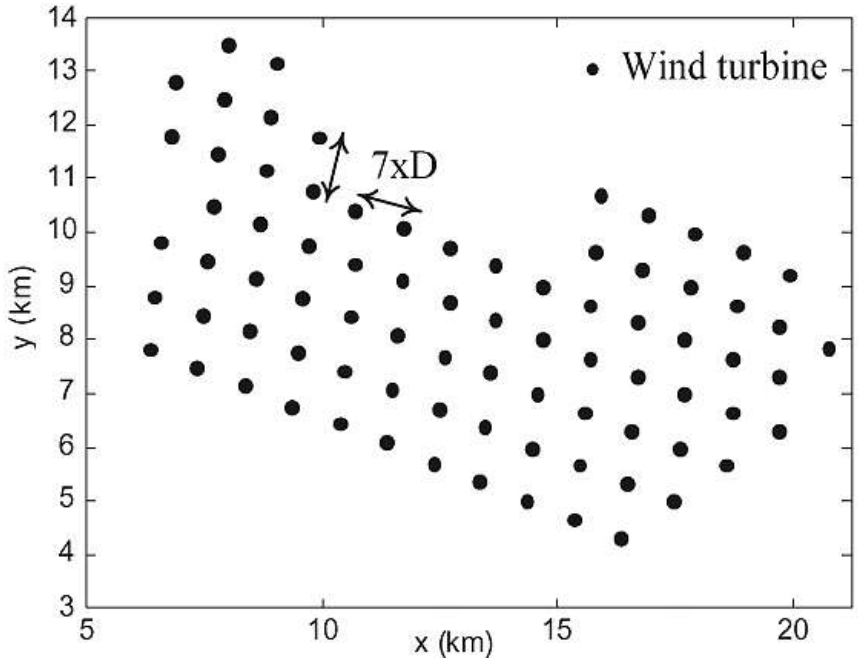

Figure 4.7: The WTs topology of the studied OWF (Dahmani et al., 2015)

The same optimization formulation that was proposed in chapter 4, is adopted to find the optimal layout of electrical interconnection and transmission systems of OWF simultaneously, by extending the number of nodes and edges in this formulation as well as considering cost of other relevant components. However, the most complex part of this optimization problem is to find the optimal electrical interconnection configuration, due to its large search space. In addition, the investment cost for platform of OS(s), offshore substation transformers transformer(s) as well as MV and HV switchgears are considered in objective function. Since no clustering is applied in this optimization problem, all feasible solutions are considered in this method. Furthermore, same as the proposed objective function in chapter 4, the power loss is considered as a penalty term, which was not considered in (Dahmani et al., 2015) and may lead to have higher power loss as well.

In this case study, the cost of MV and HV cables are assigned according to an approximated function that is related to the voltage level of subsea cables and power limitation of the corresponding cables cross sections. Note that, in optimizations, the approximate price for all edges does not apply influencing error in optimization results. This function is defined by Lundberg (2003) as follows:

$$C_{\boldsymbol{MV}}(a_{\boldsymbol{d}}) = A_p + B_p.\exp\left(C_p \times 10^{-8}.S_{\max}(a_{\boldsymbol{d}})\right) \quad (4\text{-}3)$$

where, A_p, B_p and C_p are constant cost factor of AC cables that are given in Table 4.4, according to the rated voltage of cables. $C_{\boldsymbol{MV}}(a_{\boldsymbol{d}})$ and $S_{\max}(a_{\boldsymbol{d}})$ are the cost [SEK/km] and the maximum power [MW] of the AC cables with cross section of a_d respectively, and a_d is d^{th} cross section of the cable set. Note that, identical formulation is also valid for $C_{\boldsymbol{HV}}(a_{\boldsymbol{d}})$.

$$S_{\max}(a_{\boldsymbol{d}}) = \sqrt{3}\, V_{\mathbf{rated}}.\, I_{\mathbf{max}}(a_{\boldsymbol{d}}) \quad (4\text{-}4)$$

Table 4.4: Cost factor for different voltages of AC cables

Voltage Level	A_p	B_p	C_p
33 kV	0.411×10^6	0.596×10^6	4.1×10^6
220 kV	3.181×10^6	$0.\ 11\times10^6$	1.16×10^6

The following formulation is similar to the previous case study, but the OSs are additionally considered as extra nodes in this study. Hence, the length of chromosome (number of variables) is $N+n_{OS}$.

The $C_{\boldsymbol{MV}}$ (and similarly the $C_{\boldsymbol{HV}}$) can be found as follows:

$$C_{\mathbf{MV}} = \sum_{i=1}^{N} D_{\boldsymbol{i,j}} \left(C_{sb} + \sum_{d=1}^{m} \lambda_{\boldsymbol{i}}(a_{\boldsymbol{d}}) \cdot C_{\boldsymbol{MV}}(a_{\boldsymbol{d}}) \right) \quad (4\text{-}5)$$

$$\text{s.t.} \quad \sum_{d=1}^{m} \lambda_i(a_d) = 1 \qquad \forall \lambda_i \in \{0,1\}, \quad a_d \in \text{A}$$

where, C_{sb} is considered to be \$152/m for MV subsea cables (Nandigam and Dhali, 2008; Ergun et al., 2012).

In order to find the estimated cost of the OS platform (C_{P}) and offshore substation transformers (C_{T}) are given by (Lazaridis, 2005; Zubiaga, 2009) as follows:

$$C_{\text{P}} = 2.14 + 0.0747.S_{\text{T,max}} \tag{4-6}$$

$$C_{\text{T}} = 0.03327.S_{\text{T,max}}{}^{0.7513} \tag{4-7}$$

where, C_{P} and C_{T} are the cost [Euro] of the OS platform and offshore substation transformers respectively, and $S_{\text{T,max}}$ is the power rating [VA] of the transformer that can be suitable for assigned transmitted power. The decision set to select suitable transformer are as follows:

S_{T} (MVA) = {40, 50, 100, 125, 150, 180, 200, 250, 300, 400, 630, 722, 800}

Moreover, the approximate cost of each MV and HV switchgear are assumed to be M\$0.473 and M\$0.53 respectively, thus the MV and HV bay can be easily found according to the total number of feeders.

Since the cost function for OS platform and offshore substation transformers are given based on Euro (€), the AC cables cost that are based on found Swedish Krona (SEK) and other values are based on USD (\$), identical exchange rate is used in this case, as follows:

$$1 \text{ SEK} = €0.1155 \text{ and } \$1 = €0.7694 \tag{4-8}$$

4.3.1 Comparing Both Optimization Results

In this case study, in order to demonstrate high performance of the proposed optimization method and formulation, the optimal layout of electrical interconnection and transmission systems of a real OWF has been found and compared with another study (Dahmani et al., 2015). All assumptions, constraints and OWF parameters are considered identically, where the exact found solution in that study was also simulated manually, in order to have a fair comparison. The optimization results of cost and technical variables of both studies are illustrated in Dahmani et al. (2015). Moreover, the optimal interconnection layout that found in Dahmani et al. (2015) and the proposed optimization method of this thesis are depicted in Figure 4.8 and Figure 4.9.

Table 4.5: The optimization results of both studies

The parameters	The optimal values of Dahmani et al. (2015)	The optimal values of our proposed formulation
Cost of interconnection system	45.559 M€	44.115 M€
Cost of transmission lines	97.638 M€	97.638 M€
Cost of offshore substation transformers	6.327 M€	6.327 M€
Cost of OS platforms	62.514 M€	62.514 M€
Cost of MV switchgears	7.112 M€	7.667 M€
Cost of HV switchgears	2.449 M€	2.449 M€
Total investment cost (C_{invest})	221.61 M€	220.70 M€
Length of MV cables	83.40 km	82.83 km
Length of HV cables	84.92 km	84.92 km
Number of MV feeders per OS	{7,6}	{7,7}
Number and size of HV cables	3×800 mm^2 per OS	3×800 mm^2 per OS
Number of WTs per groups	Between 3 to 7	Between 3 to 7
Transformer power, per OS	{250, 250} MVA	{250, 250} MVA
Power loss of interconnection system	3.084 MW	3.079 MW

The results reveal the improvement in the optimization results, where the most improvement is in interconnection system. The investment cost of interconnection system is decreased by 3.17% (about 1.444 M€). Nevertheless, the other parameters of transmission system and relevant components are almost the same, since their optimization are not as complex as the interconnection system. Although, the total length and power losses in interconnection system is decreased slightly, the total cost of MV switchgears has increased, because of higher number of MV feeders. Nevertheless, the total investment for this real OWF could be reduced about one million Euro.

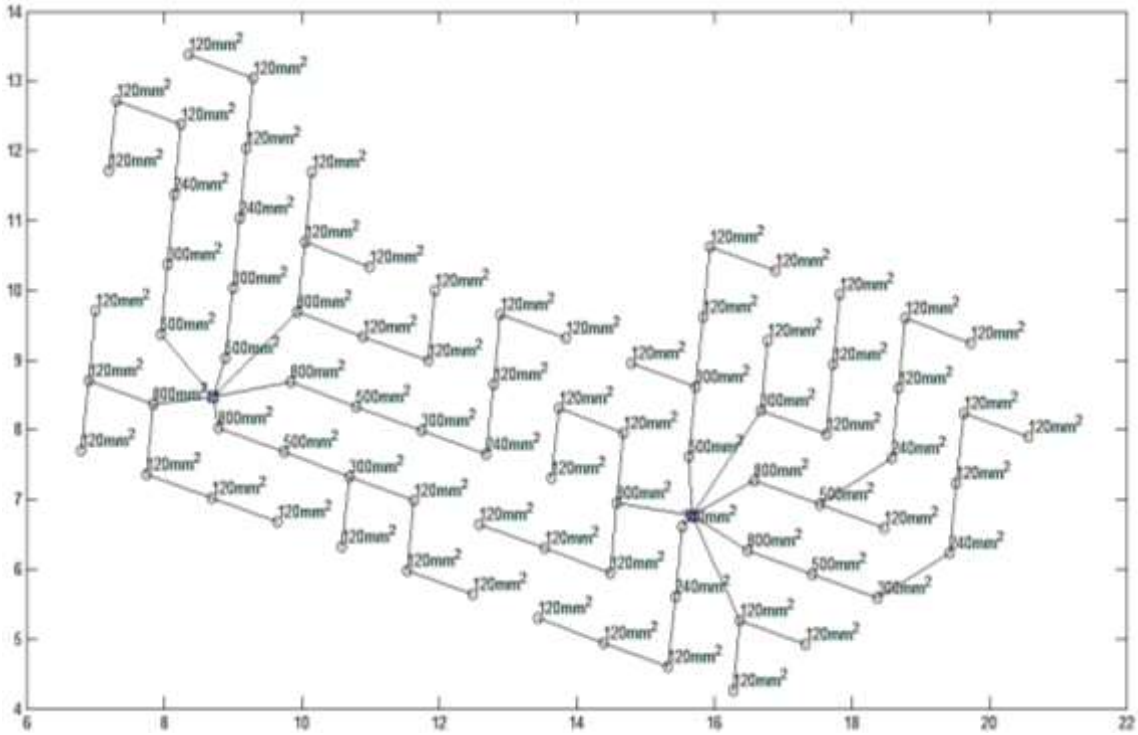

Figure 4.8: The optimal electrical interconnection layout in (Dahmani et al., 2015)

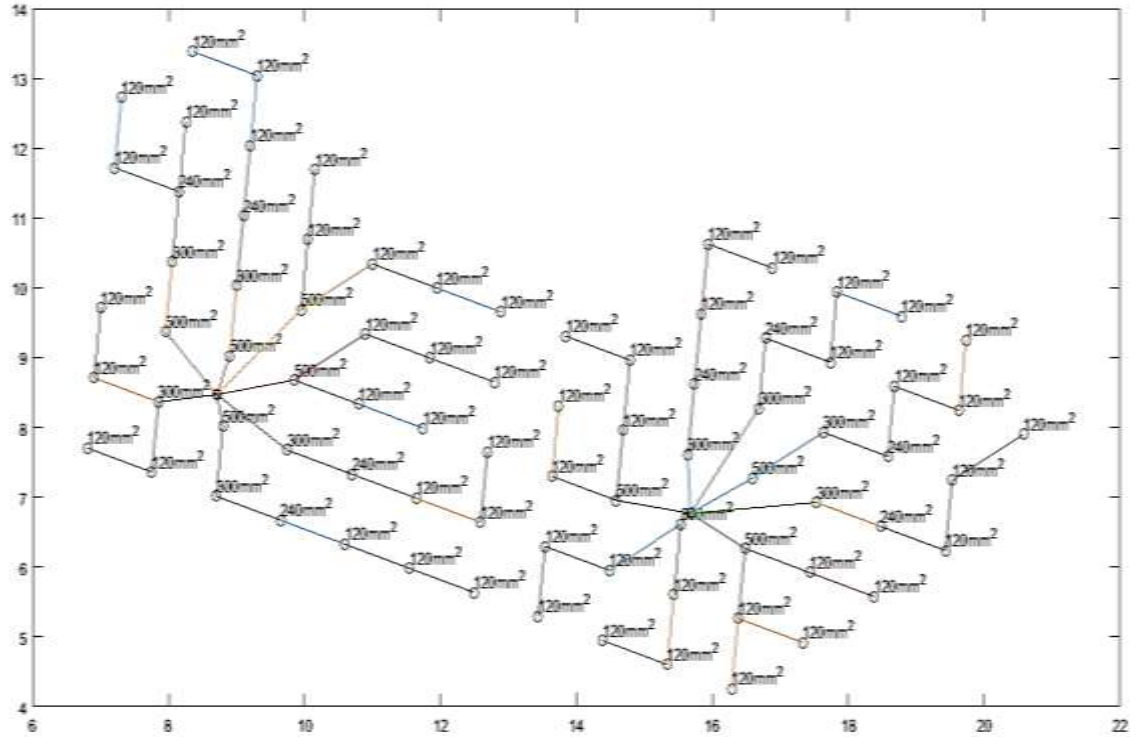

Figure 4.9: The optimal electrical interconnection layout of our proposed formulation

In order to have a comparison between both optimal configurations, as the power losses was not included in objective function in reference (Dahmani et al., 2015), some insufficient edges were selected in their optimal solution, while the total cable length and cross sections could be the same. For instance, the cable connection (edge) that is located at the position of {7.5, 12.5} or {14.5, 8} in (Dahmani et al., 2015), where another possible edges such as {7.5, 11.5} or {14.5, 7} could be replaced respectively.

Chapter 5

CONCLUSION AND FUTURE WORKS

5.1 Conclusion

This thesis proposes an optimization formulation to minimize the CAPEX of the electrical interconnection system of OWFs, in order to help designers to reach necessary balance between the technical performance and the economic costs. The simultaneous optimal electrical interconnection configuration and the cable sizing of a given topology OWF is found. The proposed formulation can be easily adopted in on-shore wind farms as well. An HS algorithm is used to solve this complex and discrete optimization problem. The optimization results are compared with an integer-based GA as a proven optimization algorithm. The results demonstrate the higher performance of the HS algorithm in comparison with the GA.

In the first case study, in order to assess the optimal interconnection layout of an identical OWF with a given topology comprehensively, full and partial optimal cable sizing are considered in the objective function of scenarios I and II, respectively. Scenario III shows a typical radial configuration to compare with these optimal scenarios. Furthermore, in the first scenario, in order to indicate the significance of this study the influences of *Csb* and WTs power rating are investigated over the CAPEX and the optimal layout of interconnection system. The results illustrate that variation in the WTs power rating completely changes the optimal interconnection layout of the identical topology OWF. Additionally, it turns out that increasing *Csb*

increases the CAPEX and usually changes the optimal interconnection layout. Comparative results in Table 4.3 reveal that, according to the CAPEX, both scenarios I and II as optimal solutions in this study would save about 24% and 20%, respectively, compared to the scenario III. However, according to the overall cost during the OWF lifetime their saving will be 11.69% and 10.55%, respectively. In conclusion, scenario I by applying full cable sizing method is the best solution in general. Nevertheless, scenario II could also be a justified solution or even the best solution, if partial cable sizing method can provide small *Csb* reduction in practice. Moreover, the total active power losses of these optimal scenarios in full capacity of the OWF turned out to be just half of the admissible value.

In the second case study, in order to demonstrate higher performance of the proposed optimization method and formulation the optimal results have been compared with another study, where an identical real OWF has been assumed. The optimal layout of electrical interconnection, transmission system and other relevant components have been found simultaneously, while all assumptions, constraints and OWF parameters are considered identically, in order to have a fair comparison. The results reveal that the interconnection cost, cable length and power loss of optimal interconnection system have been reduced. This new optimal solution for this real OWF project could save about one million Euro, according to this comparison. However, due to their simple configuration and small search space, identical optimal solutions have been found for transmission system and relevant components.

5.2 Future Works

In the future work, the proposed methodology could be similarly developed to find the optimal connection between several OWFs via high voltage links to the several on-shore grid, and the justification of HVDC solution can be investigated for different OWF with different distance and power rating. Besides, fast developing in large-scale OWFs may create a new challenge to provide 66 kV solution for interconnection system, if manufactures can offer relevant equipment with more justified prices.

REFERENCES

Banzo M., & Ramos A. (2011). Stochastic Optimization Model for Electric Power System Planning of Off-shore Wind Farms. *IEEE Transaction Power Systems*, 26(3), 1338-48.

Baring-Gould I. (2014). Offshore Wind Plant Electrical Systems. NREL, BOEM Offshore Renewable Energy Workshop.

Breton, S.P., & Moe, G. (2009). Status, Plans and Technologies for Offshore Wind Turbines in Europe and North America. *Renewable Energy, Elsevier*, 34(3), 646-654.

Cavazzi S., & Dutton A.G. (2016). An Offshore Wind Energy Geographic Information System (OWE-GIS) for assessment of the UK's offshore wind energy potential. *Renewable Energy, Elsevier*, No. 87, pp. 212-228.

Chu Ch.W., Lin M.D., Liu G.F., & Sung Y.H. (2008). Application of immune algorithms on solving minimum-cost problem of water distribution network. *Mathematical and Computer Modlling, Elsevier*, 48, 1888-1900.

Chuangpishit Sh., Tabesh A., Moradi Sh.Z., & Saeedifard M. (2014). Topology Design for Collector Systems of Offshore Wind Farms With Pure DC Power Systems. *IEEE Transaction Industrial Electronics*, 61(1), 320-328.

Blohm A., Peichel J., Ruth M., Shim Y., Williamson S., & Zhu J. (2010). Maryland Offshore Wind Development: Regulatory Environment, Potential Interconnection Points, Investment Model, and Select Conflict Areas (Report). Center for Integrative Environmental Research (CIER), University of Maryland, 2010.

BVG Associates (2010). A Guide to an Offshore Wind Farm. Report is published on behalf of The Crown Estate. Online available: https://www.thecrownestate.co.uk/media/5408/ei-a-guide-to-an-offshore-wind-farm.pdf

Cole S., Martinot P., Raroport S., Papaefthymiou G., & Gori V. (2014). Study of the Benefits of a Meshed Offshore Grid in Northern Seas Region. Brussels, report of European Commission - General for Energy.

Dahmani O., Bourguet S., Machmoum M., Guerin P., Rhein P., & Josse L. (2015). Optimization of the Connection Topology of an Offshore Wind Farm Network. *IEEE Systems J.*, 9(4), 1519-28.

Dan B., Pei-Jun Y., & Li-Xum S. (2007). Optimal Design Method of Looped Water Distribution Network. *System Engineering - Theory & Practice, Elsevier*, 27(7), 137-143.

De Prada M., Igualada L., Corchero C., Gomis-Bellmunt O., & Sumper A. (2015). Hybrid AC–DC Offshore Wind Power Plant Topology: Optimal Design. *IEEE Transaction Power Electronic*, 30(4), 1868-76.

De Prada M., Gomis-Bellmunt O., & Sumper A. (2014). Technical and economic assessment of offshore wind power plants based on variable frequency operation of clusters with a single power converter. *Applied Energy, Elsevier*, 125, 218-229.

DOE (Department of Energy) of U.S. (2008). 20% Wind Energy by 2030: Increasing Wind Energy's Contribution to U.S. Electricity Supply. Washington, D.C. Accessed April 16, 2014: http://www.nrel.gov/docs/fy08osti/41869.pdf

Dutta S. & Overbye T.J. (2012). Optimal Wind Farm Collector System Topology Design Considering Total Trenching Length. *IEEE Transaction Sustainable Energy*, 3, 339-348.

Dutta S. & Overbye T.J. (2011). A Clustering based Wind Farm Collector System Cable Layout Design. Proc. IEEE power and Energy Conf., at Illinois (PECI), at Champaign, IL, pp. 1-6.

Ederer N. (2015). The market value and impact of offshore wind on the electricity spot market: Evidence from Germany. *Applied Energy, Elsevier*, 154, 805-814.

ENTSOE (European Network of Transmission System Operators for Electricity), (2011). Offshore Transmission Technology (Report).

Ergun H., Hertem D.V., & Belmans R. (2012). Transmission System Topology Optimization for Large-Scale Offshore Wind Integration. *IEEE Transaction Sustainable Energy*, 3(4), 908-917.

Erlich I., Shewarega, F., Feltes, Ch., W. Koch, F. & Fortmann J. (2013). Off-shore Wind Power Generation Technologies. *Proc. IEEE*, 101(4), 891-905.

Erlich I., Wilich M., & Feltes Ch. (2007). Reactive Power Generation by DIFIG Based Wind Farms with AC Grid Connection. Proc. IEEE power Electronic and Application Conf., (EPE 2007), at Aalborg, pp. 1-10.

EWEA (European Wind Energy Association), (2013). Deep water, the next step for offshore wind energy. A report by the European Wind Energy Association, Belgium.

EWEA (European Wind Energy Association), (2014a). Wind energy scenarios for 2020.

EWEA (European Wind Energy Association), (2014b). The European offshore wind industry - key trends and statistics 2013 (Report).

EWEA (European Wind Energy Association), (2015). Wind energy scenarios for 2030.

EY (Ernst & Young Global Limited report), (2015). Offshore Wind in Europe: Walking the Tightrope to Success. EY report, France.

Gashi A., Kabashi G., Kabashi S., Ahmetaj S., & Veliu V. (2012). Simulation the Wind Grid Code Requirements for Wind Farms Connection in Kosovo Transmission Grid. *Energy and Power Engineering*, 4, 482-495.

Geem Z.W. (2006). Optimal Cost Design of Water Distribution Networks Using Harmony Search, in Taylor & Francis, *Engineering Optimization*, 38(3), 259-280.

Geem Z.W., Kim J.H., & Loganathan G.V. (2001). A New Heuristic Optimization Algorithm: Harmony Search, *Simulation*, 76(2), 60-68.

Gomis-Bellmunt O., Junyent-Ferré A., Sumper A. & Galceran-Arellano S. (2010). Maximum generation power evaluation of variable frequency offshore wind farms when connected to a single power converter. *Applied Energy, Elsevier*, 87, 3103-9.

González J., Payán B., & Santos J. (2013). A New and Efficient Method for Optimal Design of Large Offshore Wind Power Plants. *IEEE Transaction Power Systems*, 28, (3), 3075-84.

Gonzalez-Longatt F.M., Wall P., Regulski P., & Terzija V. (2012). Optimal Electric Network Design for a Large Off-shore Wind Farm Based on a Modified Genetic Algorithm Approach. *IEEE Systems J.*, 6(1), 164-172.

GWEC (2015). Global wind report 2015, annual market update. Global Wind Energy Council, (accessed April 2016).

Holtsmark N., Bahirat H.J.; Molinas. M., Mork B.A., & Hoidalen H.Kr. (2013). An All-DC Offshore Wind Farm with Series-Connected Turbines: An Alternative to

the Classical Parallel AC Model? *IEEE Transaction Industrial Electronics*, 60(6), 2420-8.

Hou P., Hu W., & Chen Z. (2016). Optimisation for offshore wind farm cable connection layout using adaptive particle swarm optimisation minimum spanning tree method, *IET Renew. Power Gener.*,10(5), 694 – 702.

Hou P., Hu W., Chen Z., & Chen C. (2017a). Overall Optimization for Offshore Wind Farm Electrical System," *Wind Energy, Elsevier*, 20, 1017-32.

Hou P., Hu W., M. Soltani, Chen C., & Chen Z. (2017b). Combined optimization for offshore wind turbine micro siting, *Applied Energy, Elsevier*, 189, 271-282.

Kamalakannan C., Suresh, L.P., Dash, S.S., & Panigrahi, B.K. (2014). *Power Electronics and Renewable Energy Systems. Springer*, Proc. ICPERES.

Lancheros C. (2013). Transmission systems for Offshore Wind Farms: A Technical, Environmental and Economic Assessment. Maser Thesis in Hamburg University of Technology.

Lazaridis P.L. (2005). Economic comparison of HVAC and HVDC solutions for large offshore wind farms under special consideration of reliability. (M.S. thesis), Dept. Elect. Eng., Royal Inst. Technol., Stockholm, Sweden.

Levitt A.C., Kempton W., Smith A.P., Musial W., & Firestone J. (2011). Pricing offshore wind power. *Energy Policy, Elsevier*, 39, 6408-21.

Li B., & DeCarolis J.F. (2015). A techno-economic assessment of offshore wind coupled to offshore compressed air energy storage. *Applied Energy, Elsevier*, 155, 315-322.

Lumbreras S., & Ramos A. (2013). Optimal Design of the Electrical Layout of an Off-shore Wind Farm Applying Decomposition Strategies, *IEEE Transaction Power Systems*, 28(2), 1434-41.

Lundberg S. (2003). Performance comparison of wind park configurations. Dept. Elect. Power Eng., Univ. Chalmers, Göteborg, Sweden (technical report).

Madariaga A., Martinez A.I., Martin J.L., Eguia P., & Ceballos S. (2012). Current facts about offshore wind farms. *Renewable and Sustainable Energy Reviews, Elsevier*, 16, 3105-16.

Nandigam M., & Dhali S.K. (2008). Optimal design of an offshore wind farm layout. In Proc. SPEEDAM, Ischia, Italy, pp. 1470–1474.

Nexans (2013), Submarine Power Cables, Update June 10, 2013, Available online: http://www.nexans.com/Germany/2013/SubmPowCables_FINAL_10jun13_engl.pdf

Orient Cable (2015). Ningbo Orient Wire & cable Co., Ltd. China Ningbo Subsea Cable Institute, 1st edition.

Pillai A., Chick J., Johanning L., Khorasanchi M., & de Laleu V. (2015). Offshore wind farm electrical cable layout optimization," *Engineering Optimization*, 47(12), 1689–1708.

Pookpunt S., & Ongsakul W. (2016). Design of optimal wind farm configuration using a binary particle swarm optimization at Huasai district. *Energy Conversion and Management, Elsevier*, 108, 160-180.

Projet de Parc Éolien au Large de Saint-Nazaire, P. du Banc de Guérande. Available online (2013): http://parc-eolien-en-mer-de-saint-nazaire.fr/wp-content/uploads/2013/09/SNA_dmo.pdf

Samorani M. (2013). The Wind Farm Layout Optimization Problem. *Hand Book of Power Systems*, *Springer*, IX, 21-38.

Schoenmakers D. (2008). Optimization of the coupled grid connection of offshore wind farms. Graduation project at Evelop Netherlands BV Technical University of Eindhoven.

Siemens (2014a). SCOE – Society's costs of electricity: How society should find its optimal energy mix. Siemens Wind Power, August 2014.

Siemens (2014b). Redefining the cost debate: The concept of society's cost of electricity. Wind Power and Renewables Division, Siemens AG, November 2014.

Soukissian T. (2013). Use of multi-parameter distributions for offshore wind speed modeling: The Johnson SB distribution. *Applied Energy, Elsevier*, 111, 982-1000.

Shin J.S., Kim W.W., & Kim J.O. (2011). Study on Designing for Inner Grid of Offshore Wind Farm. *J. Clean Energy Technologies*, 3(4), 265-269.

The Wind Power, Wind Energy Market Intelligence (2016). Wind farms databases. Update April 22, 2016, Available online: http://www.thewindpower.net/data/samples/Windfarms.pdf

Voormolen J.A., Junginger H.M., & Van Sark W.G.J.H.M. (2016). Unravelling historical cost developments of offshore wind energy in Europe. *Energy Policy, Elsevier*. 88, 435-444.

Wang L., Xu Y., Mao Y., & Fei M. (2010). A Discrete Harmony Search Algorithm. *Communications in Computer and Information Science, Springer*, 98, 37-43.

Xiaoxia G., Hongxing Y., & Lin L. (2016). Optimization of wind turbine layout position in a wind farm using a newly-developed two-dimensional wake model. *Applied Energy, Elsevier*, 174, 192-200.

Yun H.Y., Jeong S.J., & Kim K.S. (2013). Advanced Harmony Search with Ant Colony Optimization for Solving the Traveling Salesman Problem. *J. Applied Mathematics, Hindawi*, 2013, 1-8.

Zubiaga M., Abad G., & Barrena J.A. (2009). Evaluation and selection of AC transmission lay-outs for large offshore wind farms. In Proc. Eur. Conf. Power Electron. Appl., Barcelona, Spain, pp. 1–10.